11/07/2024

MAGIC Observations of the Blazar TON 116 in a Multi-wavelength Context

Experimental Physics PhD Thesis

MAGIC
Major Atmospheric Gamma Imaging Cerenkov Telescopes

DSFTA
DIPARTIMENTO DI SCIENZE FISICHE, DELLA TERRA E DELL'AMBIENTE

Candidate: Andrea Lorini

Supervisor: Dr. Sofia Ventura

Co-supervisor: Dr. Giacomo Bonnoli

INFN
Istituto Nazionale di Fisica Nucleare
SEZIONE DI PISA

Outline

- AGNs framework: blazars and related sequence
- VHE and multi-wavelength study of the potential outlier TON 116
- Conclusions and perspectives

Main framework

So we do not know…

- Investigation of the disputed *blazar sequence* through the blazar **TON 116**
- High Energy **overluminosity** if **$z \approx 1$ =>** potential **sequence outlier** , but **$z \geq 0.483$** from optical spectroscopy
- **Distance/nature puzzle** solvable with **MAGIC observations (VHE never explored** for TON 116!**)**
- Study extended in a modern **MWL context** to infer the most likely **emission mechanisms**

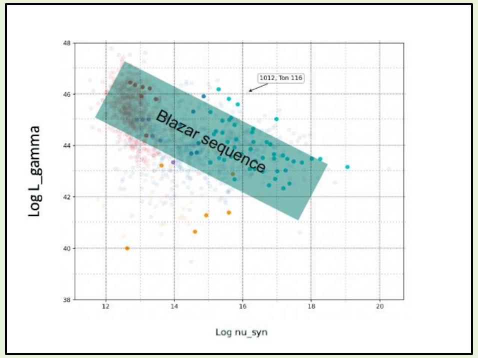


© R. Wagner

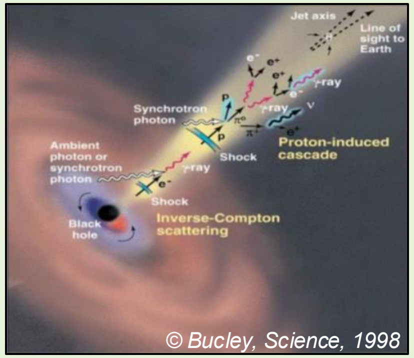

© Bucley, Science, 1998

The extragalactic source TON 116

Coordinates: RA = 12h 43' 12.7" , Dec = +36° 27' 44.0" (J2000)

Constellation: Canes Venatici (CVn)

Category/Class: AGN/BL-Lac-type Blazar

Main Catalogues: TON (*Iriarte & Chavira 1957*), Roma-BZCAT (*Massaro et al. 2015*)

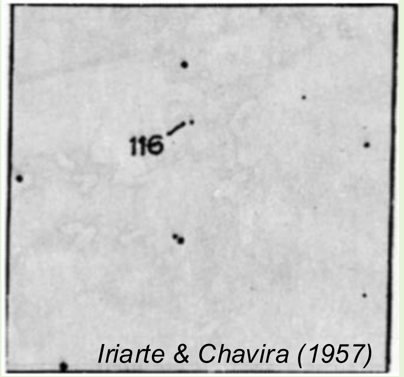

Iriarte & Chavira (1957)

The extragalactic source TON 116

<u>Coordinates</u>: RA = 12h 43' 12.7" , Dec = +36° 27' 44.0" (J2000)

<u>Constellation</u>: Canes Venatici (CVn)

<u>Category/Class</u>: AGN/BL-Lac-type Blazar

<u>Main Catalogues</u>: TON (*Iriarte & Chavira 1957*), Roma-BZCAT (*Massaro et al. 2015*)

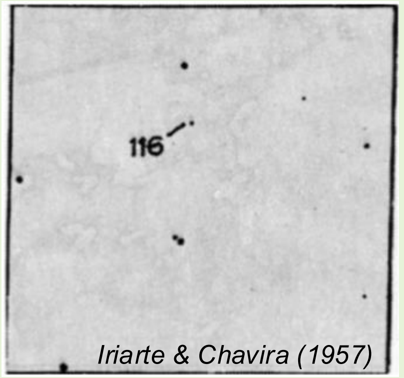

Iriarte & Chavira (1957)

Main e.m. detections

WISE Satellite
Mid-IR source *(D'abrusco et al. 2014)*

Fermi-LAT Satellite
HE γ emitter *(Ajello et al. 2020)*

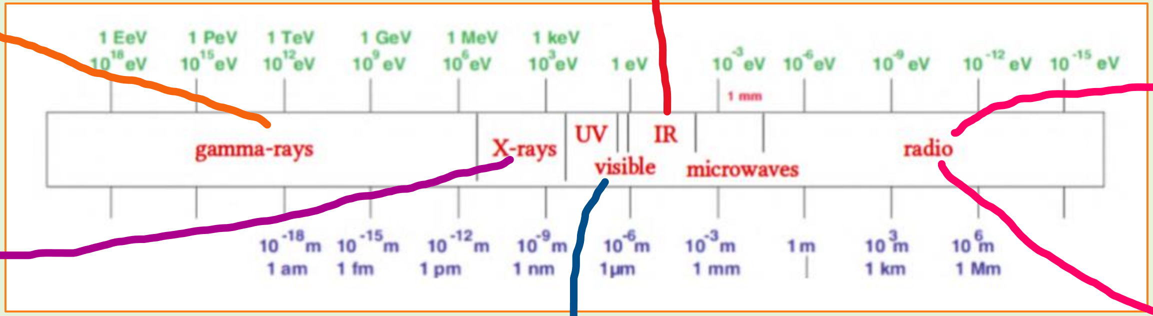

Cambridge Telescope
Radio object *(Hales et al. 1988)*

ROSAT Satellite
X-ray source (*Voges et al. 1999*)

Northern Cross Telescope
Radio object *(Colla et al. 1973)*

<u>Discovery at OANTON telescope</u>
<u>B-UV faint star *(Iriarte & Chavira 1957)*</u>

Active Galactic Nuclei

Extremely high flux at all wavelengths for ~ 1% of all known galaxies

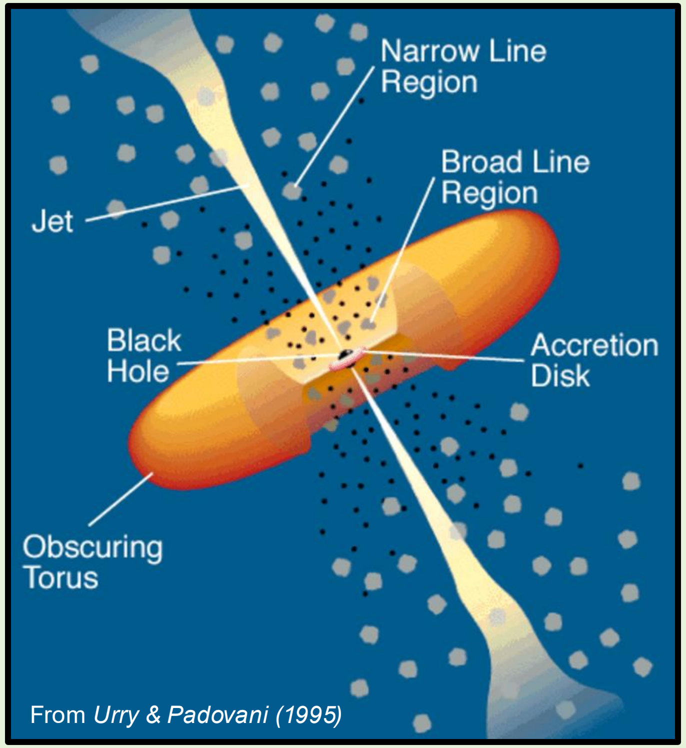

Accretion onto a Super Massive Black Hole (SMBH) of ~ 10^6-10^{10} $M_\odot$

Accretion disk of infalling material (black-body emission)

+

Fast/slow-moving (BLR/NLR) excited or ionized clumps

+

Optically-thick dusty torus (Vis-UV absorber and IR emitter)

+

Radio jet of ultra-high-speed particles reaching up to ~ 1 Mpc

The Unified Model

Many empirical AGN classes defined over time

BUT...

All basically the same objects; differences due to spatial orientation

(*Urry & Padovani 1995*)

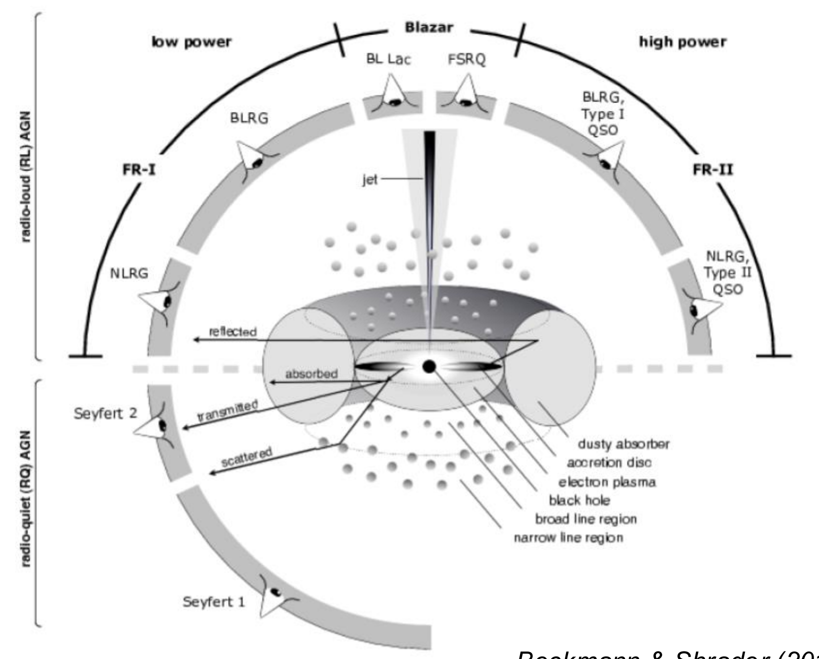

Beckmann & Shrader (2012)

- The most powerful, persistent sources (of UHECRs also)
- Small l.o.s.-axis angle => inner parts more appreciable
- AGNs with jets ~ towards Earth ($\theta < 20°$) are called ***blazars***

Variable flux at all λs

Blazars

Around 10% of AGNs are radio-loud ($F_{5\ GHz}$ / $F_{250\ nm}$ > 10), and ~ 1% of them are blazars

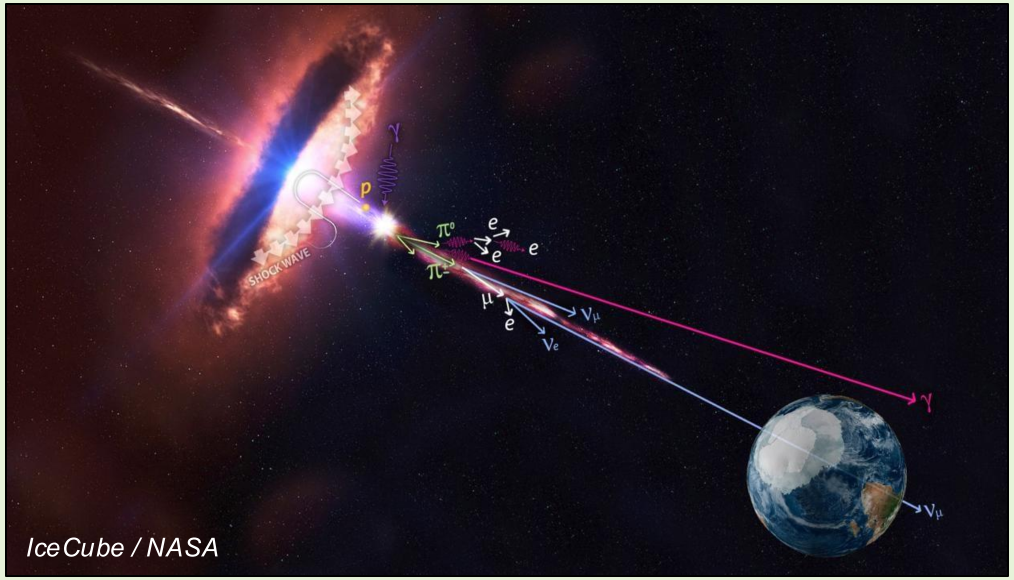

Jets towards us => extreme properties:

- Very beamed, boosted radiation (also *superluminal motion*)
- Bolometric luminosity up to 10^{48} erg/s
- High polarization and variability (down to min scale!)
- Candidates for direct UHECRs and neutrinos

Blazar subclasses

FSRQs	BL Lacs
EW > 5 Å Broad emission lines on optical continuum	**EW < 5 Å** No/faint emission lines on optical continuum
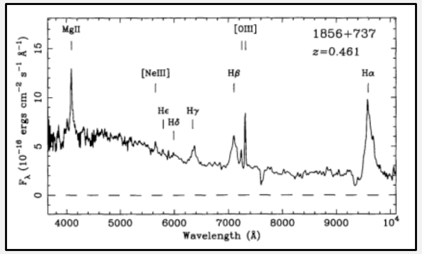 *Henstock et al. (1997)*	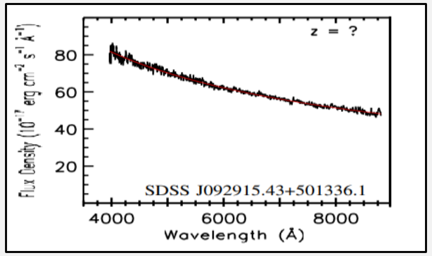 *Plotkin et al. (2010)*

Standard classification
(*Stocke et al. 1991*)

Blazar subclasses

FSRQs	BL Lacs
EW > 5 Å Broad emission lines on optical continuum	**EW < 5 Å** No/faint emission lines on optical continuum
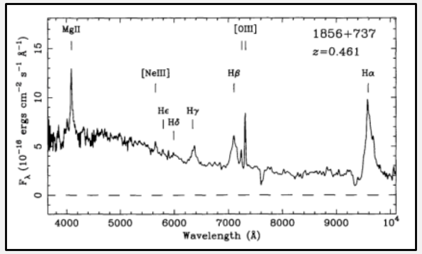	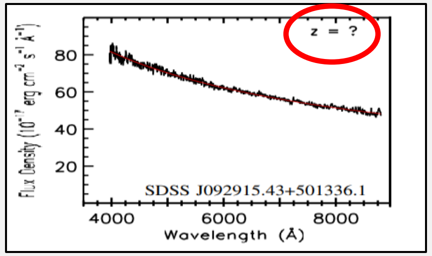
Henstock et al. (1997)	*Plotkin et al. (2010)*

Standard classification (*Stocke et al. 1991*)

but may be variability-dependent (also masquerading BL Lacs)...

Blazar subclasses

	FSRQs	BL Lacs
Standard classification (*Stocke et al. 1991*)	**EW > 5 Å** Broad emission lines on optical continuum 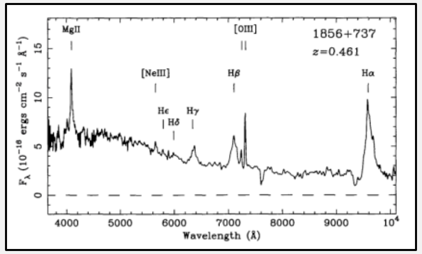 *Henstock et al. (1997)*	**EW < 5 Å** No/faint emission lines on optical continuum 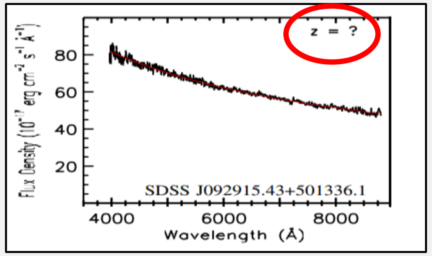 *Plotkin et al. (2010)*
Proposed classification (*Ghisellini et al. 2011*)	**$L_{BLR} / L_{EDD} > 5 \cdot 10^{-4}$** Efficient accretion rate  *M. Weiss, CfA*	**$L_{BLR} / L_{EDD} < 5 \cdot 10^{-4}$** Inefficient accretion rate 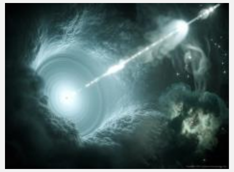 DESY

but may be variability-dependent (also masquerading BL Lacs)...

Blazar subclasses

	FSRQs	BL Lacs
Standard classification (*Stocke et al. 1991*)	**EW > 5 Å** Broad emission lines on optical continuum 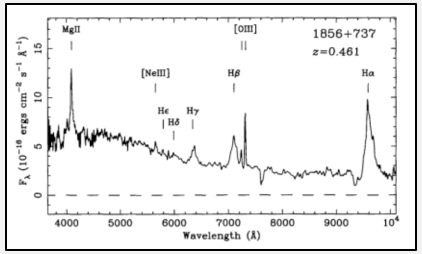 *Henstock et al. (1997)*	**EW < 5 Å** No/faint emission lines on optical continuum 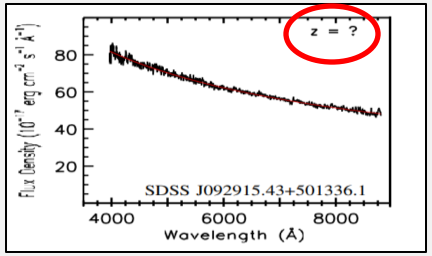 *Plotkin et al. (2010)*
Proposed classification (*Ghisellini et al. 2011*)	**$L_{BLR} / L_{EDD} > 5 \cdot 10^{-4}$** Efficient accretion rate  *M. Weiss, CfA*	**$L_{BLR} / L_{EDD} < 5 \cdot 10^{-4}$** Inefficient accretion rate 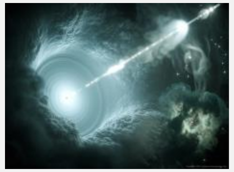 DESY

but may be variability-dependent (also masquerading BL Lacs)...

$L_{edd} \approx 1.3 \cdot 10^{38}\, M_{SMBH} / M_{\odot}$ erg/s
intrinsic properties considered...

Intrinsic differences

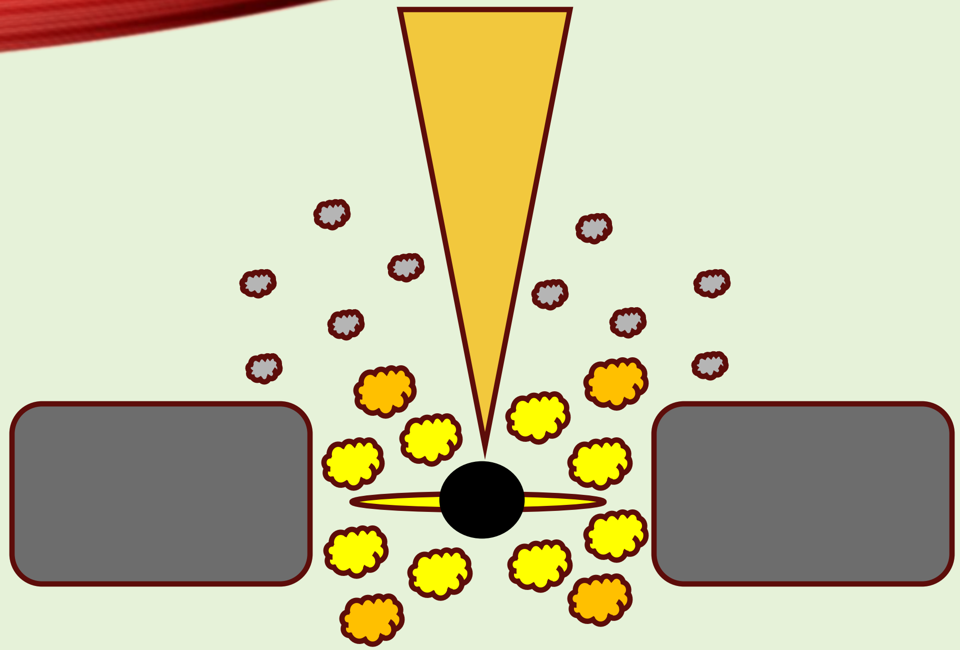

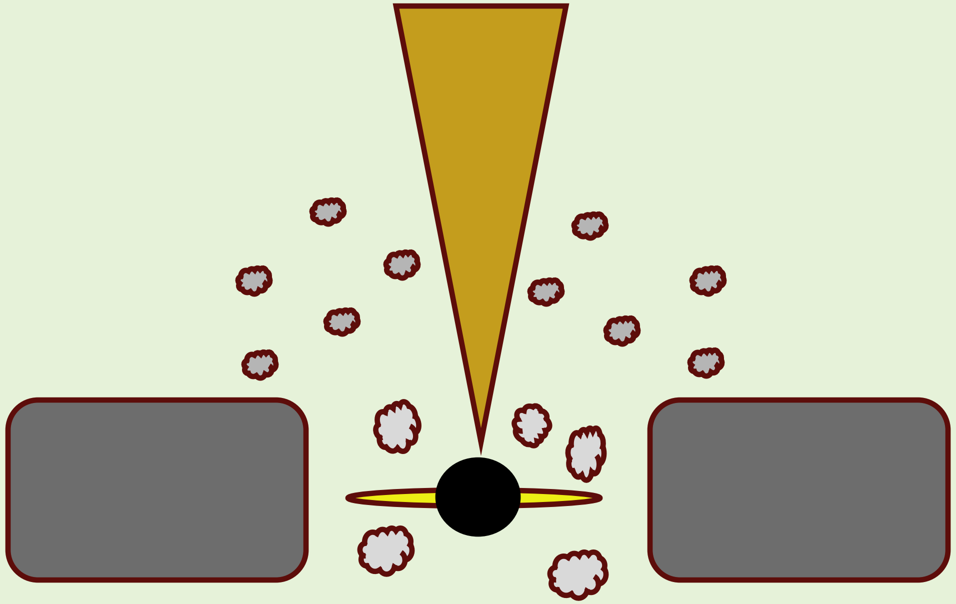

Flat Spectrum Radio Quasars (FSRQs)

Shakura-Sunyaev disk (SSD) + dense BLR
Rich environment with diffuse radiation fields

⇩

Efficient accretion

BL Lac Objects (BL Lacs)

Advection-Dominated Accretion Flow (ADAF) disk + poor BLR
Scarce environment with dim radiation fields

⇩

Inefficient accretion

AGN classification

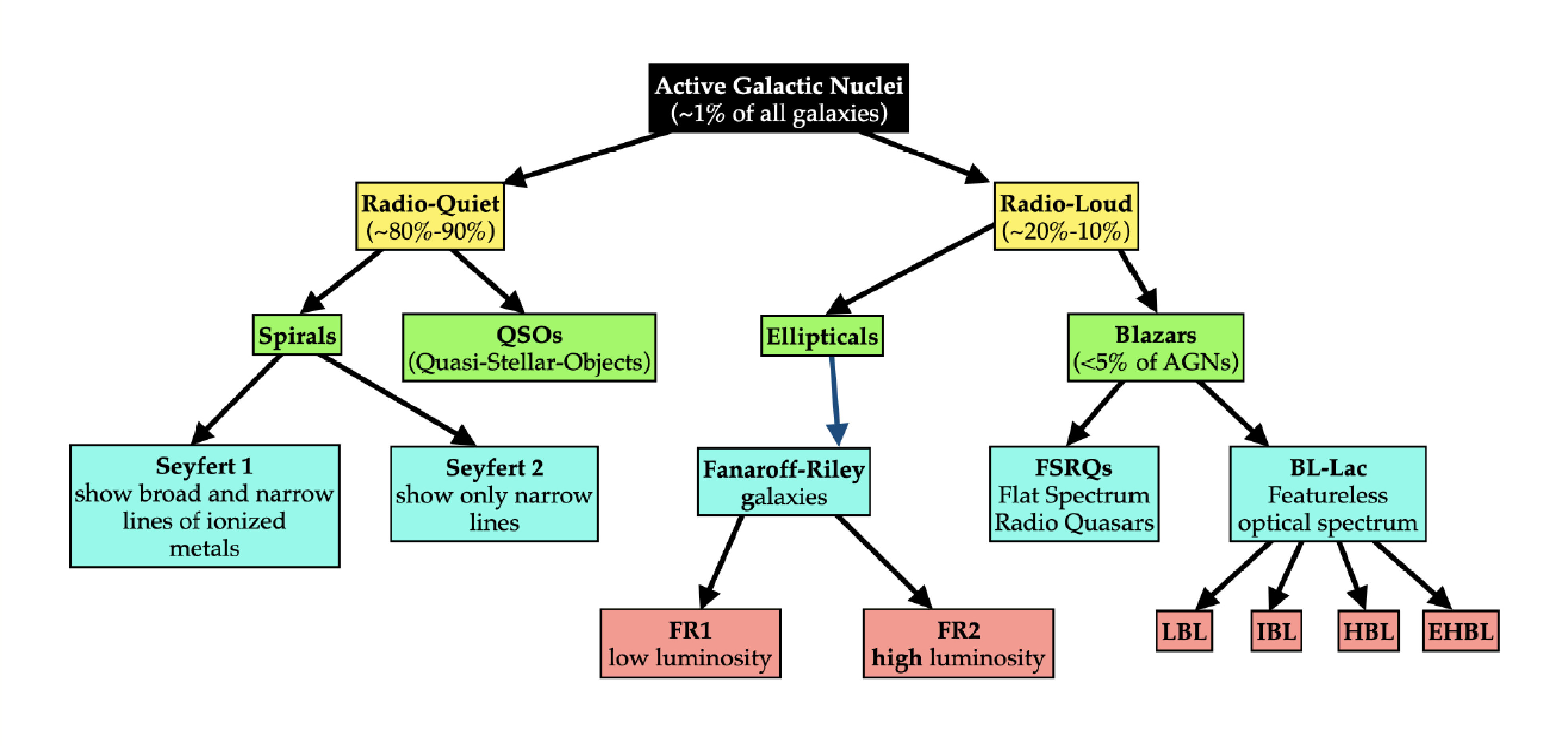

AGN classification

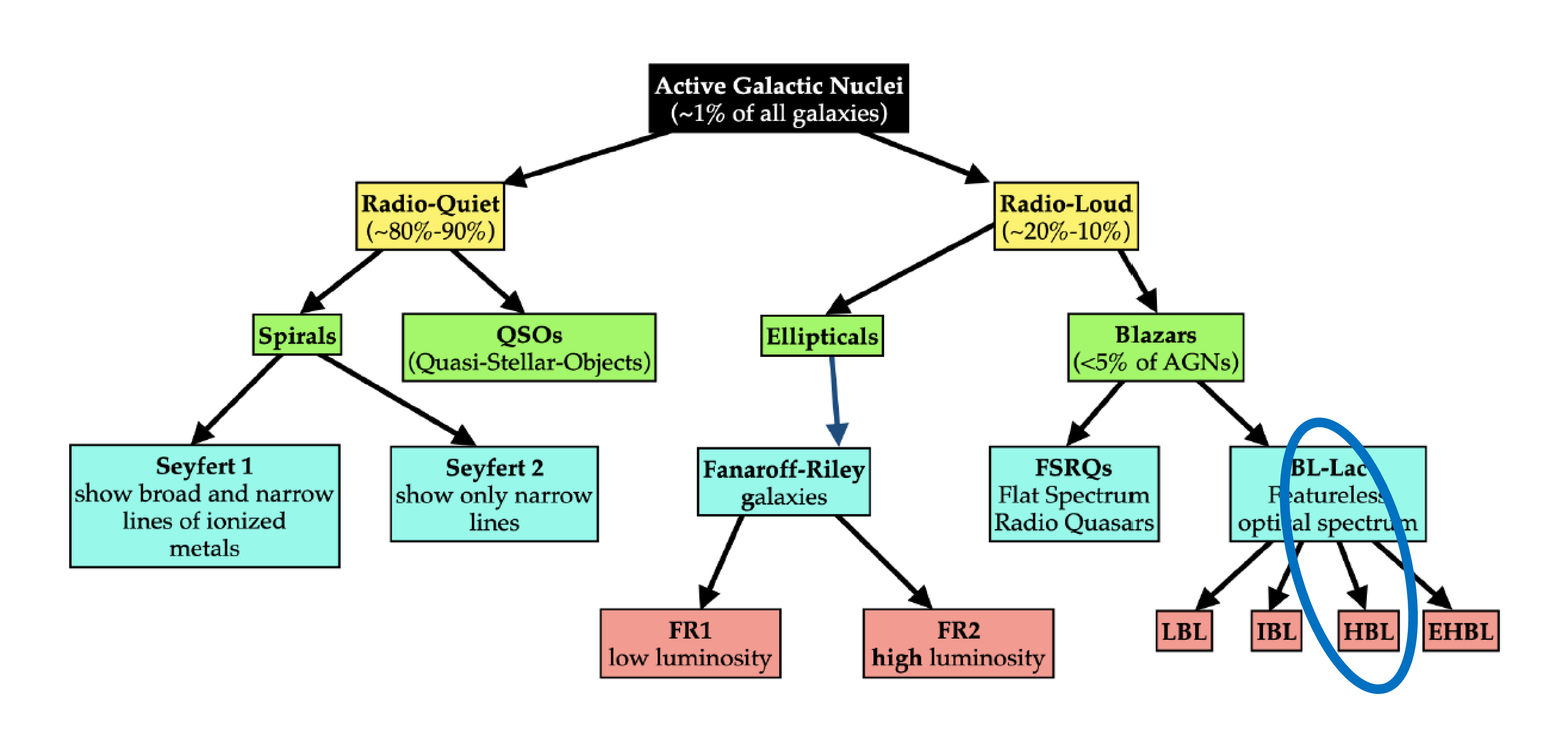

Spectral Energy Distribution

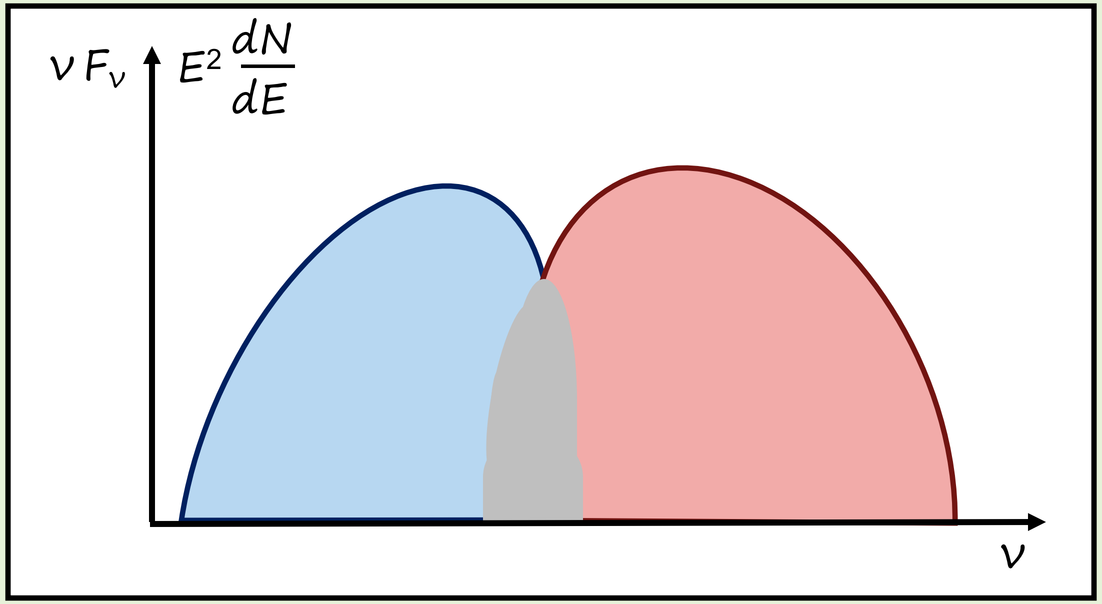

Spectral Energy Distribution

Synchrotron radiation

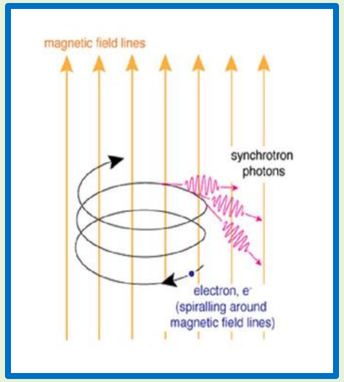

https://imagine.gsfc.nasa.gov/

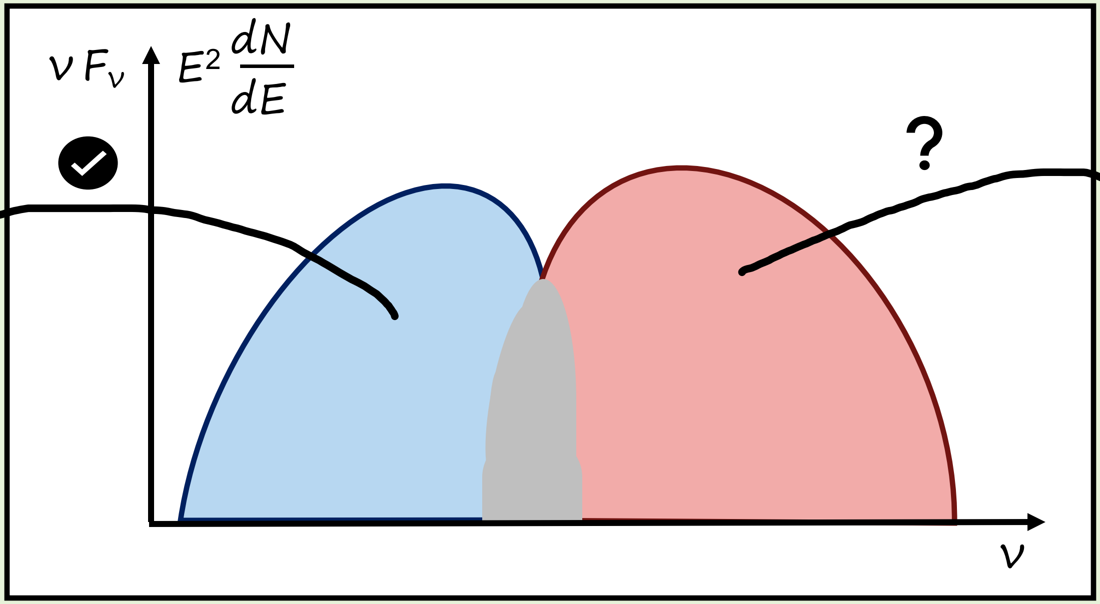

Inverse-Compton radiation

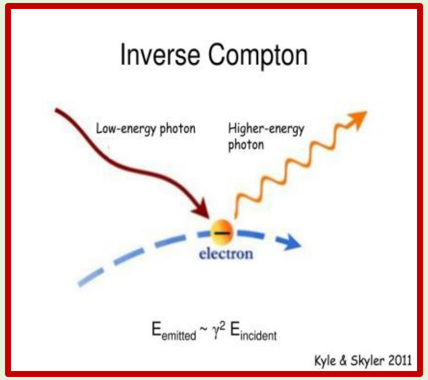

- **Low-energy (peak in IR-X bands) and high-energy (peak in γ MeV-TeV band) broad bumps**

Spectral Energy Distribution

Synchrotron radiation

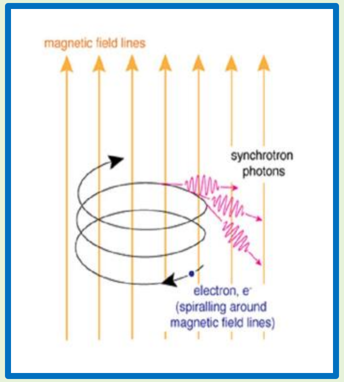

https://imagine.gsfc.nasa.gov/

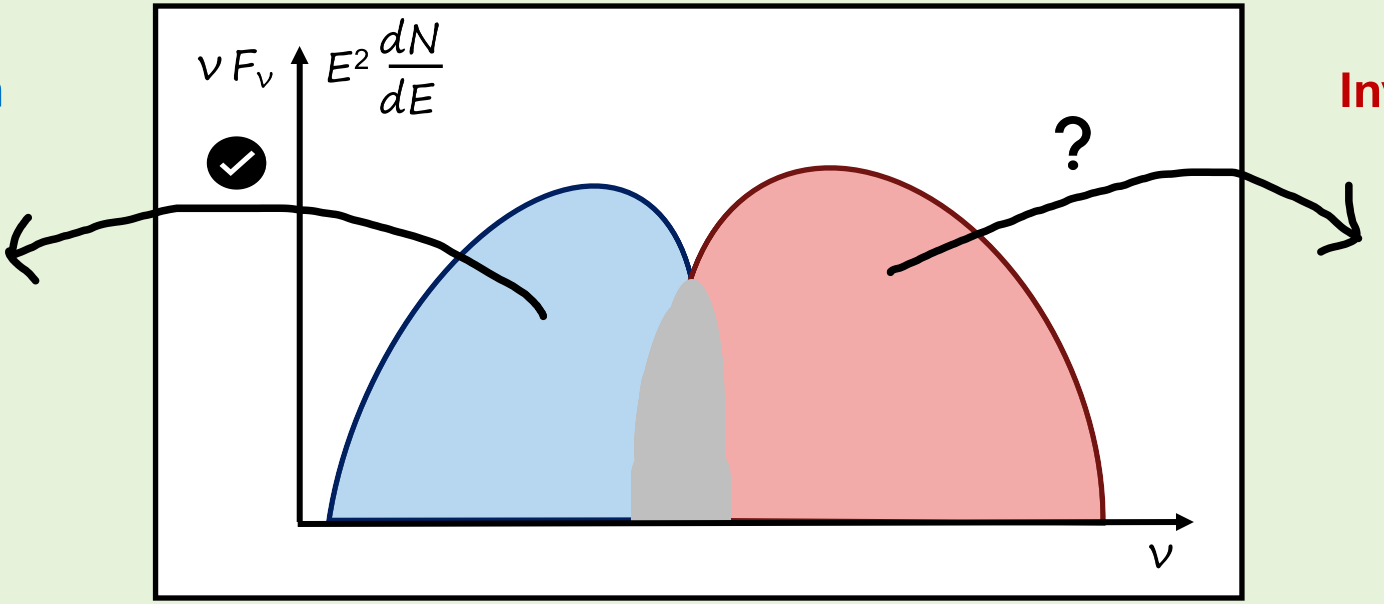

Inverse-Compton radiation

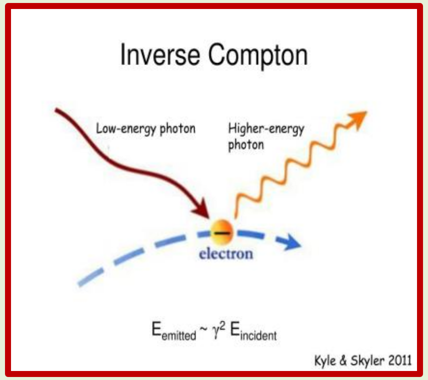

- **Low-energy (peak in IR-X bands) and high-energy (peak in γ MeV-TeV band) broad bumps**
- **Simple SSC (+EC) leptonic model usually assumed, but lepto-hadronic ones possible (at HE)**

Proton synchrotron

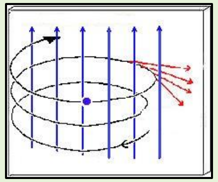

From *universe-review.ca*

Bethe-Heitler process

$p + \xi \longrightarrow p + e^- + e^+$

$$p+\xi \longrightarrow \Delta^+ \longrightarrow \begin{cases} p+\pi^0 \\ n+\pi^\pm \end{cases} \quad \begin{cases} \pi^0 \longrightarrow \gamma+\gamma \\ \pi^+ \longrightarrow \mu^+ + \nu_\mu \\ \pi^- \longrightarrow \mu^- + \overline{\nu}_\mu \end{cases} \quad \begin{cases} \mu^+ \longrightarrow e^+ + \overline{\nu}_\mu + \nu_e \\ \mu^- \longrightarrow e^- + \nu_\mu + \overline{\nu}_e \end{cases}$$

Photo-production

Synchrotron Self-Compton model

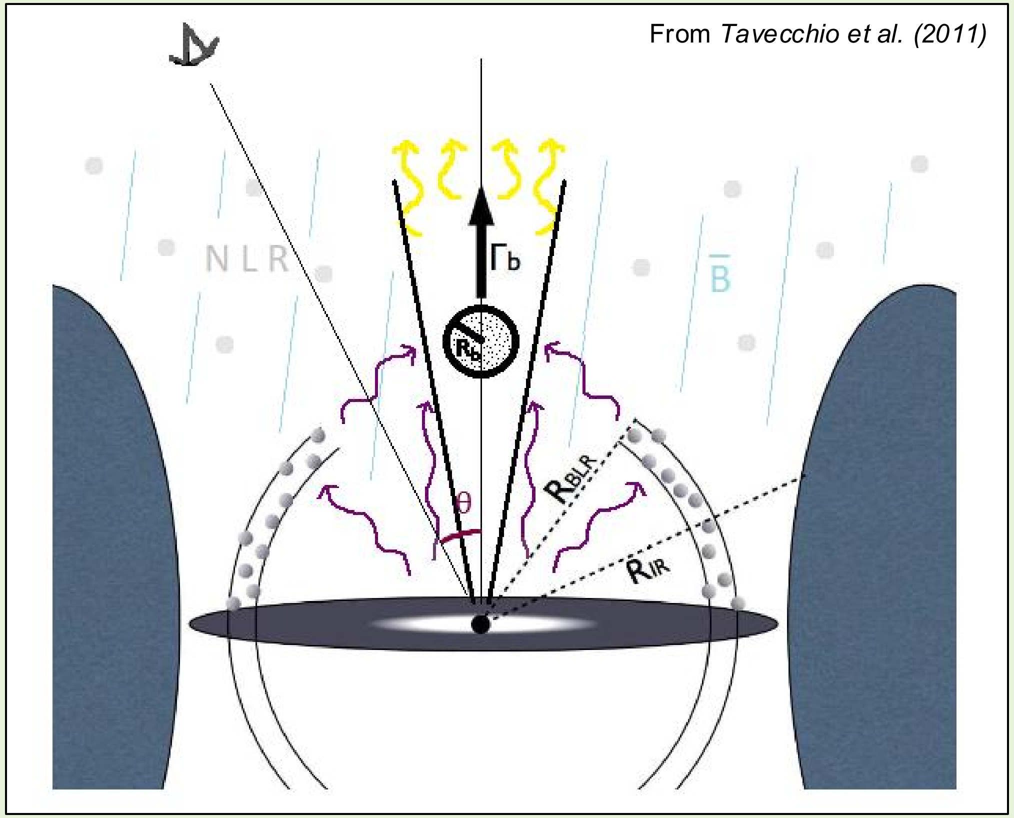

A *blob* assumed spherical (radius R_b) and filled with particles, relativistically moving (Lorentz factor Γ_b) nearly towards us through a tangled magnetic field ($\bar{B}$)

$$R_b = \frac{c\,t_{var}\,\delta_D}{1+z}$$

Synchrotron Self-Compton model

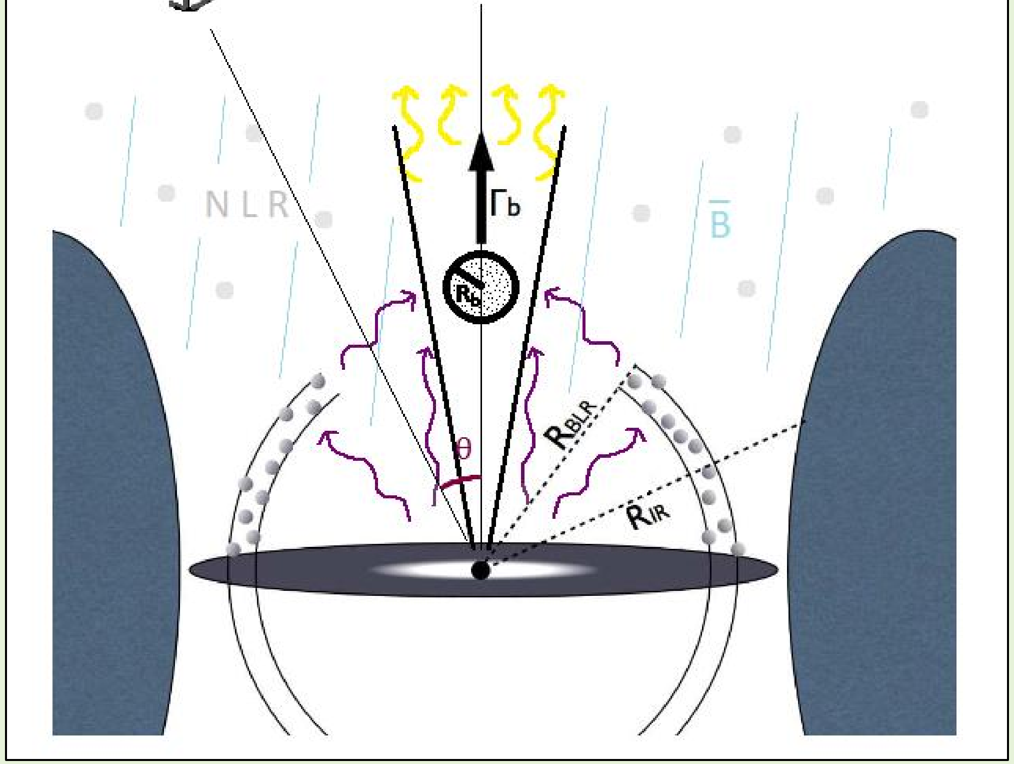

From *Tavecchio et al. (2011)*

A *blob* assumed spherical (radius R_b) and filled with particles, relativistically moving (Lorentz factor Γ_b) nearly towards us through a tangled magnetic field ($\bar{B}$)

$$R_b = \frac{c\, t_{var}\, \delta_D}{1+z}$$

Speed of light in vacuum (c)

Minimum time of flux variability (t_{var})

Doppler factor (boosting) (δ_D)

$$\delta_D = \frac{1}{\Gamma_b\,(1-\beta\cos\theta)}$$

$F_{obs} = \delta_D^4\, F'_{em}$

$\beta := v / c$

Redshift (z)

Synchrotron Self-Compton model

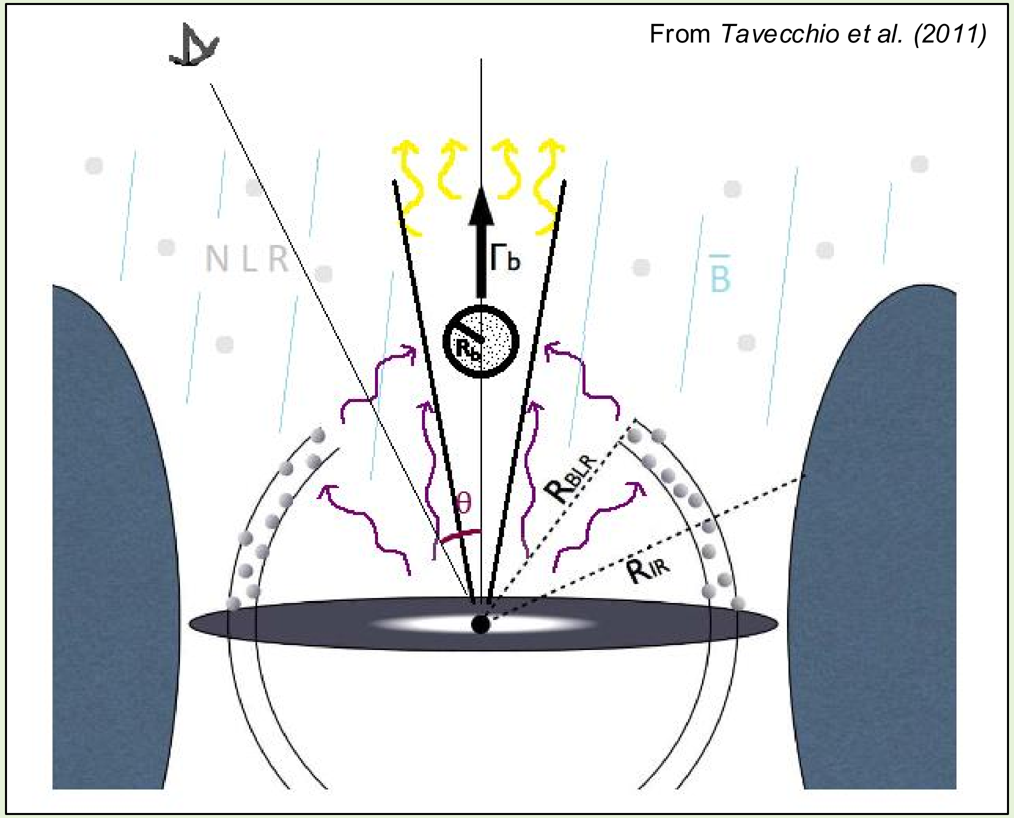

From *Tavecchio et al. (2011)*

A *blob* assumed spherical (radius R_b) and filled with particles, relativistically moving (Lorentz factor Γ_b) nearly towards us through a tangled magnetic field ($\bar{B}$)

$$R_b = \frac{c\,t_{var}\,\delta_D}{1+z}$$

- c: Speed of light in vacuum
- t_{var}: Minimum time of flux variability
- δ_D: Doppler factor (boosting)
- z: Redshift

$$\delta_D = \frac{1}{\Gamma_b\,(1-\beta\cos\theta)}$$

$\beta := v / c$

$F_{obs} = \delta_D^4 F'_{em}$

Electron energy distribution in finite interval $[\gamma_{min}, \gamma_{max}]$:

power-law (PL), broken power-law (BPL), log-parabola (LP), ...

$$n(\gamma) = k\gamma^{-p}$$

$$n(\gamma) = \begin{cases} k\gamma^{-p_1} & \gamma < \gamma_{br} \\ k\gamma^{-p_2} & \gamma \geq \gamma_{br} \end{cases}$$

$$n(\gamma) = k\left(\frac{\gamma}{\gamma_0}\right)^{-(p+q\log_{10}(\gamma/\gamma_0))}$$

Synchrotron Self-Compton model

Mostly for BL Lacs (lack of external fields)

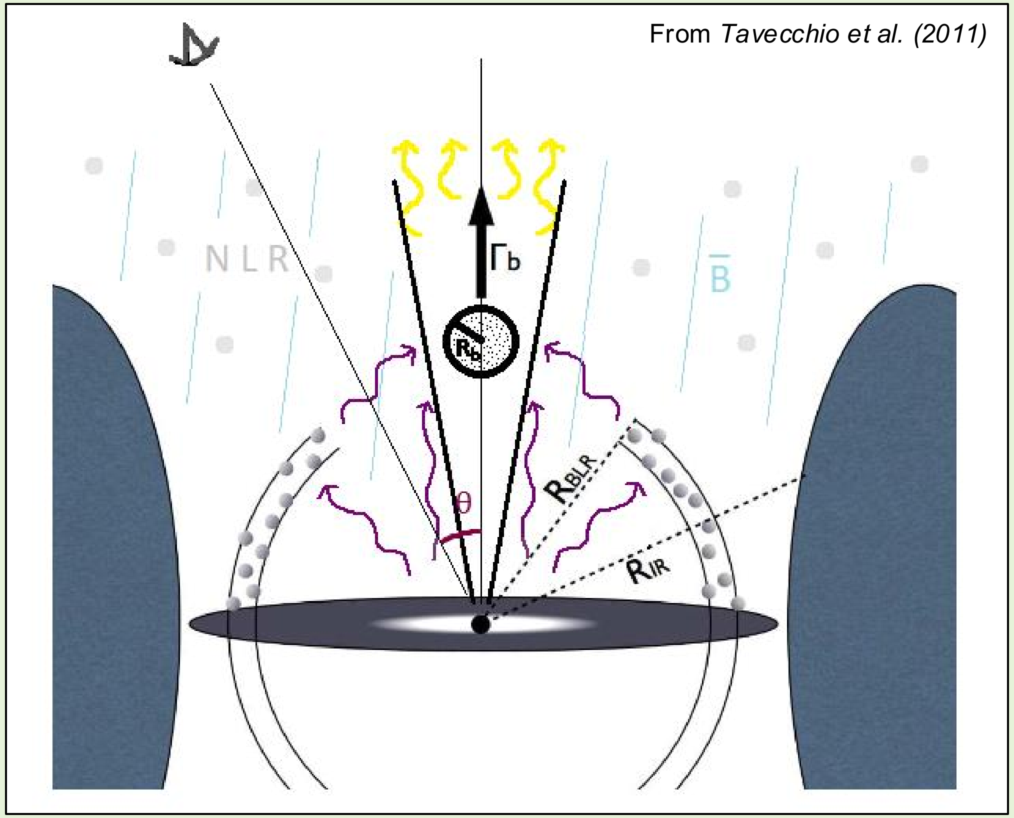

Parameters: B, R_b, δ_D, k, p_1, p_2, γ_{min}, γ_{br}, γ_{max}

Links and constraints on γ_{br}, cooling, particles' escape

A *blob* assumed spherical (radius R_b) and filled with particles, relativistically moving (Lorentz factor Γ_b) nearly towards us through a tangled magnetic field ($\bar{B}$)

$$R_b = \frac{c\, t_{var}\, \delta_D}{1+z}$$

Speed of light in vacuum (c); Minimum time of flux variability (t_{var}); Doppler factor (boosting) (δ_D); Redshift (z)

$$\delta_D = \frac{1}{\Gamma_b (1 - \beta \cos\theta)}$$

$\beta := v / c$

$F_{obs} = \delta_D^4 F'_{em}$

Electron energy distribution in finite interval $[\gamma_{min}, \gamma_{max}]$:

power-law (PL), broken power-law (BPL), log-parabola (LP), ...

$$n(\gamma) = k\gamma^{-p}$$

$$n(\gamma) = \begin{cases} k\gamma^{-p_1} & \gamma < \gamma_{br} \\ k\gamma^{-p_2} & \gamma \geq \gamma_{br} \end{cases}$$

$$n(\gamma) = k\left(\frac{\gamma}{\gamma_0}\right)^{-(p+q\log_{10}(\gamma/\gamma_0))}$$

Blazar sequence

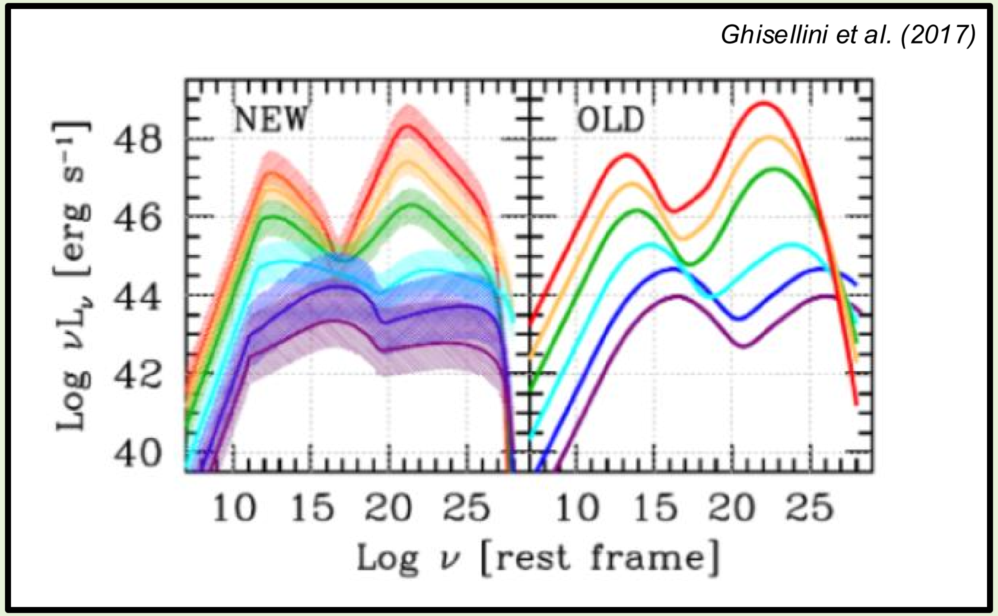

Fossati et al. (1998)

- Set of 126 well-sampled blazars binned in radio luminosity ($L_{5\ GHz}$)
- $\nu_{p,c} / \nu_{p,s} \approx 5 \cdot 10^8$
- SED peaks towards smaller frequencies with increasing bolometric L (FRSQs more luminous)

Blazar sequence

Ghisellini et al. (2017)

- Set of 747 γ-emitting blazars binned in γ luminosity, trend confirmed

  But increasing L_γ …

- FSRQs more Compton-dominated and with harder X-ray slope
- BL Lacs with redder-when-brigther behaviour

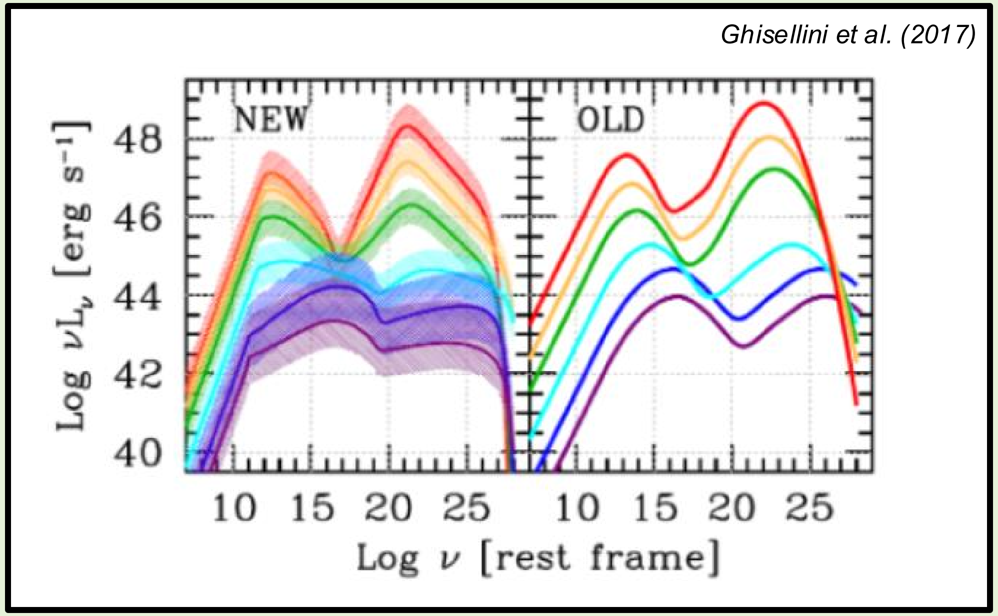

Fossati et al. (1998)

- Set of 126 well-sampled blazars binned in radio luminosity ($L_{5\ GHz}$)
- $\nu_{p,c} / \nu_{p,s} \approx 5 \cdot 10^8$
- SED peaks towards smaller frequencies with increasing bolometric L (FRSQs more luminous)

Sequence...just a selection bias?

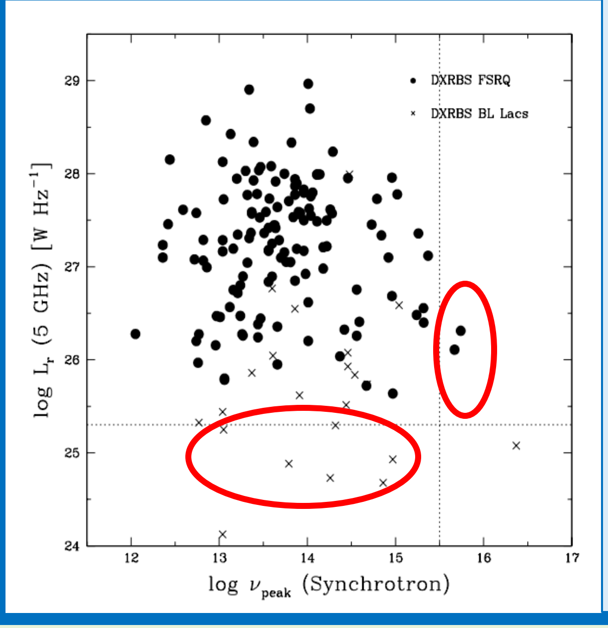

Padovani (2007)

- **No $\nu_{p,s}$ - $L_{5\ GHz}$ anti-correlation**
  (+ large power scatter at given $\nu_{p,s}$)

- **FSRQs detected with high $\nu_{p,s}$** (UV - X)

- **$\nu_{p,s}$ (FSRQs) $\lesssim$ 10-100 $\nu_{p,s}$ (BL Lacs)**
  (at most, to be better investigated)

Sequence...just a selection bias?

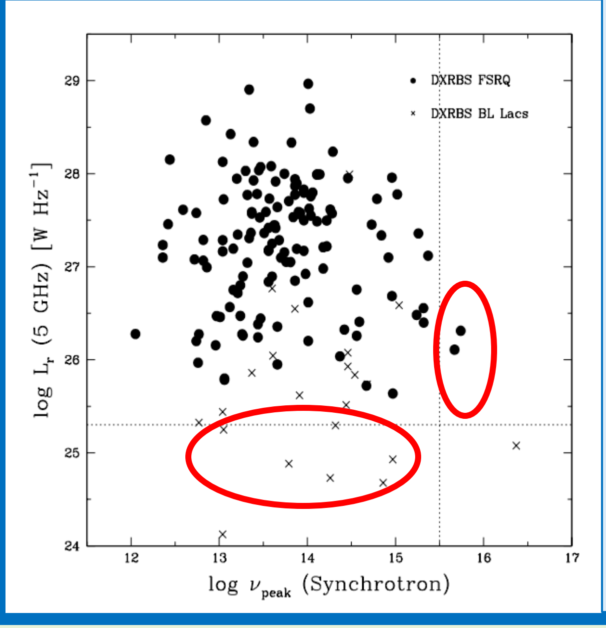

Padovani (2007)

- **No $\nu_{p,s}$ - $L_{5\,GHz}$ anti-correlation** (+ large power scatter at given $\nu_{p,s}$)
- **FSRQs detected with high $\nu_{p,s}$** (UV - X)
- **$\nu_{p,s}$ (FSRQs) $\lesssim$ 10-100 $\nu_{p,s}$ (BL Lacs)** (at most, to be better investigated)

Giommi et al. (2012)

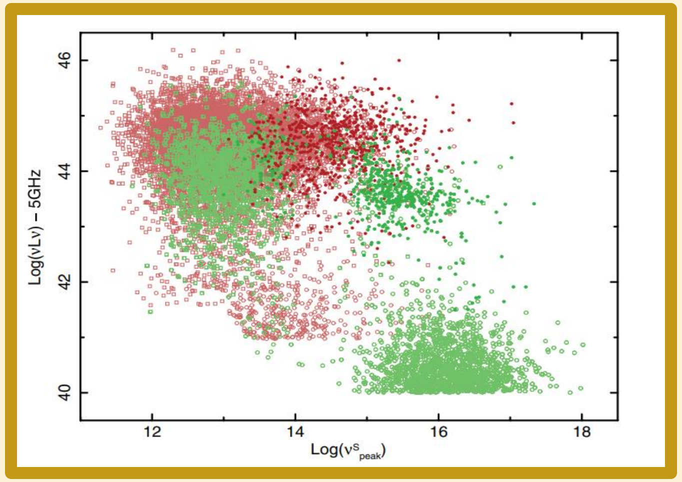

✖ **~ all blazar classifications and trends are selection-affected**

Sequence...just a selection bias?

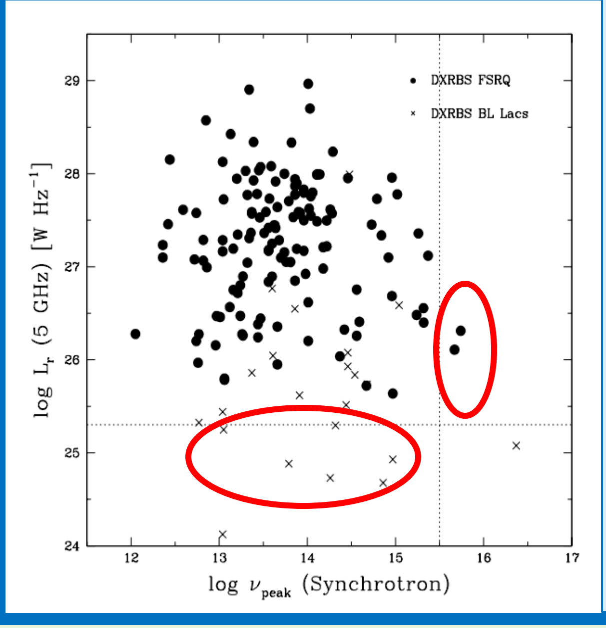

Padovani (2007)

- **No $\nu_{p,s}$ - $L_{5\ GHz}$ anti-correlation**
  (+ large power scatter at given $\nu_{p,s}$)
- **FSRQs detected with high $\nu_{p,s}$** (UV - X)
- **$\nu_{p,s}$ (FSRQs) $\lesssim$ 10-100 $\nu_{p,s}$ (BL Lacs)**
  (at most, to be better investigated)

Giommi et al. (2012)

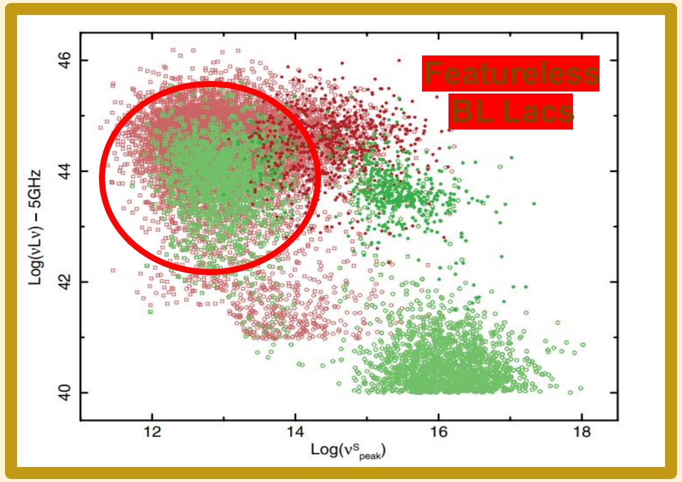

✕ **~ all blazar classifications and trends are selection-affected**

Huge MWL datasets
+
Extensive MC simulations

⇩

Blazar sequence from shallow radio-X surveys

Sequence...just a selection bias?

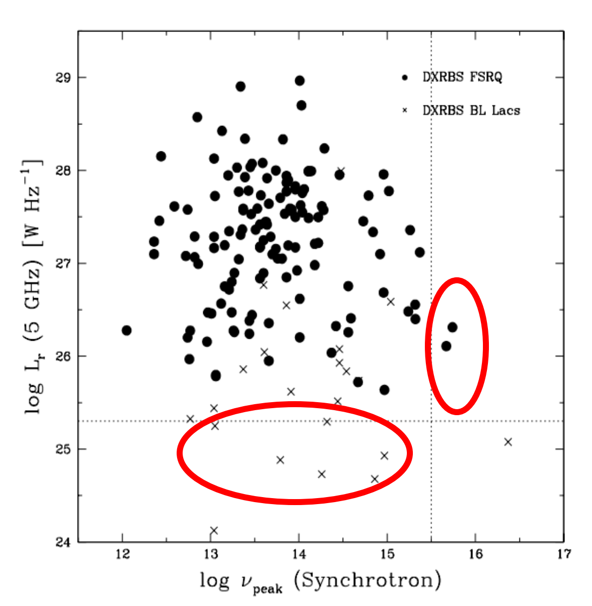

Padovani (2007)

- **No $\nu_{p,s}$ - $L_{5\,GHz}$ anti-correlation**
  (+ large power scatter at given $\nu_{p,s}$)
- **FSRQs detected with high $\nu_{p,s}$** (UV - X)
- **$\nu_{p,s}$ (FSRQs) $\lesssim$ 10-100 $\nu_{p,s}$ (BL Lacs)**
  (at most, to be better investigated)

Giommi et al. (2012)

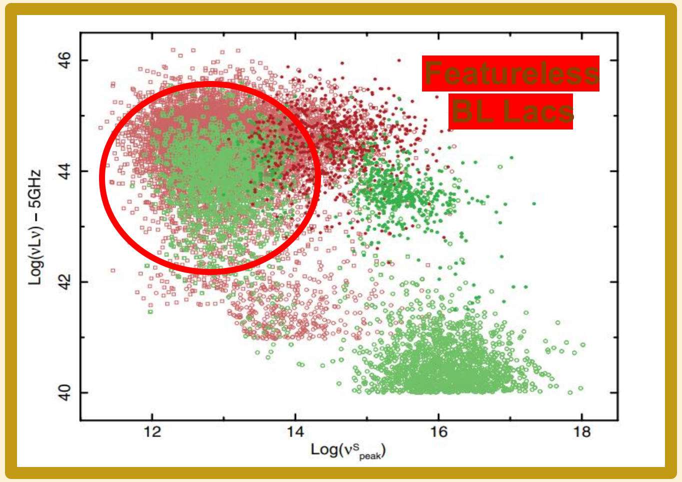

✖ **~ all blazar classifications and trends are selection-affected**

[*Huge MWL datasets*
+
Extensive MC simulations]

⬇

Blazar sequence from shallow radio-X surveys

Keenan et al. (2021)

† *End of the blazar sequence* †

(from ~ 2000 accurate SEDs of jetted AGNs)

Yet jets' dichotomy:

1 -> Weakly-accreting LERGs (mostly HBLs)
2 -> Efficiently-accreting HERGs (FSRQs, LBLs)

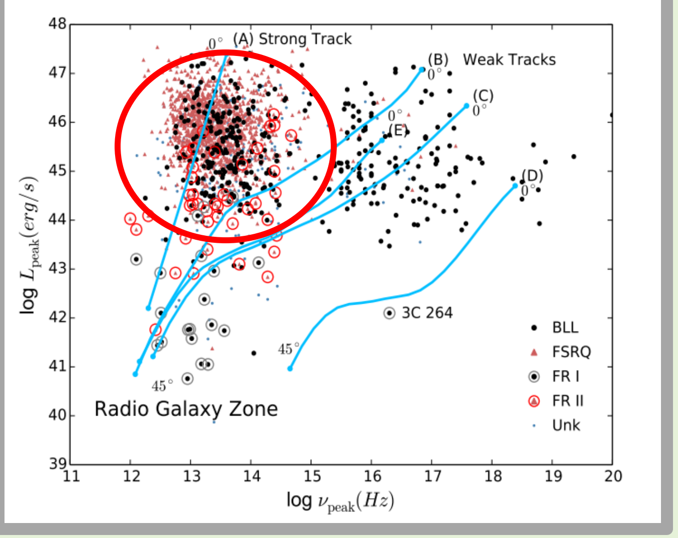

TON 116 vs blazar sequence

High HE state from *Fermi*-LAT (4LAC, *Ajello et al. 2020*) assuming z ≈ 1

$\nu_{p,s} > 10^{15}$ Hz and $L_{HE} > 10^{46}$ erg/s ⟹ out of blazar sequence!

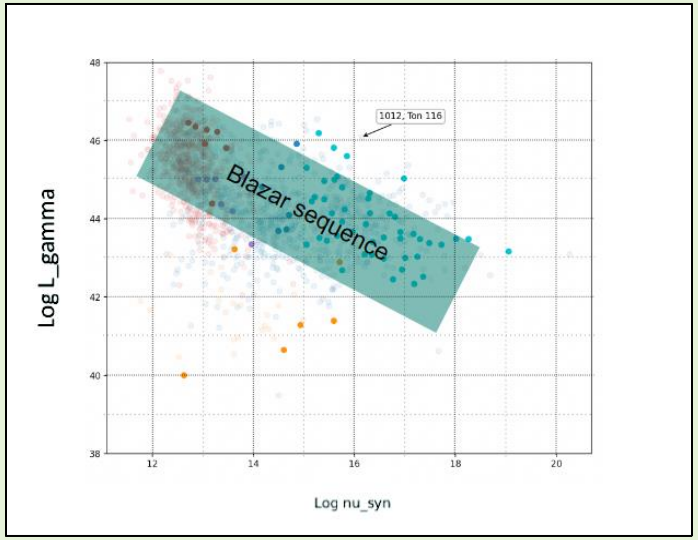

TON 116 vs blazar sequence

High HE state from *Fermi*-LAT (4LAC, *Ajello et al. 2020*) assuming z ≈ 1

$\nu_{p,s}$ > 10^{15} Hz and L_{HE} > 10^{46} erg/s ⟹ out of blazar sequence!

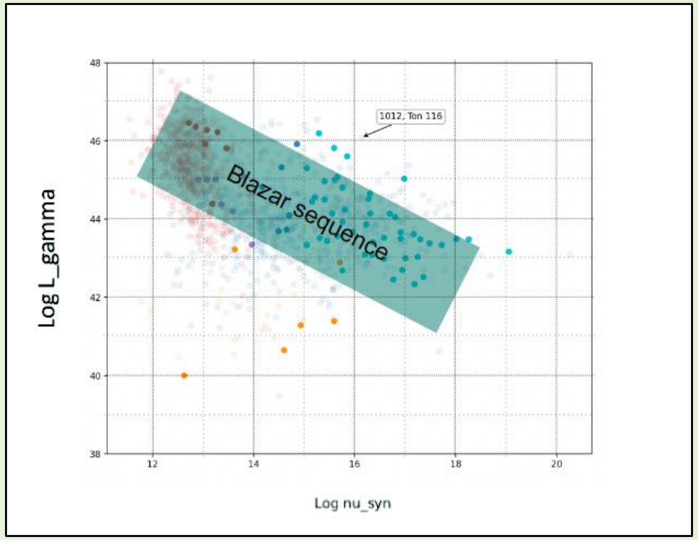

But from GTC observation in optical: z > 0.483 (*Paiano et al. 2017*)

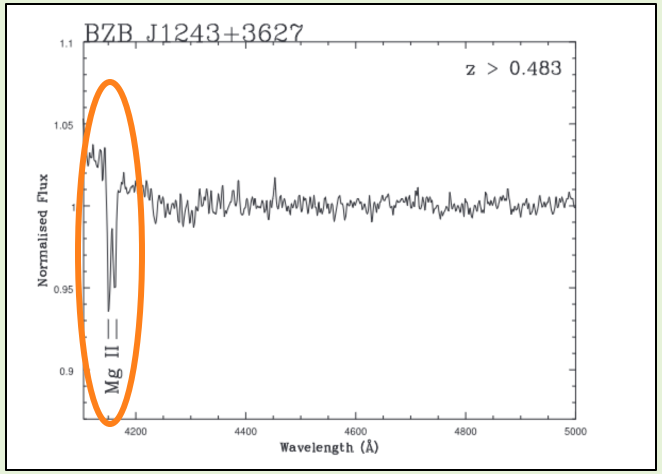

MgII absorption doublet at 4160 Å due to intervening matter

- Previously: z > 0.485 (*Plotkin et al. 2010*), z ≈ 0.50 (*Meisner & Romani 2010*)
- *Is TON 116 overluminous due to proximity, or to intrinsic properties?*

Gamma band distance constraint

From HE (*Fermi*-LAT) and VHE (MAGIC) spectrum ⟹ upper limit on redshift (z*)

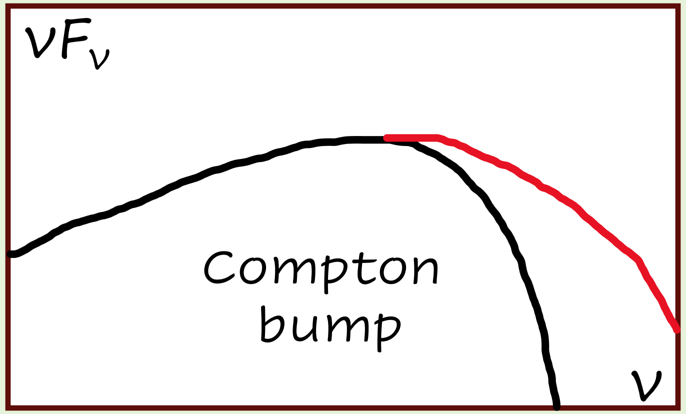

VHE affected by EBL absorption (increasing with energy and distance):

$$\gamma + \gamma \longrightarrow e^- + e^+$$

Gamma band distance constraint

From HE (*Fermi*-LAT) and VHE (MAGIC) spectrum ⟹ upper limit on redshift (z*)

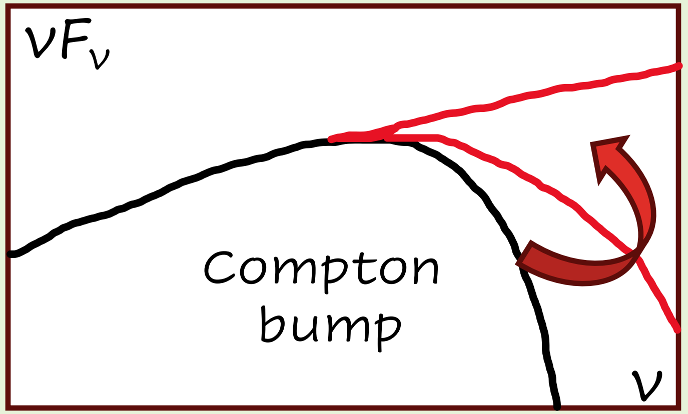

VHE affected by EBL absorption (increasing with energy and distance):

$$\gamma + \gamma \longrightarrow e^- + e^+$$

The EBL-corrected spectrum cannot be harder than HE trend!

Gamma band distance constraint

From HE (*Fermi*-LAT) and VHE (MAGIC) spectrum ⟹ upper limit on redshift (z*)

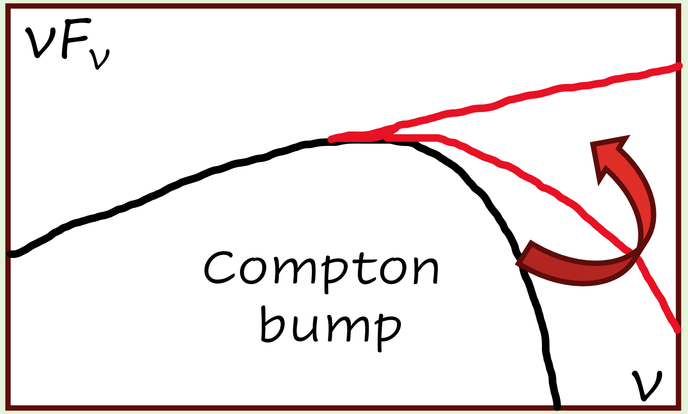

VHE affected by EBL absorption (increasing with energy and distance):

$$\gamma + \gamma \longrightarrow e^- + e^+$$

The EBL-corrected spectrum cannot be harder than HE trend!

***Prandini et al. (2010)*:**

Change of intrinsic VHE spectrum with z (sample of known TeV *Fermi* sources)

⇓

TON 116 distance can be constrained!

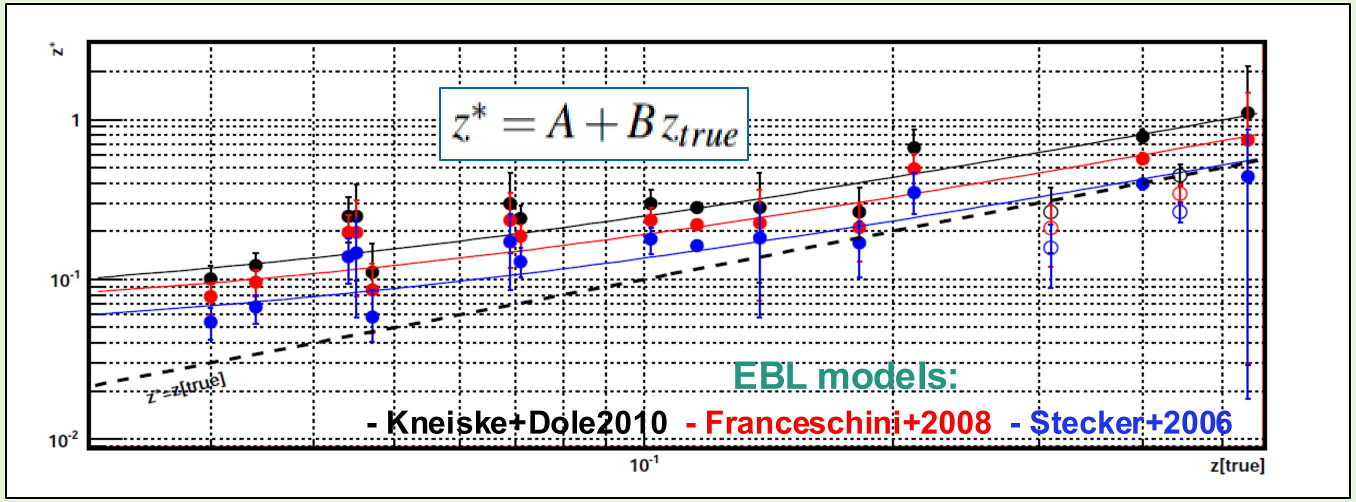

Exploited Instruments

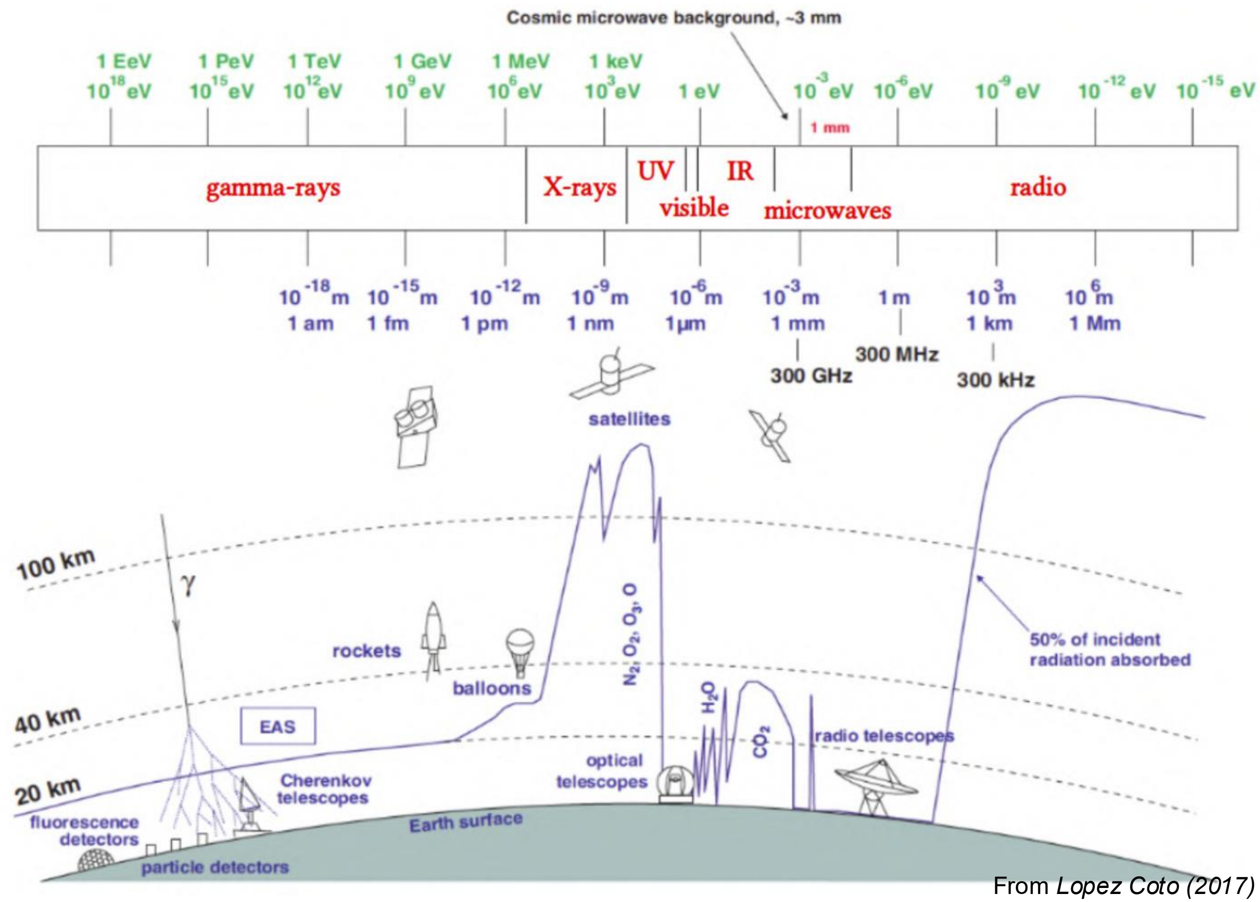

From *Lopez Coto (2017)*

Exploited Instruments

Fermi-LAT

HE γ–rays
≳ 30 MeV – 300 GeV
e^--e^+ pair production

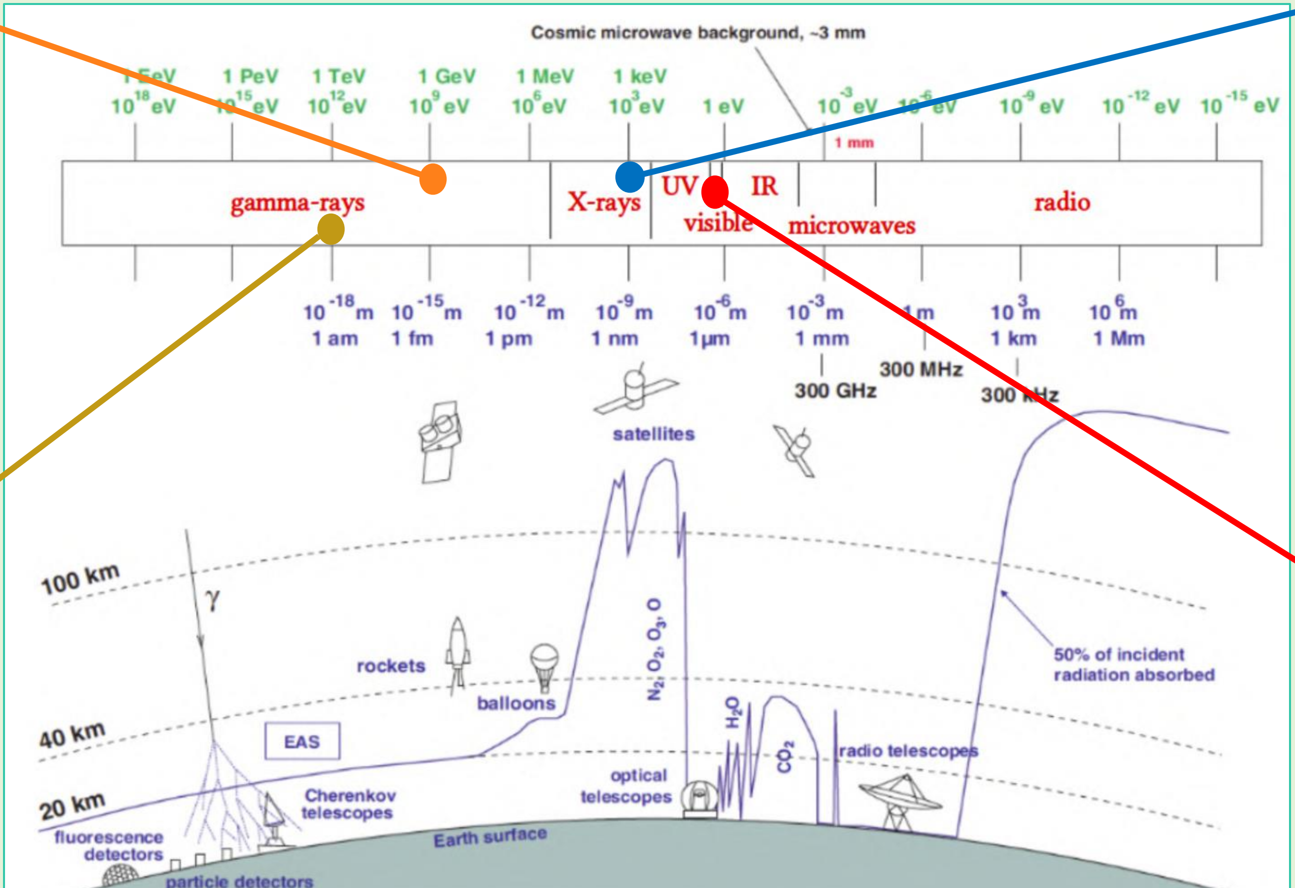

From *Lopez Coto (2017)*

MAGIC

VHE γ–rays
≈ 50 GeV – 50 TeV
EAS Cherenkov radiation

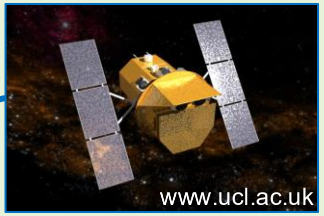

Swift-XRT

Soft *X*–rays
0.3 – 10 keV
Focused light collector

OSN

Optical R band
≈ 640.7 nm (J-C filter)
Photometry (+ polarimetry)

MAGIC

Major Atmospheric Gamma Imaging Cherenkov

- One of the currently active IACTs
- Located on La Palma (29° N, 18° W, Canary Islands, Spain), at ~ 2,200 m a.s.l.
- Two dishes of 17 m diameter, 85 m aside, each with ~ 250 mirrors of 1 m side (M1, M2 since 2004, 2009)
- Total area ≈ 236 m^2 , FoV ≈ 3.5°, angular resolution ≈ 0.1°

MAGIC

Major Atmospheric Gamma Imaging Cherenkov

- One of the currently active IACTs
- Located on La Palma (29° N, 18° W, Canary Islands, Spain), at ~ 2,200 m a.s.l.
- Two dishes of 17 m diameter, 85 m aside, each with ~ 250 mirrors of 1 m side (M1, M2 since 2004, 2009)
- Total area ≈ 236 m^2 , FoV ≈ 3.5°, angular resolution ≈ 0.1°

Aiming at indirectly detecting primary γ-rays in the ~ 30 GeV – 50 TeV range through the Cherenkov technique

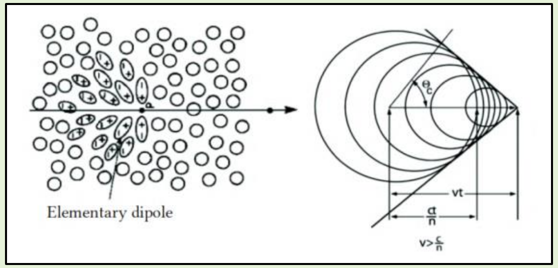

From *De Naurois & Mazin (2015)*

VHE photons revelation

Primary VHE γ-ray interacting with atmospheric nuclei (h ~ 10 km)

Cascade of generated e^--e^+ (pair production) and γ (bremsstrahlung)

Cherenkov pool (~ ns pulse) focused by M1 and M2 reflectors

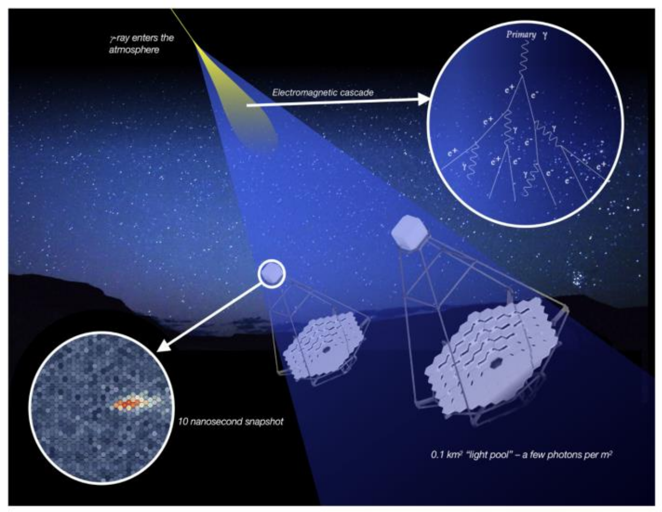

VHE photons revelation

Primary VHE γ-ray interacting with atmospheric nuclei (h ~ 10 km)

Cascade of generated e^--e^+ (pair production) and γ (bremsstrahlung)

Cherenkov pool (~ ns pulse) focused by M1 and M2 reflectors

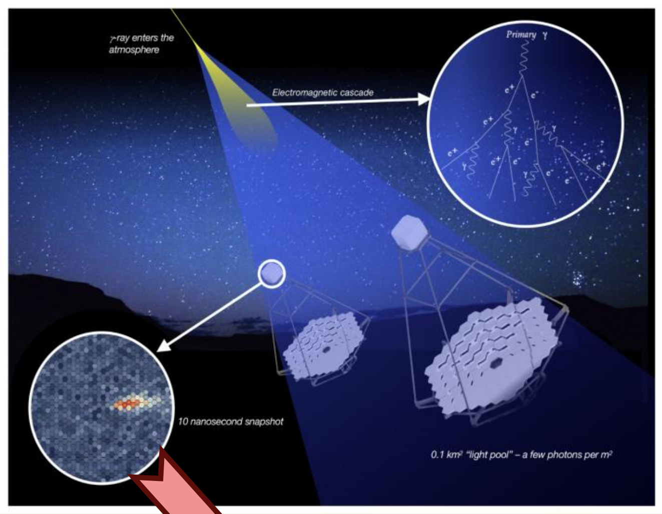

MAGIC Analysis and Reconstruction Software (MARS)

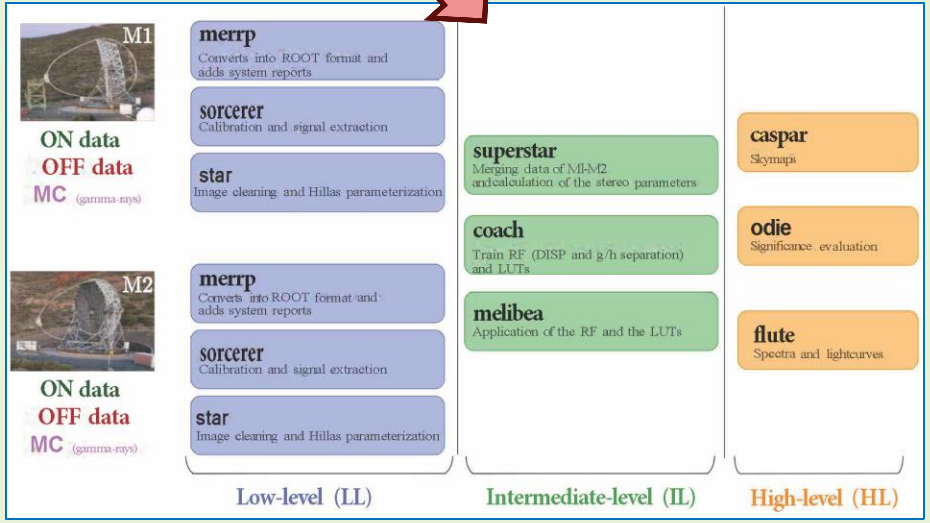

Fundamental quantities reconstructed:

Direction **Energy** **Hadronness**

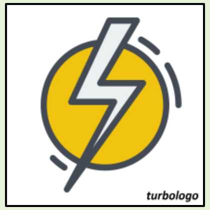

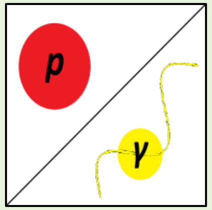

MAGIC signal

Reconstructed γ events versus θ^2

θ ⟹ angle from ON/OFF region centre

- **ON counts**
- **OFF counts**

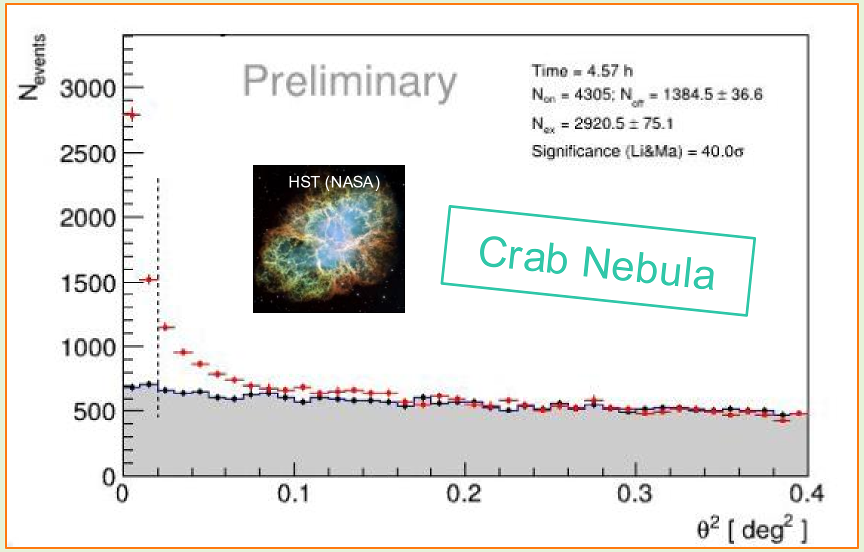

8th MAGIC SW School (Dr. C. Nigro)

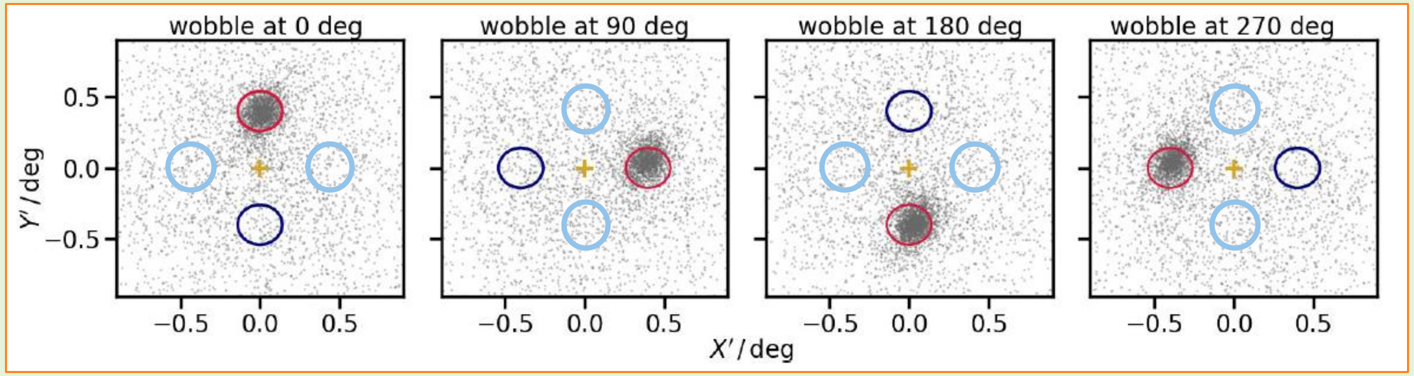

Actual pointing **ON region** **OFF region(s)**

MAGIC signal

ON counts

OFF counts

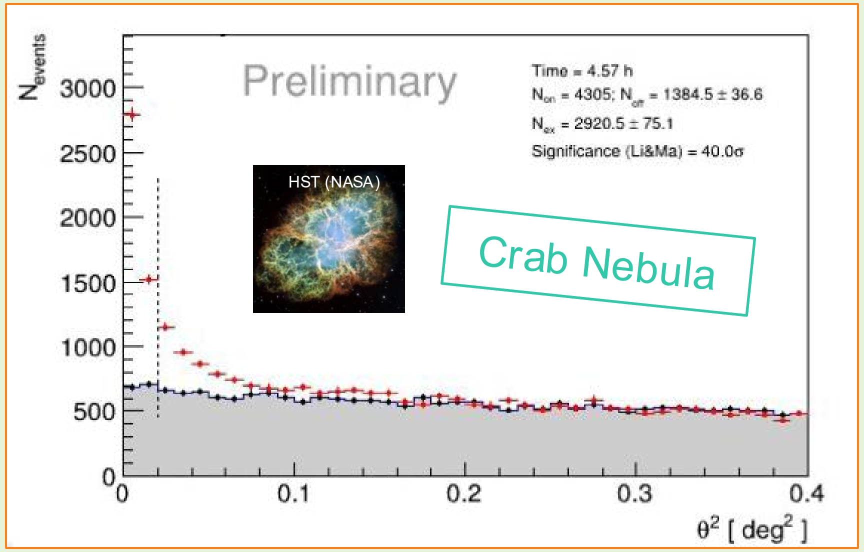

8th MAGIC SW School (Dr. C. Nigro)

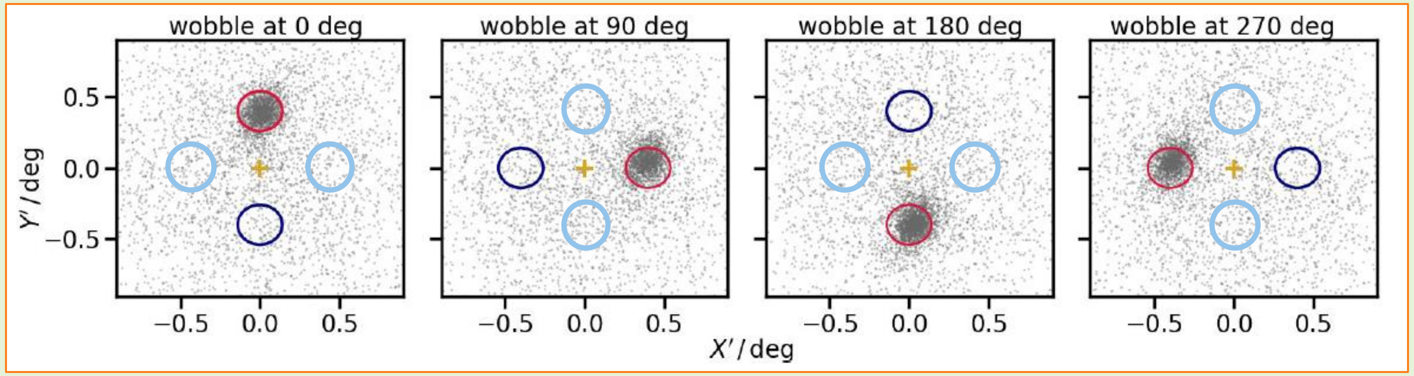

Actual pointing   ON region   OFF region(s)

Reconstructed γ events versus θ^2

θ ⟹ angle from ON/OFF region centre

Source Hypothesis Test:

H_0 (no γ emission) or H_1 (γ emission)?

$$\mathbb{S}_3 = \sqrt{2}\left\{N_{\rm on}\ln\left(\frac{1+\alpha}{\alpha}\frac{N_{\rm on}}{N_{\rm on}+N_{\rm off}}\right)+N_{\rm off}\ln\left[(1+\alpha)\frac{N_{\rm off}}{N_{\rm on}+N_{\rm off}}\right]\right\}^{1/2}$$

Signal significance (*Li & Ma 1983*)

MAGIC signal

- ON counts
- OFF counts

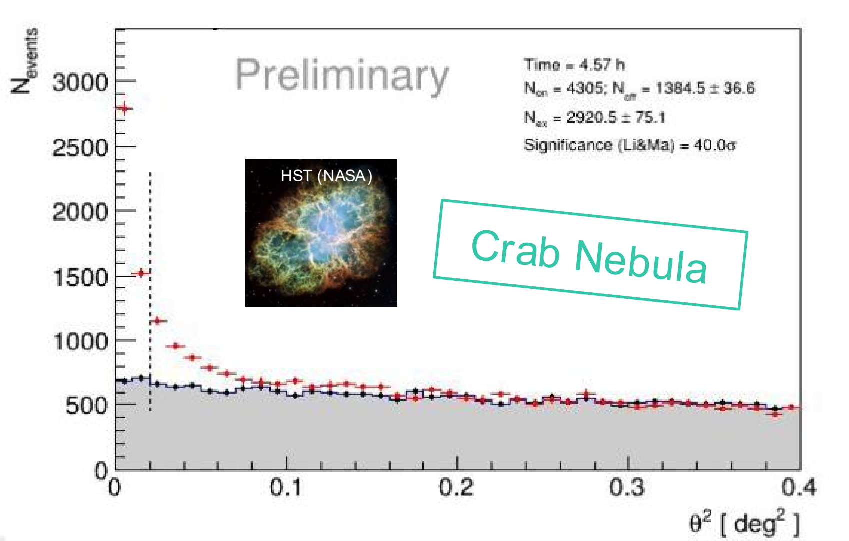

8th MAGIC SW School (Dr. C. Nigro)

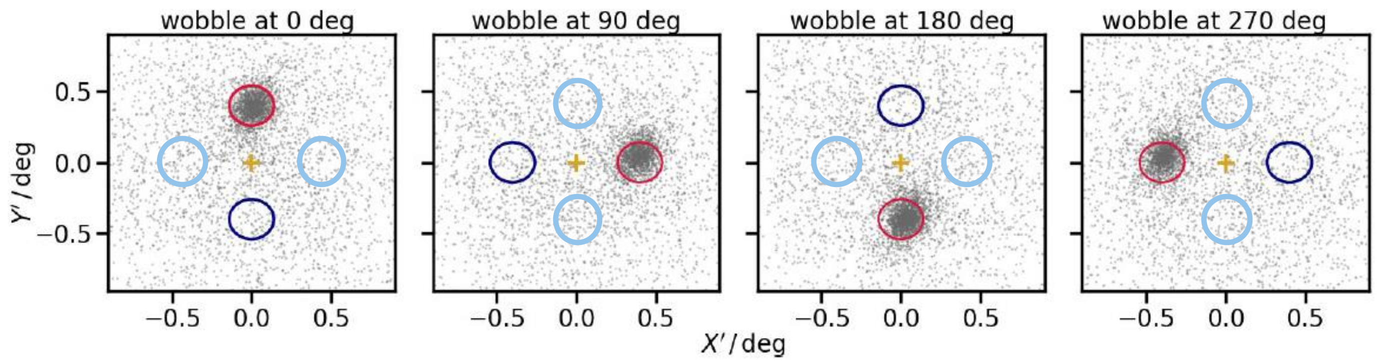

Actual pointing   ON region   OFF region(s)

Reconstructed γ events versus θ^2

θ ⇒ angle from ON/OFF region centre

Source Hypothesis Test:

H_0 (no γ emission) or H_1 (γ emission)?

$$\mathbb{S}_3 = \sqrt{2}\left\{N_{\rm on}\ln\left(\frac{1+\alpha}{\alpha}\frac{N_{\rm on}}{N_{\rm on}+N_{\rm off}}\right)+N_{\rm off}\ln\left[(1+\alpha)\frac{N_{\rm off}}{N_{\rm on}+N_{\rm off}}\right]\right\}^{1/2}$$

Signal significance (*Li & Ma 1983*)

Standard observation mode: ***Wobble***

Source & background events efficiently taken!

TON 116 by MAGIC (2021, 2022)

Zenith: 7°-36°; DTs: Dark Extragalactic; DCMax = 3000 nA; LIDAR@9km: > 0.7; Cloudiness: < 30; En. range: LE

2021 (~ 17.8/18.7 h)

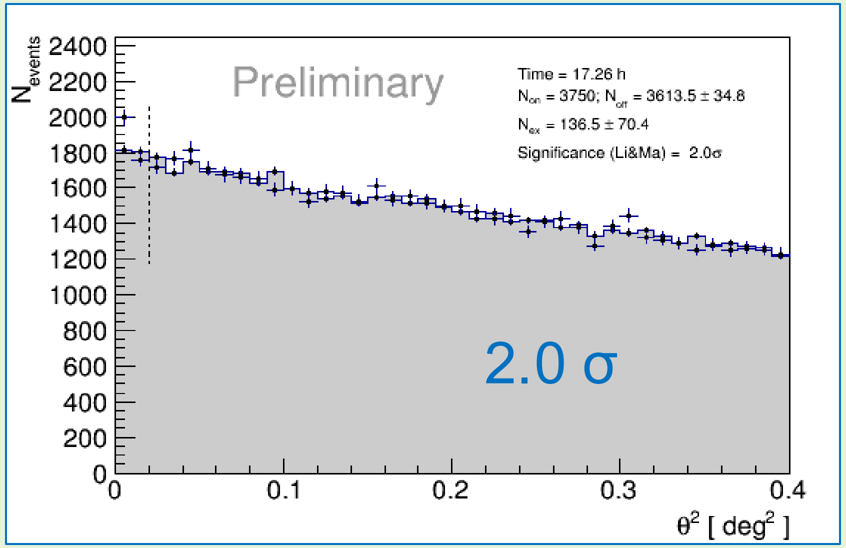

2022 (~ 7.0/8.0 h)

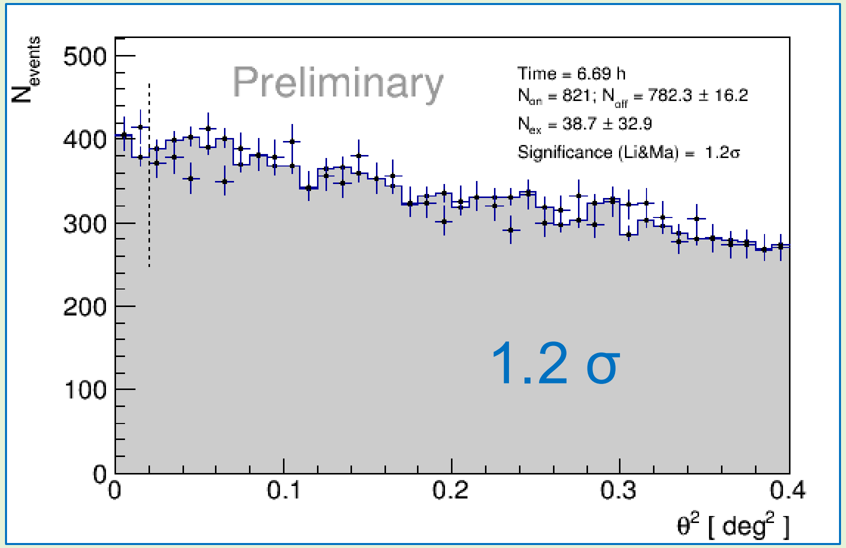

2021+2022 (~ 24.8/26.7 h)

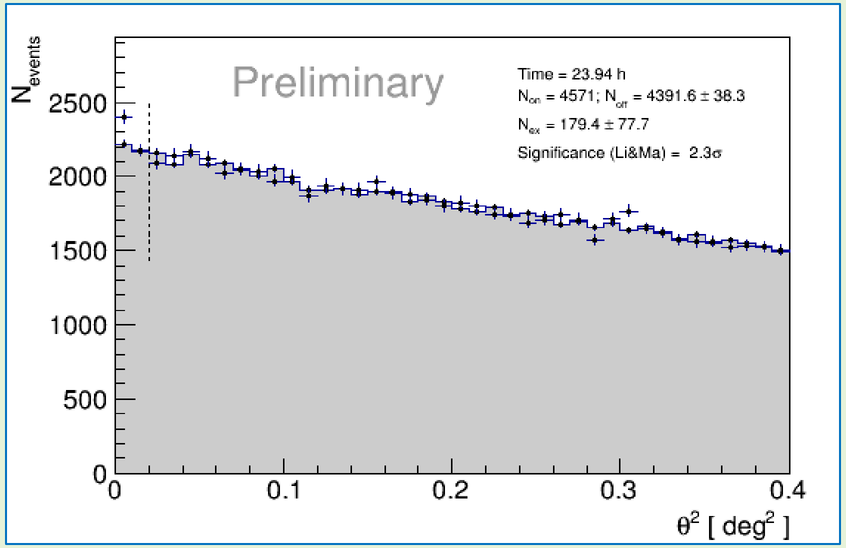

TON 116 by MAGIC (2021, 2022)

Zenith: 7°-36°; DTs: Dark Extragalactic; DCMax = 3000 nA; LIDAR@9km: > 0.7; Cloudiness: < 30; En. range: LE

2021 (~ 17.8/18.7 h)

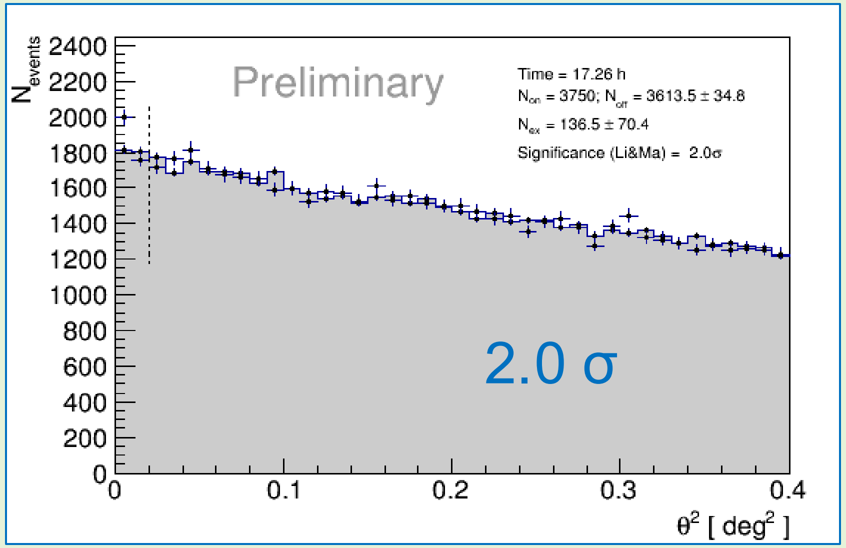

2022 (~ 7.0/8.0 h)

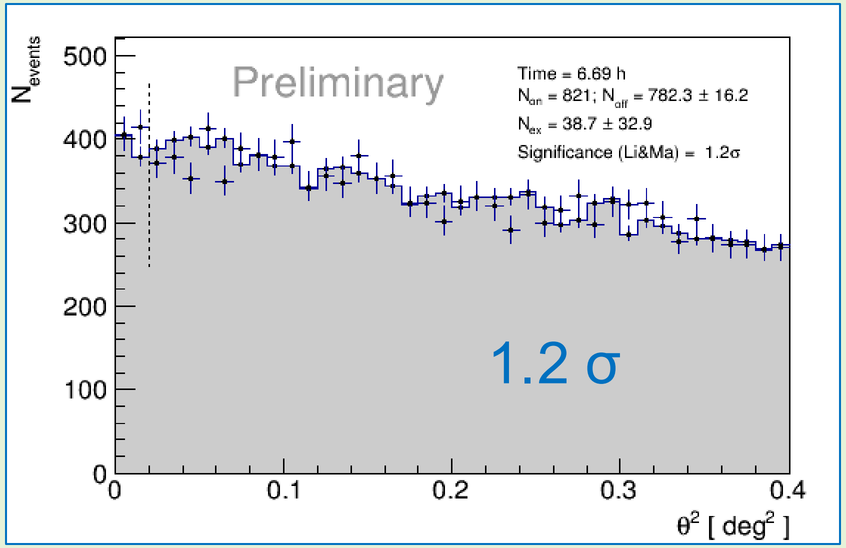

2021+2022 (~ 24.8/26.7 h)

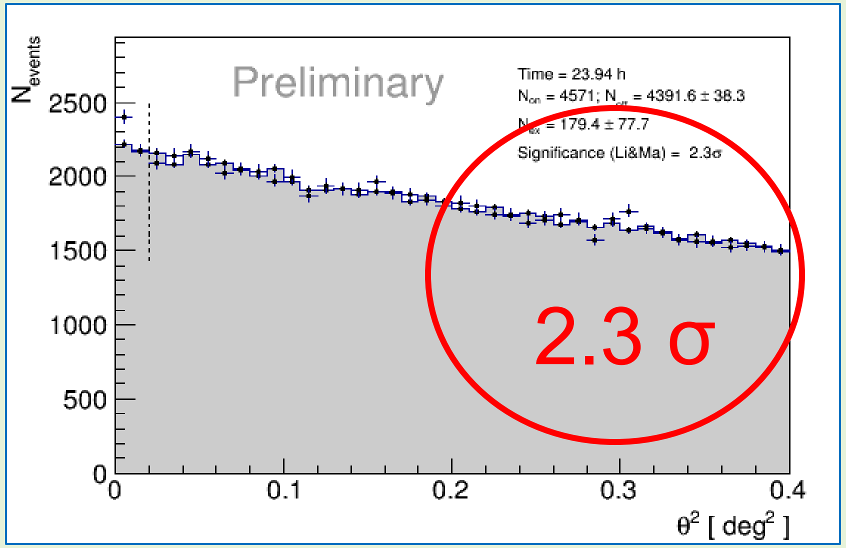

VHE excess hint

2021 (~ 18h, flute)

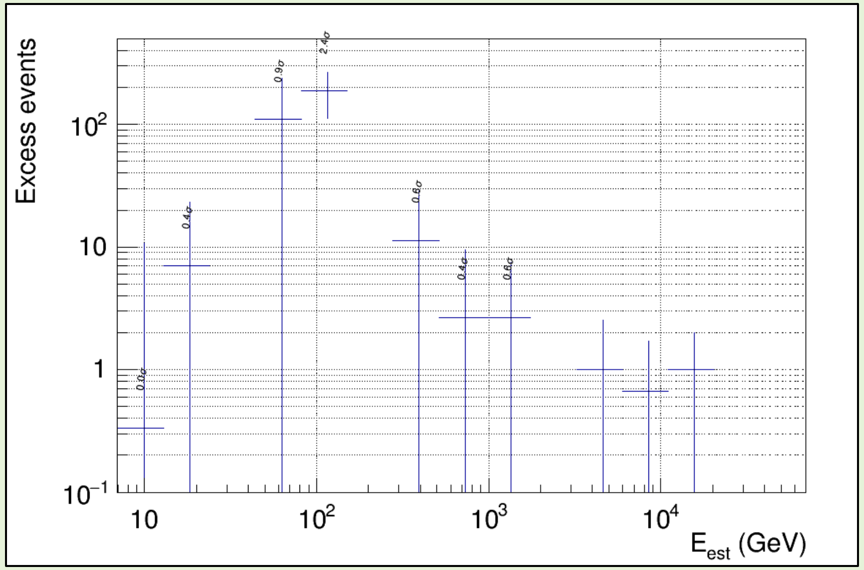

2021+2022 (~ 25h, foam)

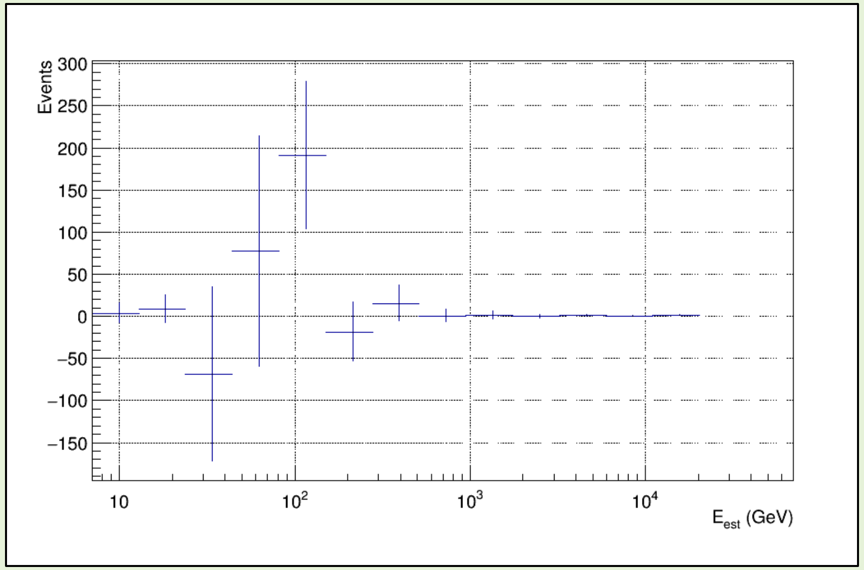

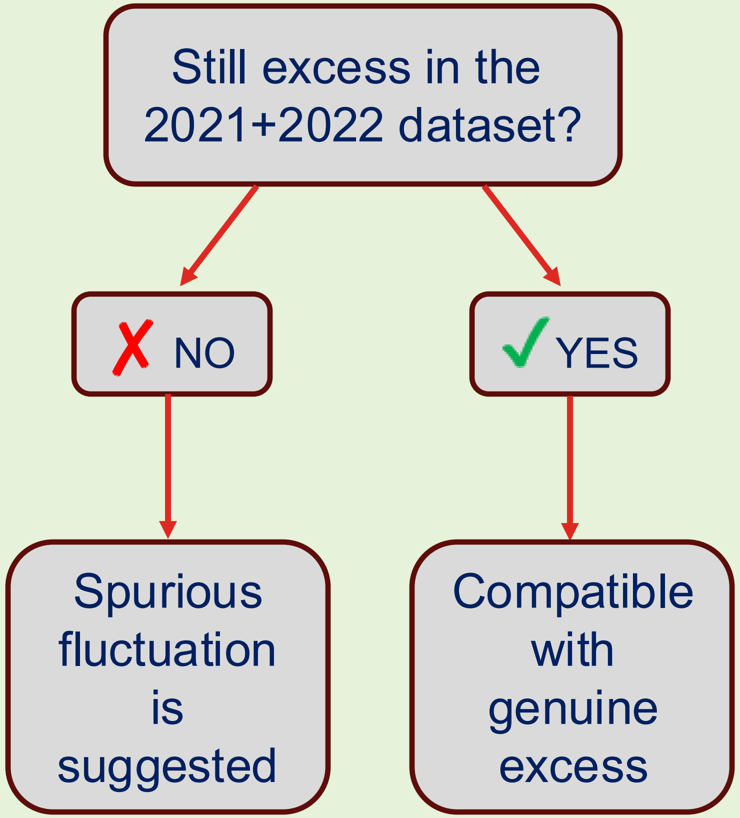

VHE excess hint

2021 (~ 18h, flute)

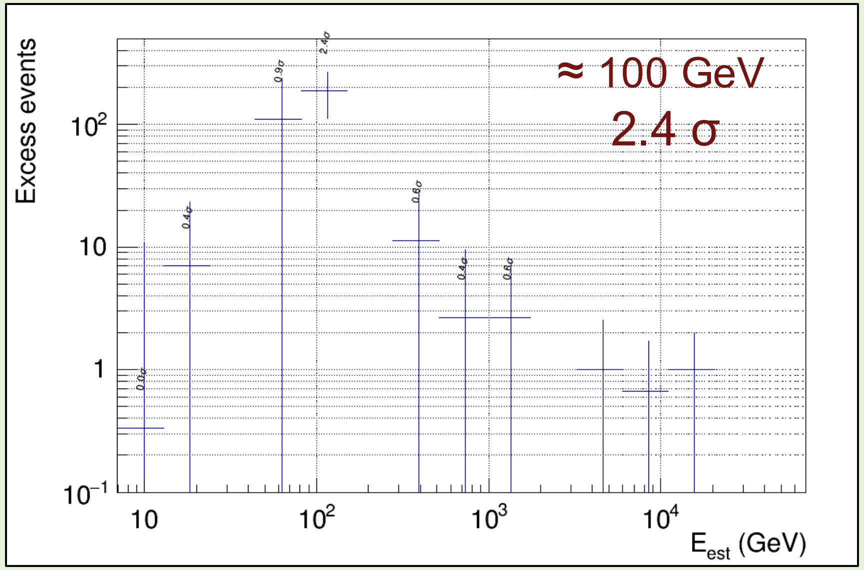

2021+2022 (~ 25h, foam)

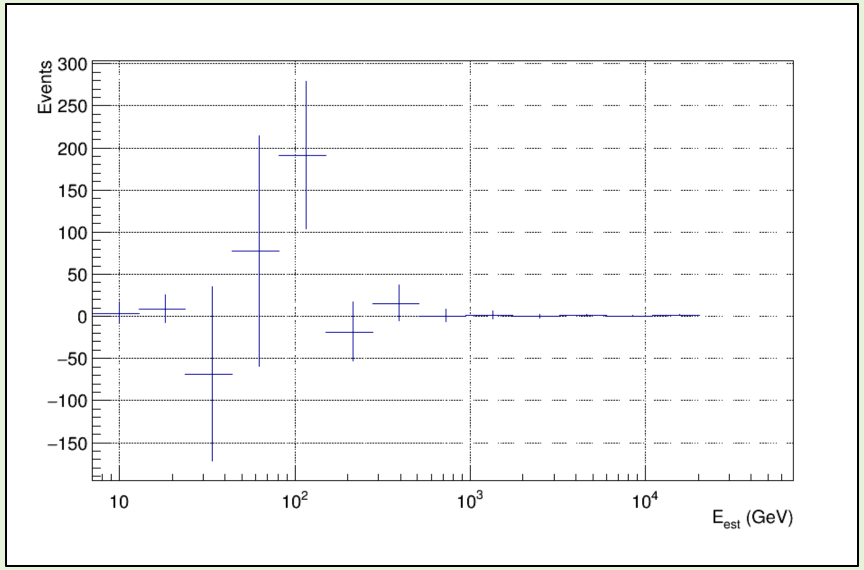

Still excess in the 2021+2022 dataset?

✗ NO → Spurious fluctuation is suggested

✓ YES → Compatible with genuine excess

VHE excess hint

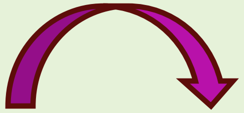

2021 (~ 18h, flute)

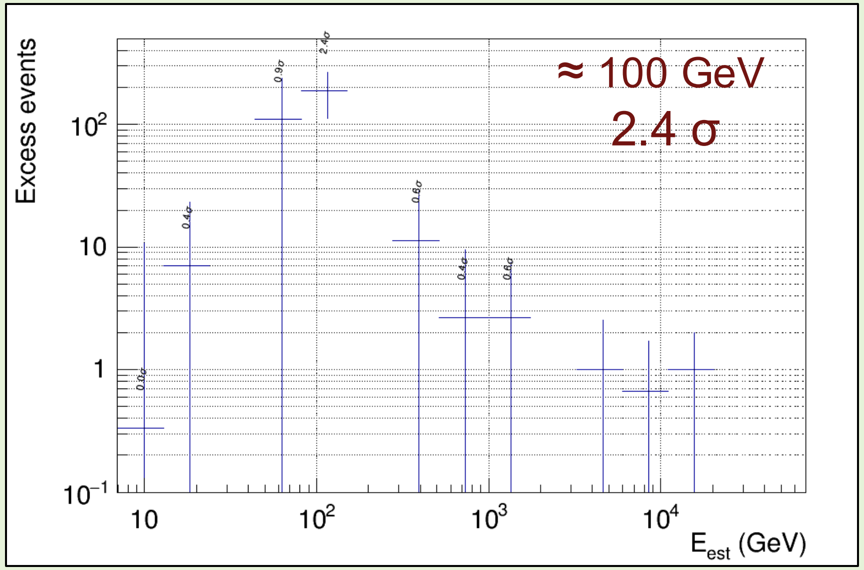

2021+2022 (~ 25h, foam)

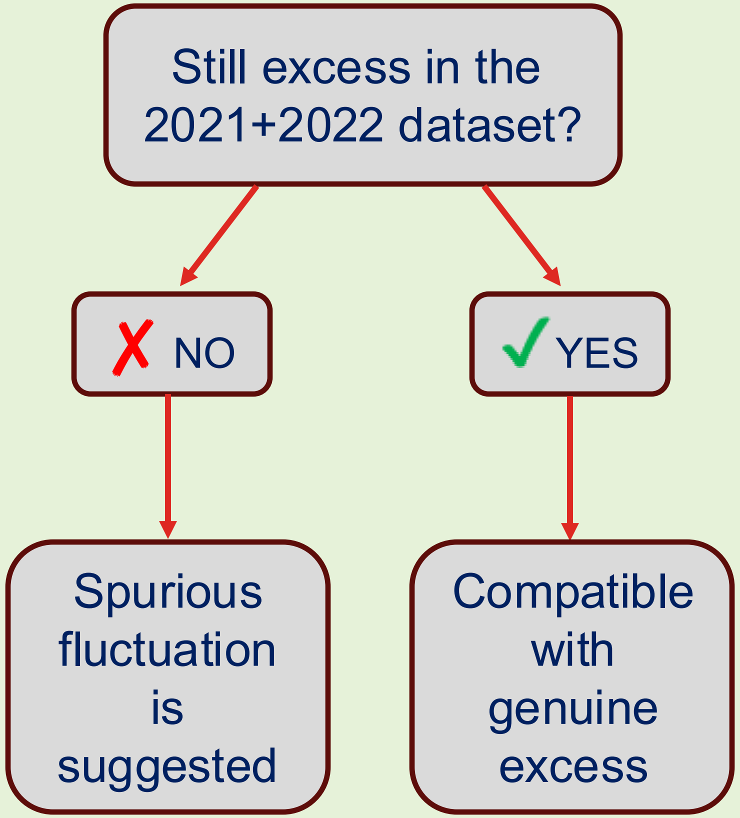

Dedicated odie execution
(standard/fitted ON & OFF distrib.):

$2.0\ \sigma \lesssim s \lesssim 2.6\ \sigma$

TON 116 by MAGIC (2023, total)

Zenith: 7°-36°; DTs: Dark Extragalactic; DCMax = 3000 nA; LIDAR@9km: > 0.7; Cloudiness: < 30; En. range: LE

2023
(~ 12.4/27.3 h)

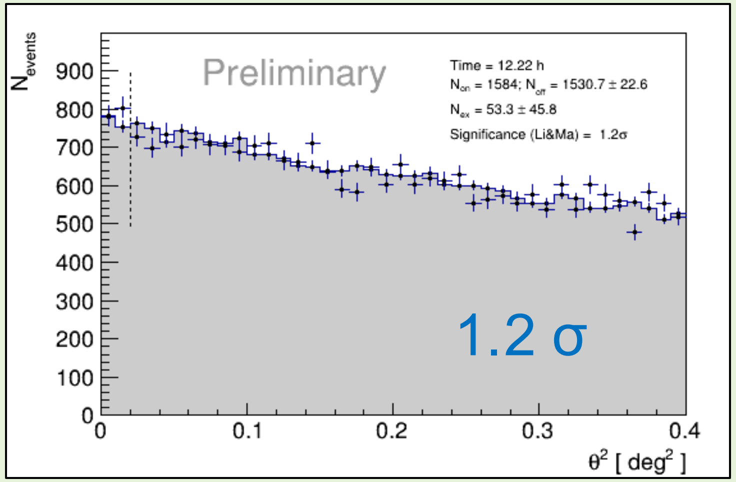

New proposal for 2023 (observational cycle 18)

- Worse weather conditions
- Atypical analysis settings required for ST.03.18 and ST.03.19 MC periods

≲ ½ time selected (from March on)

TON 116 by MAGIC (2023, total)

Zenith: 7°-36°; DTs: Dark Extragalactic; DCMax = 3000 nA; LIDAR@9km: > 0.7; Cloudiness: < 30; En. range: LE

2023
(~ 12.4/27.3 h)

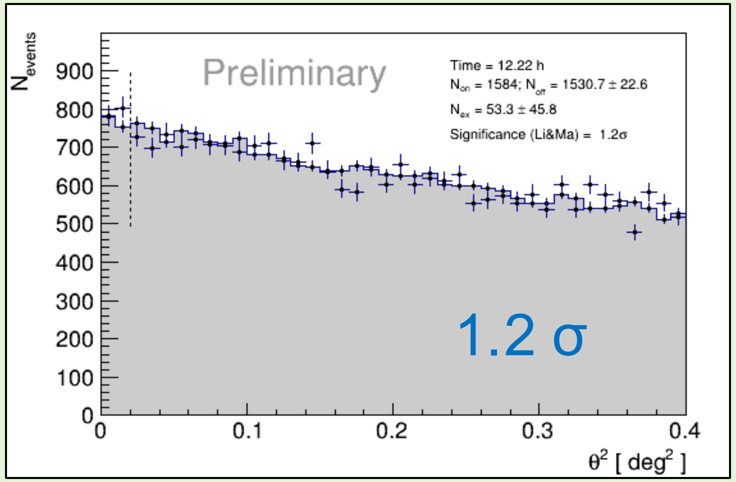

New proposal for 2023 (observational cycle 18)

- Worse weather conditions
- Atypical analysis settings required for ST.03.18 and ST.03.19 MC periods

≲ ½ time selected (from March on)

Odie results about joint 2021-2023 dataset:

t ~ 37 h, s = 2.2 σ

↓

still not enough for a signal...

No detection

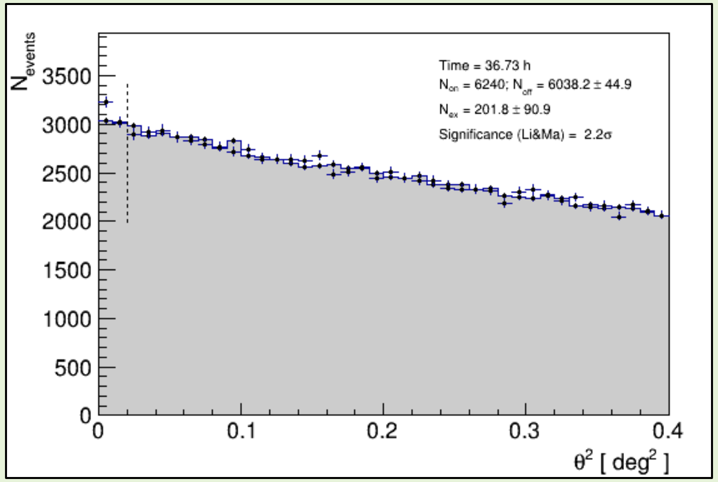

2021 + 2022 + 2023

MAGIC Flux of TON 116

N_{bin} (E_{est}) = 20; N_{bin} (Az) = 1; z = 0.5; LC E_{min}/binning = 100 GeV / night-wise; CL = 95%; EBL Model: Domìnguez+11

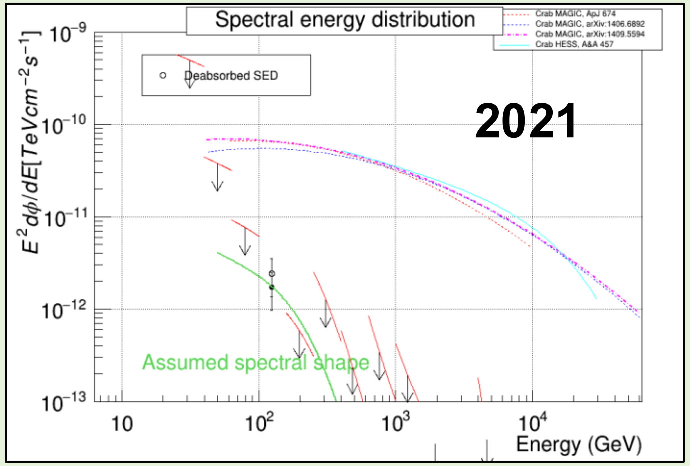

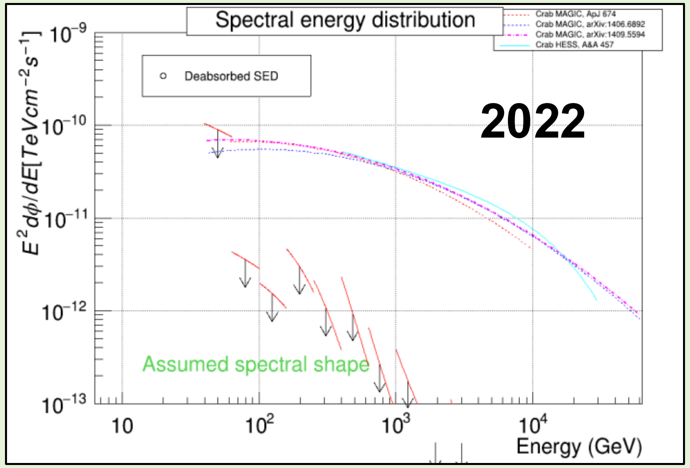

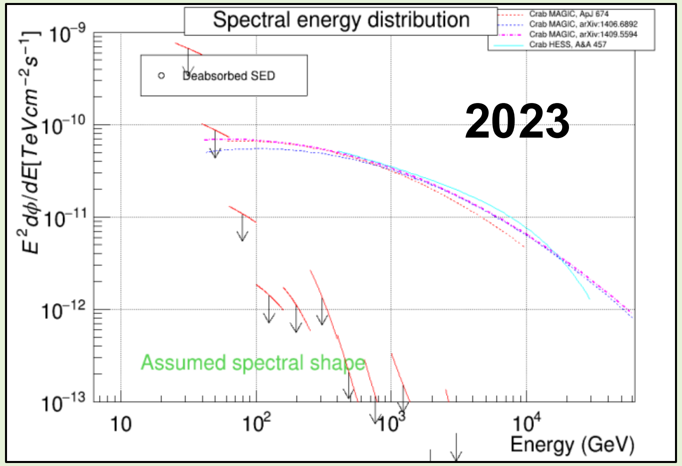

MAGIC Flux of TON 116

N_{bin} (E_{est}) = 20; N_{bin} (Az) = 1; z = 0.5; LC E_{min}/binning = 100 GeV / night-wise; CL = 95%; EBL Model: Domìnguez+11

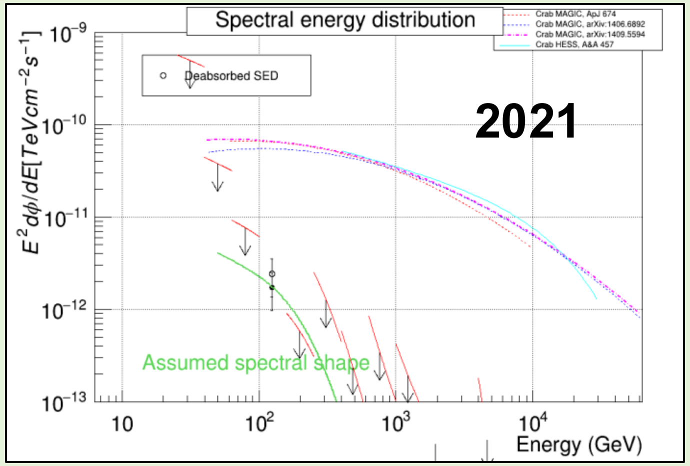

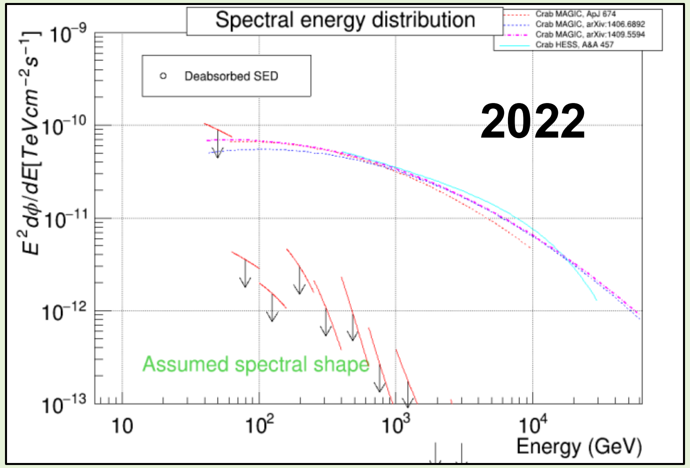

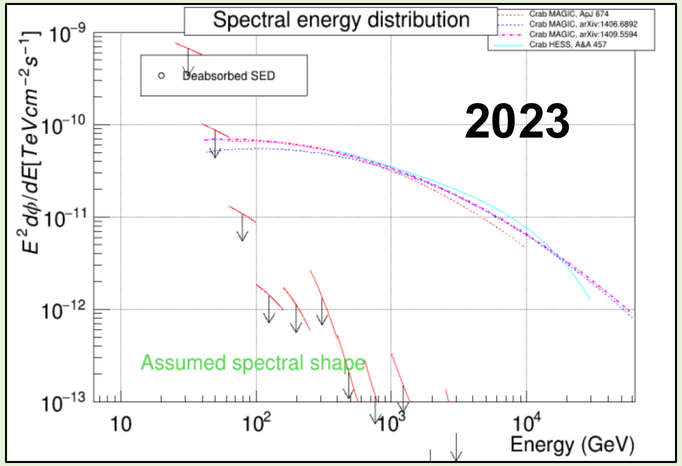

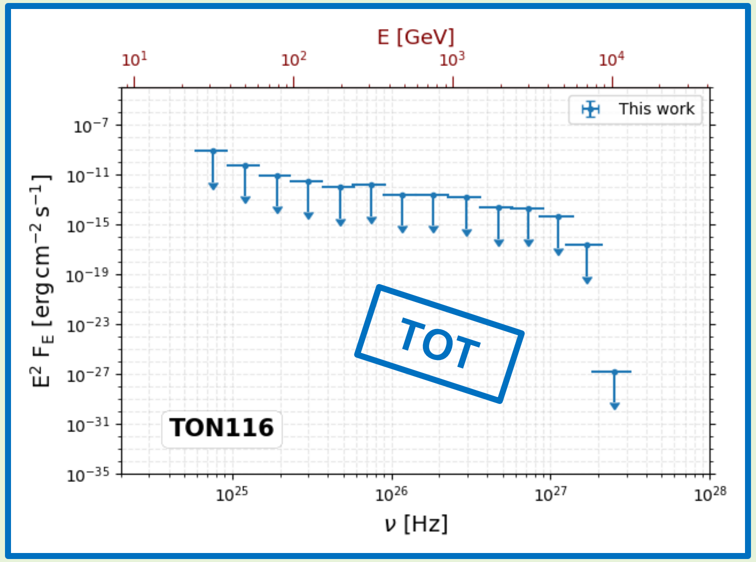

- ✓ **First unveiling of VHE side for the source ever!**
- ✓ No detection ⟹ upper limits (ULs)
- ✓ Constraint on the blue-tail of the Compton bump
- ✓ $E_{p,c} \lesssim$ 100 GeV and strong suppression before 1 TeV

TON 116 by Fermi-LAT

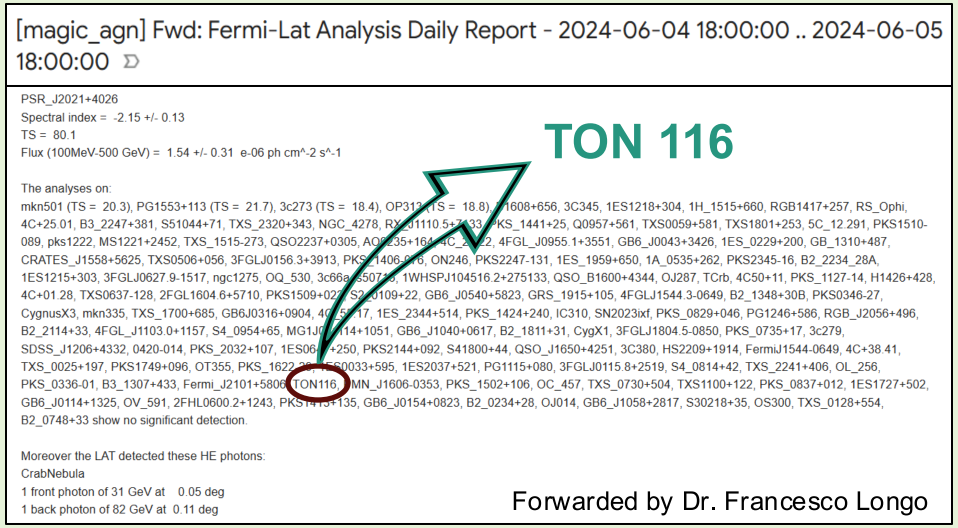

[magic_agn] Fwd: Fermi-Lat Analysis Daily Report - 2024-06-04 18:00:00 .. 2024-06-05 18:00:00

PSR_J2021+4026
Spectral index = -2.15 +/- 0.13
TS = 80.1
Flux (100MeV-500 GeV) = 1.54 +/- 0.31 e-06 ph cm^-2 s^-1

The analyses on:
mkn501 (TS = 20.3), PG1553+113 (TS = 21.7), 3c273 (TS = 18.4), OP313 (TS = 18.8), [illegible]1608+656, 3C345, 1ES1218+304, 1H_1515+660, RGB1417+257, RS_Ophi, 4C+25.01, B3_2247+381, S51044+71, TXS_2320+343, NGC_4278, RX_J1110.5+7[illegible]33, [illegible]PKS_1441+25, Q0957+561, TXS0059+581, TXS1801+253, 5C_12.291, PKS1510-089, pks1222, MS1221+2452, TXS_1515-273, QSO2237+0305, AO[illegible]235+164, 4C_2[illegible]2, 4FGL_J0955.1+3551, GB6_J0043+3426, 1ES_0229+200, GB_1310+487, CRATES_J1558+5625, TXS0506+056, 3FGLJ0156.3+3913, PKS_1406-[illegible]6, ON246, PKS2247-131, 1ES_1959+650, 1A_0535+262, PKS2345-16, B2_2234_28A, 1ES1215+303, 3FGLJ0627.9-1517, ngc1275, OQ_530, 3c66a, [illegible]s507[illegible], 1WHSPJ104516.2+275133, QSO_B1600+4344, OJ287, TCrb, 4C50+11, PKS_1127-14, H1426+428, 4C+01.28, TXS0637-128, 2FGL1604.6+5710, PKS1509+02[illegible], S2[illegible]0109+22, GB6_J0540+5823, GRS_1915+105, 4FGLJ1544.3-0649, B2_1348+30B, PKS0346-27, CygnusX3, mkn335, TXS_1700+685, GB6J0316+0904, 4C[illegible]5[illegible].17, 1ES_2344+514, PKS_1424+240, IC310, SN2023ixf, PKS_0829+046, PG1246+586, RGB_J2056+496, B2_2114+33, 4FGL_J1103.0+1157, S4_0954+65, MG1J0[illegible]114+1051, GB6_J1040+0617, B2_1811+31, CygX1, 3FGLJ1804.5-0850, PKS_0735+17, 3c279, SDSS_J1206+4332, 0420-014, PKS_2032+107, 1ES06[illegible]+250, PKS2144+092, S41800+44, QSO_J1650+4251, 3C380, HS2209+1914, FermiJ1544-0649, 4C+38.41, TXS_0025+197, PKS1749+096, OT355, PKS_1622[illegible], [illegible]S0033+595, 1ES2037+521, PG1115+080, 3FGLJ0115.8+2519, S4_0814+42, TXS_2241+406, OL_256, PKS_0336-01, B3_1307+433, Fermi_J2101+5806, TON116, [illegible]MN_J1606-0353, PKS_1502+106, OC_457, TXS_0730+504, TXS1100+122, PKS_0837+012, 1ES1727+502, GB6_J0114+1325, OV_591, 2FHL0600.2+1243, PKS[illegible]+135, GB6_J0154+0823, B2_0234+28, OJ014, GB6_J1058+2817, S30218+35, OS300, TXS_0128+554, B2_0748+33 show no significant detection.

Moreover the LAT detected these HE photons:
CrabNebula
1 front photon of 31 GeV at 0.05 deg
1 back photon of 82 GeV at 0.11 deg

- Monitoring since ~ satellite launch (HE emitter + TeV candidate)
- Enhanced HE (4LAC, *Ajello et al. 2020*) => MAGIC proposals
- 2022

TON 116 by Fermi-LAT

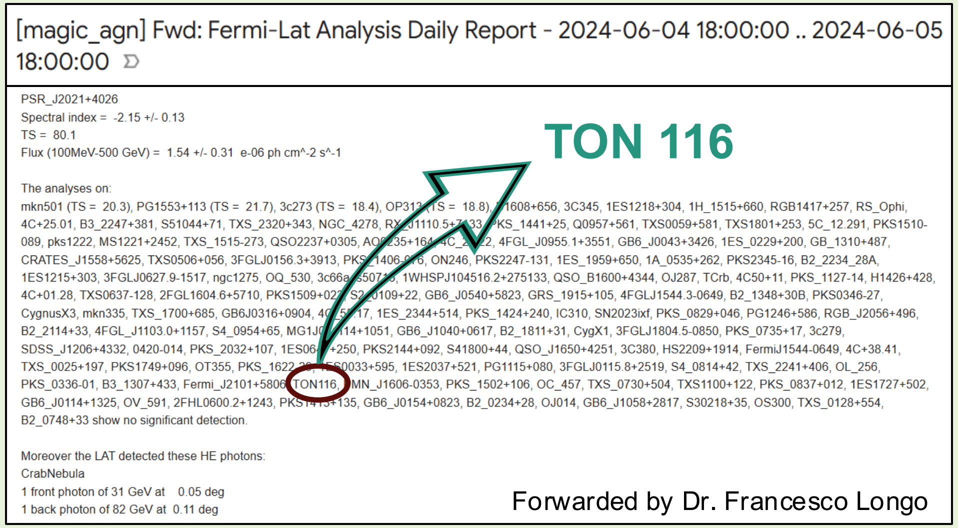
[magic_agn] Fwd: Fermi-Lat Analysis Daily Report - 2024-06-04 18:00:00 .. 2024-06-05 18:00:00

PSR_J2021+4026
Spectral index = -2.15 +/- 0.13
TS = 80.1
Flux (100MeV-500 GeV) = 1.54 +/- 0.31 e-06 ph cm^-2 s^-1

The analyses on:
mkn501 (TS = 20.3), PG1553+113 (TS = 21.7), 3c273 (TS = 18.4), OP31[illegible] (TS = 18.8), [illegible]1608+656, 3C345, 1ES1218+304, 1H_1515+660, RGB1417+257, RS_Ophi, 4C+25.01, B3_2247+381, S51044+71, TXS_2320+343, NGC_4278, RX[illegible]J1110.5+[illegible]33, [illegible]KS_1441+25, Q0957+561, TXS0059+581, TXS1801+253, 5C_12.291, PKS1510-089, pks1222, MS1221+2452, TXS_1515-273, QSO2237+0305, AO[illegible]235+164, 4C_[illegible]2, 4FGL_J0955.1+3551, GB6_J0043+3426, 1ES_0229+200, GB_1310+487, CRATES_J1558+5625, TXS0506+056, 3FGLJ0156.3+3913, PKS[illegible]1406-[illegible]6, ON246, PKS2247-131, 1ES_1959+650, 1A_0535+262, PKS2345-16, B2_2234_28A, 1ES1215+303, 3FGLJ0627.9-1517, ngc1275, OQ_530, 3c66a, [illegible]s507[illegible], 1WHSPJ104516.2+275133, QSO_B1600+4344, OJ287, TCrb, 4C50+11, PKS_1127-14, H1426+428, 4C+01.28, TXS0637-128, 2FGL1604.6+5710, PKS1509+02[illegible], S2[illegible]0109+22, GB6_J0540+5823, GRS_1915+105, 4FGLJ1544.3-0649, B2_1348+30B, PKS0346-27, CygnusX3, mkn335, TXS_1700+685, GB6J0316+0904, 4C[illegible]55.17, 1ES_2344+514, PKS_1424+240, IC310, SN2023ixf, PKS_0829+046, PG1246+586, RGB_J2056+496, B2_2114+33, 4FGL_J1103.0+1157, S4_0954+65, MG1J0[illegible]14+1051, GB6_J1040+0617, B2_1811+31, CygX1, 3FGLJ1804.5-0850, PKS_0735+17, 3c279, SDSS_J1206+4332, 0420-014, PKS_2032+107, 1ES06[illegible]+250, PKS2144+092, S41800+44, QSO_J1650+4251, 3C380, HS2209+1914, FermiJ1544-0649, 4C+38.41, TXS_0025+197, PKS1749+096, OT355, PKS_1622[illegible], [illegible]S0033+595, 1ES2037+521, PG1115+080, 3FGLJ0115.8+2519, S4_0814+42, TXS_2241+406, OL_256, PKS_0336-01, B3_1307+433, Fermi_J2101+5806, TON116, [illegible]MN_J1606-0353, PKS_1502+106, OC_457, TXS_0730+504, TXS1100+122, PKS_0837+012, 1ES1727+502, GB6_J0114+1325, OV_591, 2FHL0600.2+1243, PKS[illegible]+135, GB6_J0154+0823, B2_0234+28, OJ014, GB6_J1058+2817, S30218+35, OS300, TXS_0128+554, B2_0748+33 show no significant detection.

Moreover the LAT detected these HE photons:
CrabNebula
1 front photon of 31 GeV at 0.05 deg
1 back photon of 82 GeV at 0.11 deg

- Monitoring since ~ satellite launch (HE emitter + TeV candidate)
- Enhanced HE (4LAC, *Ajello et al. 2020*) => MAGIC proposals
- 2022 → $\Gamma \approx 1.75$, $F_{1GeV} \approx 1.64$ MeV cm^{-2} s^{-1}, $E_{p,c} \approx 70$ GeV (*very fast analysis*)

  → LogParabola (LP) spectrum (4FGL, *Abdollahi et al. 2022*)

TON 116 by Fermi-LAT

[magic_agn] Fwd: Fermi-Lat Analysis Daily Report - 2024-06-04 18:00:00 .. 2024-06-05 18:00:00

PSR_J2021+4026
Spectral index = -2.15 +/- 0.13
TS = 80.1
Flux (100MeV-500 GeV) = 1.54 +/- 0.31 e-06 ph cm^-2 s^-1

The analyses on:
mkn501 (TS = 20.3), PG1553+113 (TS = 21.7), 3c273 (TS = 18.4), OP313 (TS = 18.8), 1608+656, 3C345, 1ES1218+304, 1H_1515+660, RGB1417+257, RS_Ophi, 4C+25.01, B3_2247+381, S51044+71, TXS_2320+343, NGC_4278, RX_J1110.5+7133, PKS_1441+25, Q0957+561, TXS0059+581, TXS1801+253, 5C_12.291, PKS1510-089, pks1222, MS1221+2452, TXS_1515-273, QSO2237+0305, AO0235+164, 4C_2122, 4FGL_J0955.1+3551, GB6_J0043+3426, 1ES_0229+200, GB_1310+487, CRATES_J1558+5625, TXS0506+056, 3FGLJ0156.3+3913, PKS_1406-076, ON246, PKS2247-131, 1ES_1959+650, 1A_0535+262, PKS2345-16, B2_2234_28A, 1ES1215+303, 3FGLJ0627.9-1517, ngc1275, OQ_530, 3c66a, s50716, 1WHSPJ104516.2+275133, QSO_B1600+4344, OJ287, TCrb, 4C50+11, PKS_1127-14, H1426+428, 4C+01.28, TXS0637-128, 2FGL1604.6+5710, PKS1509+022, S2_0109+22, GB6_J0540+5823, GRS_1915+105, 4FGLJ1544.3-0649, B2_1348+30B, PKS0346-27, CygnusX3, mkn335, TXS_1700+685, GB6J0316+0904, 4C_55.17, 1ES_2344+514, PKS_1424+240, IC310, SN2023ixf, PKS_0829+046, PG1246+586, RGB_J2056+496, B2_2114+33, 4FGL_J1103.0+1157, S4_0954+65, MG1J0114+1051, GB6_J1040+0617, B2_1811+31, CygX1, 3FGLJ1804.5-0850, PKS_0735+17, 3c279, SDSS_J1206+4332, 0420-014, PKS_2032+107, 1ES0647+250, PKS2144+092, S41800+44, QSO_J1650+4251, 3C380, HS2209+1914, FermiJ1544-0649, 4C+38.41, TXS_0025+197, PKS1749+096, OT355, PKS_1622-29, 1ES0033+595, 1ES2037+521, PG1115+080, 3FGLJ0115.8+2519, S4_0814+42, TXS_2241+406, OL_256, PKS_0336-01, B3_1307+433, Fermi_J2101+5806, TON116, PMN_J1606-0353, PKS_1502+106, OC_457, TXS_0730+504, TXS1100+122, PKS_0837+012, 1ES1727+502, GB6_J0114+1325, OV_591, 2FHL0600.2+1243, PKS1413+135, GB6_J0154+0823, B2_0234+28, OJ014, GB6_J1058+2817, S30218+35, OS300, TXS_0128+554, B2_0748+33 show no significant detection.

Moreover the LAT detected these HE photons:
CrabNebula
1 front photon of 31 GeV at 0.05 deg
1 back photon of 82 GeV at 0.11 deg

TON 116

Forwarded by Dr. Francesco Longo

- Monitoring since ~ satellite launch (HE emitter + TeV candidate)
- Enhanced HE (4LAC, *Ajello et al. 2020*) => MAGIC proposals
- 2022 → $\Gamma \approx 1.75$, $F_{1GeV} \approx 1.64$ MeV $cm^{-2}\,s^{-1}$, $E_{p,c} \approx 70$ GeV (*very fast analysis*)

→ LogParabola (LP) spectrum (4FGL, *Abdollahi et al. 2022*)

Taken advantage of long observation history of the source

2008-2023 (15-year) period | 2021-2023 (MAGIC) period

TON 116 by Fermi-LAT (2008-2023)

E range: 300 MeV – 500 GeV; N_{bin} /decade: 10; RoI/bin width: 10°/0.1°; Zenith cuts: standard;
Event class/type: 128 (point-like) / 3 (front+back); Models: isotropic, gal. diffuse, 4FGL-DR3; Likelihood zone: 15°

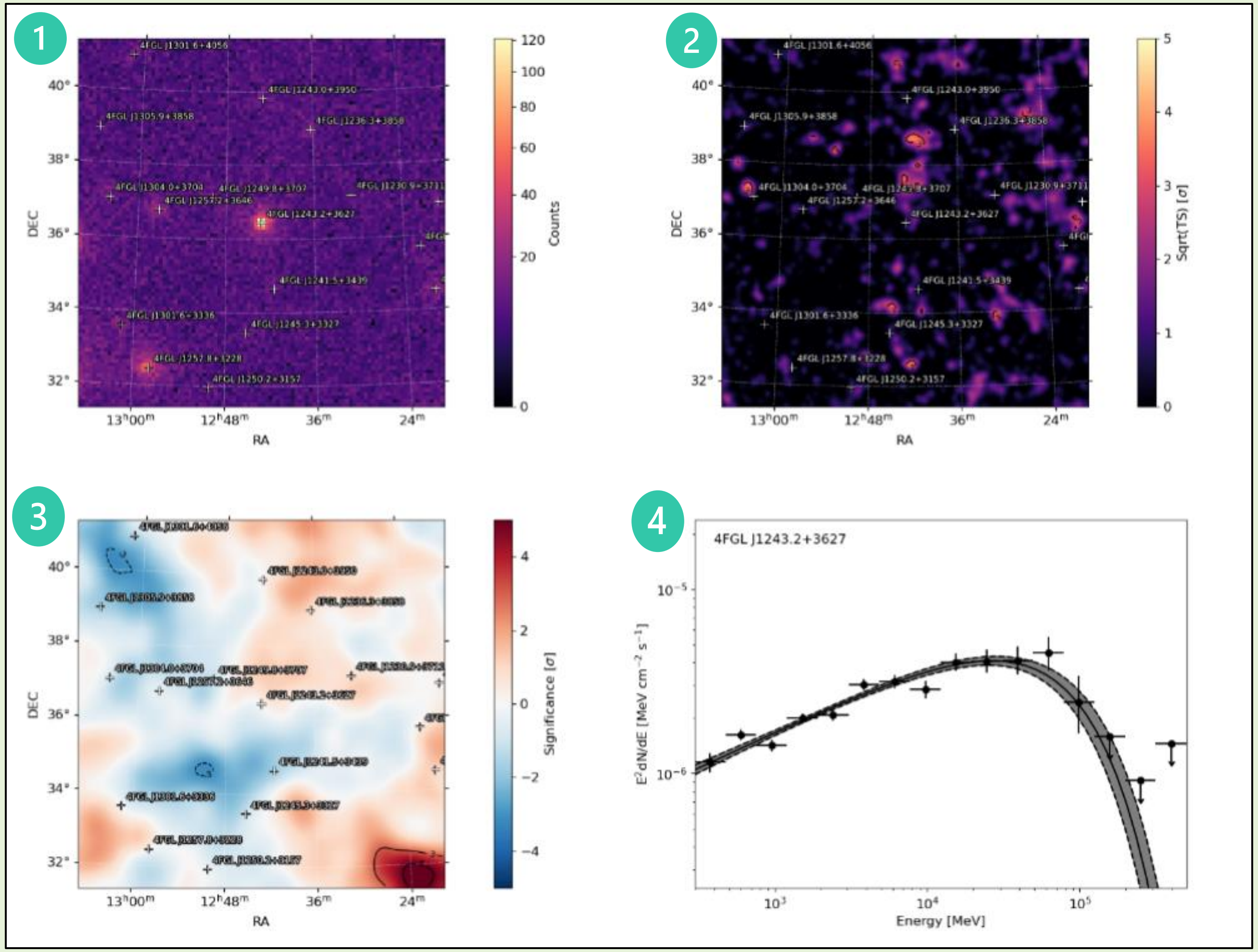

1 Counts' map
2 TS map
3 Residuals' map
4 Fitted SED

TON 116 by Fermi-LAT (2008-2023)

E range: 300 MeV – 500 GeV; N_{bin} /decade: 10; RoI/bin width: 10°/0.1°; Zenith cuts: standard;
Event class/type: 128 (point-like) / 3 (front+back); Models: isotropic, gal. diffuse, 4FGL-DR3; Likelihood zone: 15°

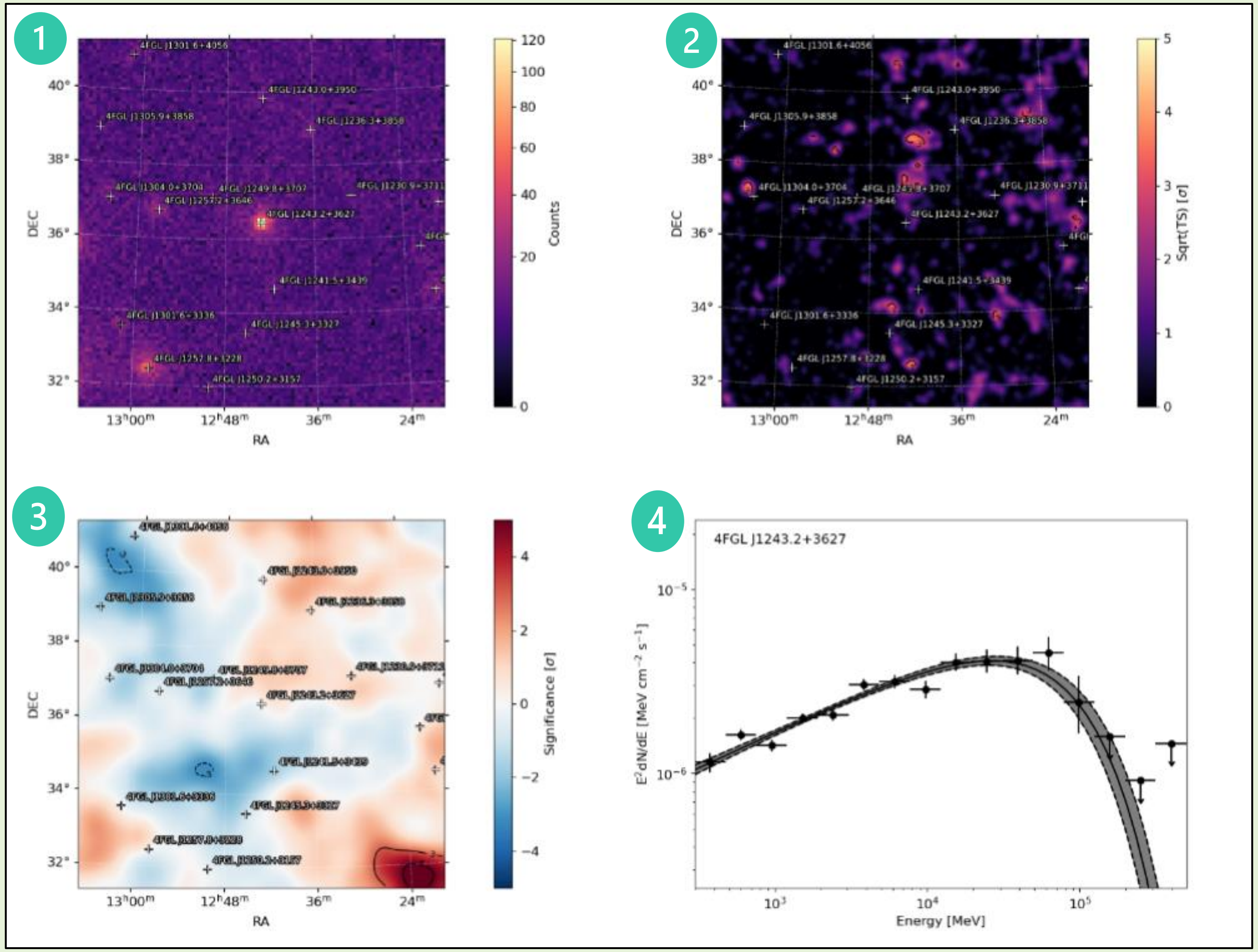

1 Counts' map
2 TS map
3 Residuals' map
4 Fitted SED

Best-fit model for spectral dataset:

~~**Power-law (PL)**~~ ~~**Log-parabola (LP)**~~

Power-law with exponential cut-off **(PLEC)**

$$\frac{dN}{dE} = N_0 \cdot \left(\frac{E}{10^3\ \mathrm{MeV}}\right)^{-\gamma} \cdot \exp[-(E - E_b)/p_1]$$

Through $\mathbf{TS_{curvature}}$ **test**

TON 116 by Fermi-LAT (2021-2023)

E range: 300 MeV – 500 GeV; N_{bin} /decade: 10; RoI/bin width: 10°/0.1°; Zenith cuts: standard;
Event class/type: 128 (point-like) / 3 (front+back); Models: isotropic, gal. diffuse, 4FGL-DR3; Likelihood zone: 15°

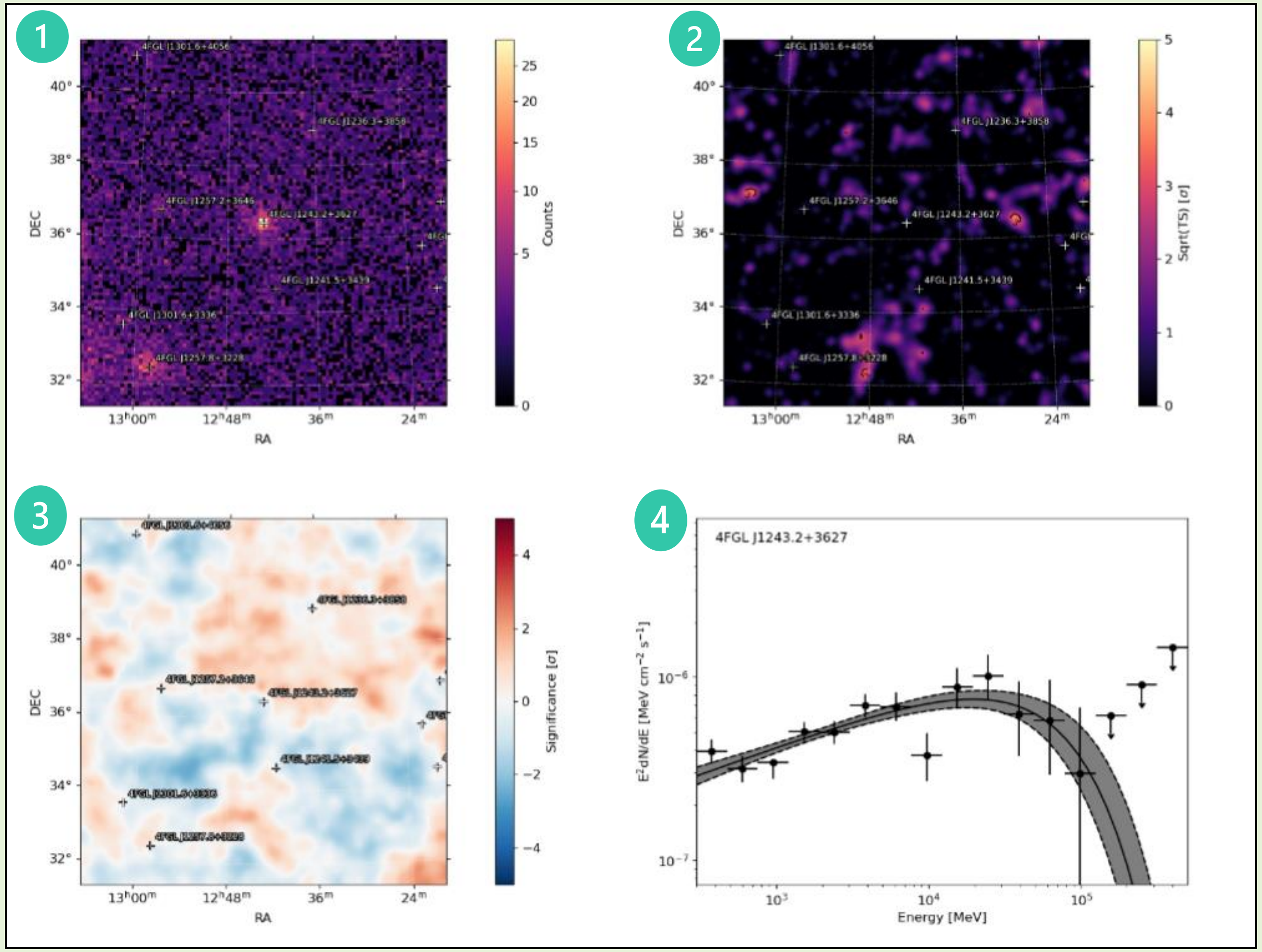

1 Counts' map
2 TS map
3 Residuals' map
4 Fitted SED

TON 116 by Fermi-LAT (2021-2023)

E range: 300 MeV – 500 GeV; N_{bin} /decade: 10; RoI/bin width: 10°/0.1°; Zenith cuts: standard;
Event class/type: 128 (point-like) / 3 (front+back); Models: isotropic, gal. diffuse, 4FGL-DR3; Likelihood zone: 15°

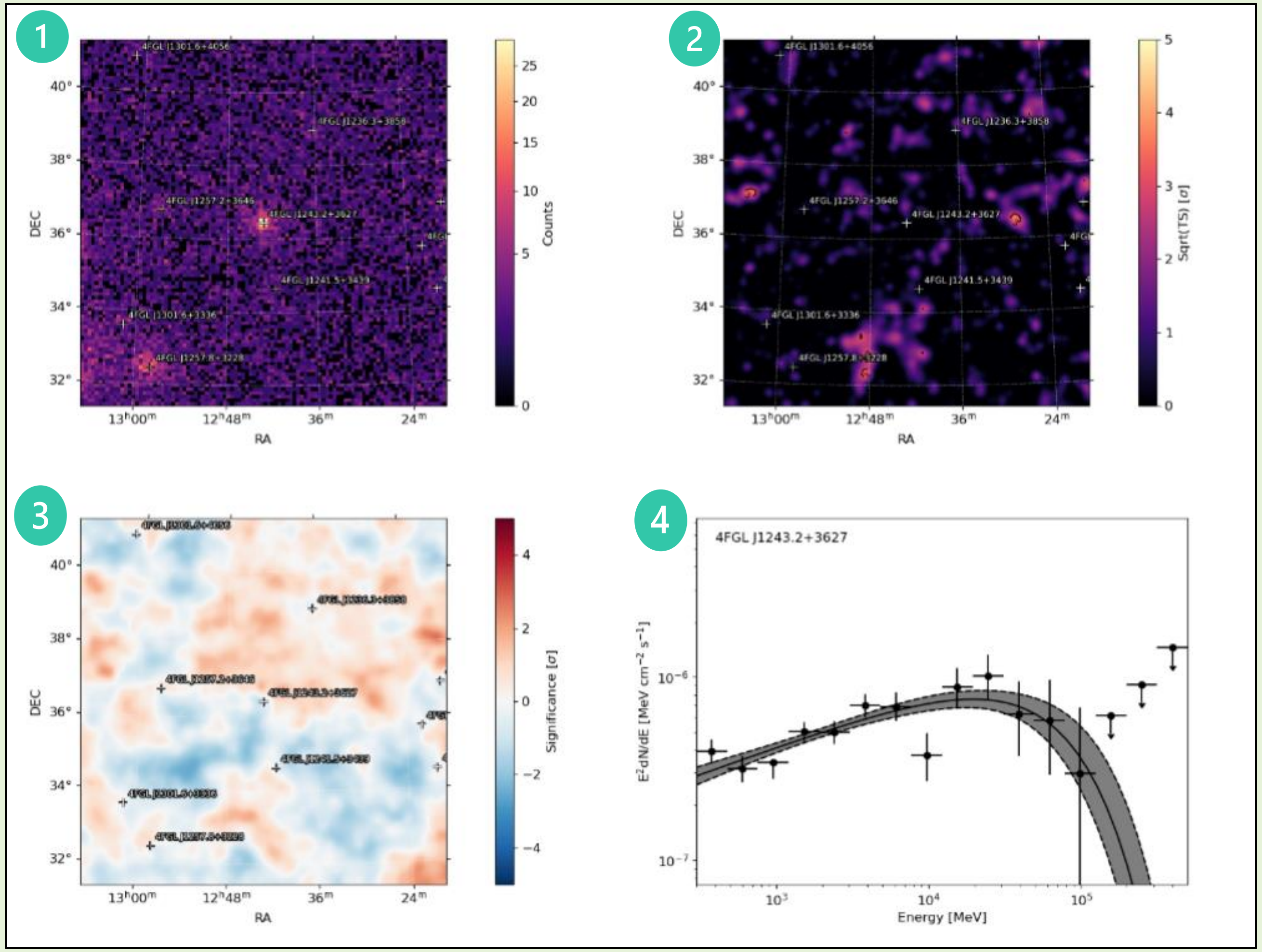

1 Counts' map
2 TS map
3 Residuals' map
4 Fitted SED

Again, spectral trend consistent with:

***Power-law with exponential cut-off* (PLEC)**

$$\frac{dN}{dE} = N_0 \cdot \left(\frac{E}{10^3\ \mathrm{MeV}}\right)^{-\gamma} \cdot \exp[-(E - E_b)/p_1]$$

✓

TON 116 by Fermi-LAT (recap)

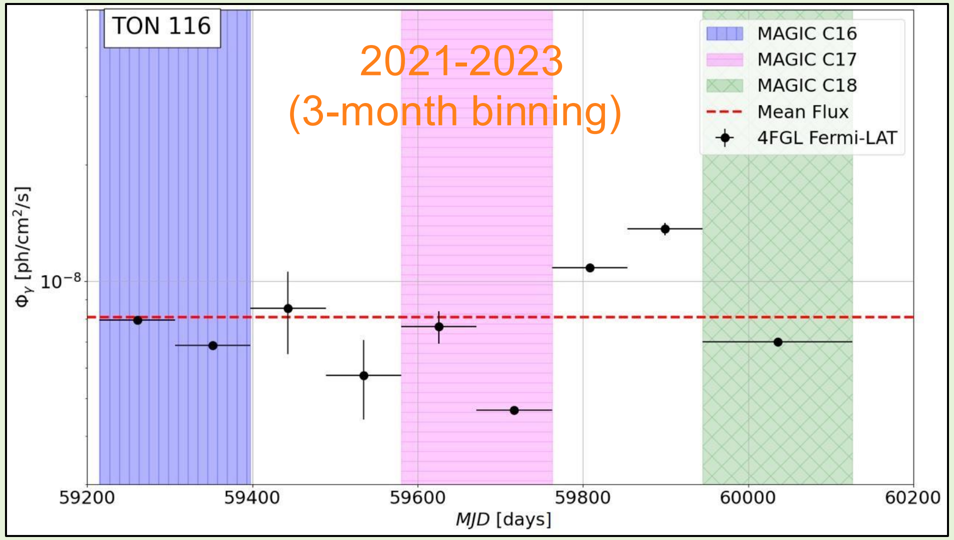

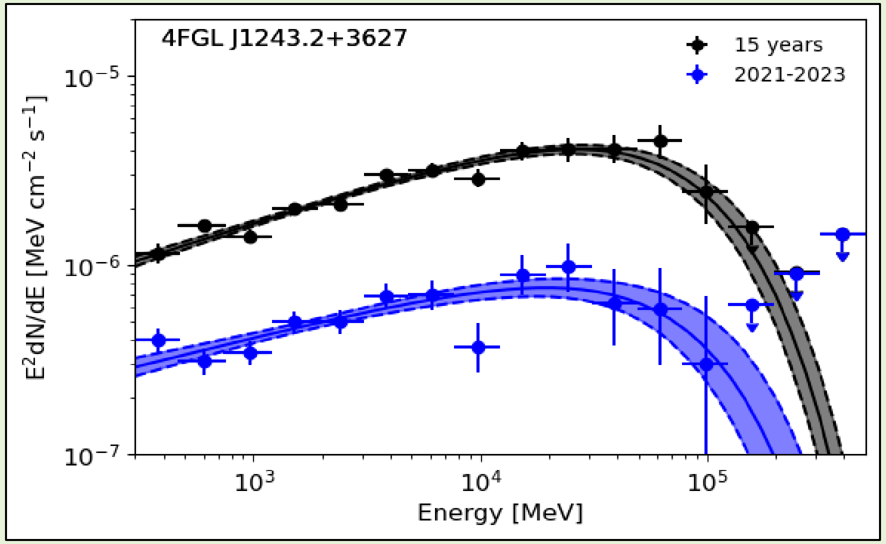

TON 116 by Fermi-LAT (recap)

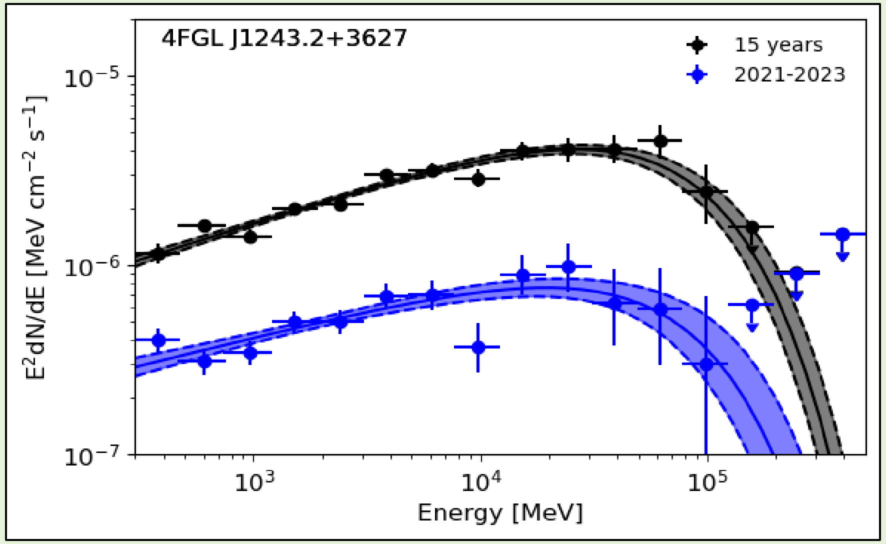

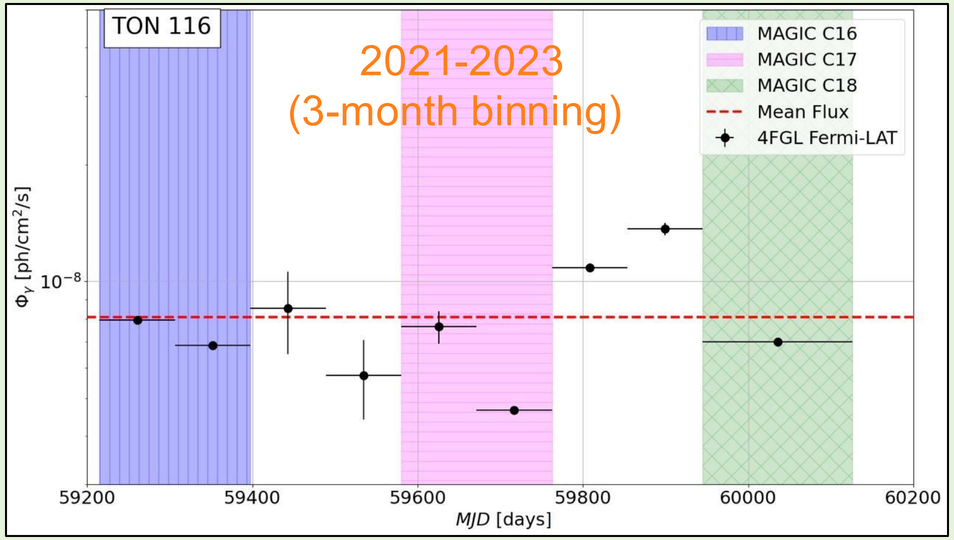

300 MeV – 500 GeV range, 2021-2023 period:

- *Overall non-variability (LC)*
- *Particularly low activity (SED) also preventing VHE detection (but still possible in case of flare...)*

TON 116 by Swift-XRT

- **10 "visits"** on the source in the 2021-2023 period

9 in Mar 2021 + 1 in Mar 2022, ~ 1.6 ks duration (~ 27 min)
1 previously discarded due to scarce time (2021-04-02)

- **Photon Counting (PC)** readout mode

Events within R ~ 6 pixels from the centre excluded to avoid pile-up occurrence; signal up to ~ 30 pixels, compared with PSF

- **Dedicated analysis software** in the 0.2 - 10 keV range

xspec (HEASoft v.6.32.1) with ancillary files for detector response

Swift Master Catalog (swiftmastr) Bulletin
Search radius used: 25.00'

https://heasarc.gsfc.nasa.gov/db-perl/W3Browse/w3table.pl

Select All	Related Links	Services	name	obsid	ra	dec	start time	processing date	xrt exposure [s]	uvot exposure [s]	bat exposure [s]	archive date	Search Offset [']
	BAT UVOT XRT	O R N S D B	TXCVN	00090484001	12 44 36.19	+36 45 17.2	2010-04-08 16:46:00	2016-07-11	4488.16200	4480.38100	4551.00000	2010-04-19	24.261 (TON 116)
	BAT UVOT XRT	O R N S D B	TXCVN	00090484002	12 44 33.79	+36 45 13.7	2010-04-21 06:28:00	2016-07-12	3420.78900	3416.20100	3488.00000	2010-05-02	23.888 (TON 116)
	BAT UVOT XRT	O R N S D B	TXCVN	00090484004	12 44 39.89	+36 43 47.2	2010-05-18 04:21:00	2016-07-13	2861.86000	2859.82200	2912.00000	2010-05-29	23.742 (TON 116)
	BAT UVOT XRT	O R N S D B	1RXSJ124312.5	00038445002	12 43 12.44	+36 30 08.7	2010-10-19 02:25:59	2016-08-15	2403.15100	2397.25500	2538.00000	2010-10-30	2.413 (TON 116)
	BAT UVOT XRT	O R N S D B	1RXSJ124312.5	00038445001	12 43 16.40	+36 28 29.6	2009-02-13 20:37:00	2015-12-27	2143.72100	2071.67300	2196.00000	2009-02-24	1.058 (TON 116)
	BAT UVOT XRT	O R N S D B	1RXSJ124312.5	00038445028	12 43 13.17	+36 27 59.7	2024-01-06 04:15:55	2024-01-16	2141.23400	2110.16600	2172.00000	2024-01-17	0.275 (TON 116)
	BAT UVOT XRT	O R N S D B	1RXSJ124312.5	00038445004	12 43 15.82	+36 29 08.3	2017-12-27 00:24:57	2018-01-06	2075.93700	2060.72800	2090.00000	2018-01-07	1.536 (TON 116)
	BAT UVOT XRT	O R N S D B	1RXSJ124312.5	00038445027	12 43 14.92	+36 26 22.4	2022-03-09 01:17:36	2022-03-19	1978.96300	1904.96400	2000.00000	2022-03-20	1.429 (TON 116)
	BAT UVOT XRT	O R N S D B	1RXSJ124312.5	00038445016	12 43 14.36	+36 28 14.7	2021-02-18 10:35:36	2021-02-28	1955.68500	1954.23900	1873.00000	2021-03-01	0.607 (TON 116)
	BAT UVOT XRT	O R N S D B	1RXSJ124312.5	00038445017	12 43 06.79	+36 28 56.0	2021-02-18 08:54:34	2021-02-28	1880.40800	1879.62300	2038.00000	2021-03-01	1.693 (TON 116)
	BAT UVOT XRT	O R N S D B	1RXSJ124312.5	00038445021	12 43 12.39	+36 27 00.6	2021-02-22 11:20:35	2021-03-04	1699.41800	1698.69400	1706.00000	2021-03-05	0.727 (TON 116)
	BAT UVOT XRT	O R N S D B	1RXSJ124312.5	00038445019	12 43 19.30	+36 27 49.2	2021-02-20 09:58:35	2021-03-02	1689.38800	1689.60300	1697.00000	2021-03-03	1.323 (TON 116)
	BAT UVOT XRT	O R N S D B	1RXSJ124312.5	00038445018	12 43 14.04	+36 29 33.4	2021-02-19 11:40:35	2021-03-01	1671.83600	1670.57200	1678.00000	2021-03-02	1.842 (TON 116)
	BAT UVOT XRT	O R N S D B	1RXSJ124312.5	00038445020	12 43 21.42	+36 24 24.6	2021-02-21 11:27:34	2021-03-03	1633.85600	1634.53800	1642.00000	2021-03-04	3.754 (TON 116)
	BAT UVOT XRT	O R N S D B	1RXSJ124312.5	00038445023	12 43 10.93	+36 26 30.9	2021-03-12 08:05:35	2021-03-22	1429.59900	1428.28900	1444.00000	2021-03-23	1.271 (TON 116)
	BAT UVOT XRT	O R N S D	TXCVN	00091453007	12 44 37.83	+36 44 38.9	2013-03-10 05:58:59	2017-11-04	1387.57100	1381.92800	1413.00000	2013-03-21	24.036 (TON 116)
	BAT UVOT XRT	O R N S D B	1RXSJ124312.5	00038445025	12 43 10.13	+36 26 31.9	2021-03-19 08:52:35	2021-03-29	1368.18100	1367.67400	1376.00000	2021-03-30	1.311 (TON 116)
	BAT UVOT XRT	O R N S D B	1RXSJ124312.5	00038445006	12 43 15.52	+36 27 56.1	2018-01-24 13:44:57	2018-02-03	1318.83500	1311.03100	1326.00000	2018-02-04	0.595 (TON 116)
	BAT UVOT XRT	O R N S D B	1RXSJ124312.5	00038445024	12 43 10.01	+36 25 40.9	2021-03-16 09:13:35	2021-03-26	1303.16400	1300.77000	1309.00000	2021-03-27	2.124 (TON 116)
	BAT UVOT XRT	O R N S D	TXCVN	00091453008	12 44 40.75	+36 43 44.4	2013-03-25 16:10:59	2017-11-06	1278.22800	1278.10900	1285.00000	2013-04-05	23.839 (TON 116)
	BAT UVOT XRT	O R N S D B	1RXSJ124312.5	00038445010	12 43 14.83	+36 26 45.9	2018-03-21 15:03:57	2018-04-23	1119.68200	1104.87000	1133.00000	2018-04-01	1.057 (TON 116)
	BAT UVOT XRT	O R N S D B	1RXSJ124312.5	00038445014	12 42 57.16	+36 27 47.3	2018-05-02 15:54:56	2018-05-12	1118.20300	1109.55800	1124.00000	2018-05-13	3.132 (TON 116)
	BAT UVOT XRT	O R N S D B	1RXSJ124312.5	00038445008	12 43 23.25	+36 26 15.1	2018-02-21 14:17:57	2018-03-03	1020.46900	1012.14900	1027.00000	2018-03-04	2.583 (TON 116)
	BAT UVOT XRT	O R N S D B	1RXSJ124312.5	00038445007	12 43 16.68	+36 27 26.3	2018-02-07 18:56:57	2018-02-17	1007.93000	998.56700	1013.00000	2018-02-18	0.846 (TON 116)
	BAT UVOT XRT	O R N S D B	1RXSJ124312.5	00038445003	12 43 18.62	+36 28 51.7	2017-12-13 17:12:57	2017-12-23	1002.91600	993.73500	1008.00000	2017-12-24	1.634 (TON 116)

TON 116 by Swift-XRT

- **10 "visits"** on the source in the 2021-2023 period

9 in Mar 2021 + 1 in Mar 2022, ~ 1.6 ks duration (~ 27 min)
1 previously discarded due to scarce time (2021-04-02)

- **Photon Counting (PC)** readout mode

Events within R ~ 6 pixels from the centre excluded to avoid pile-up occurrence; signal up to ~ 30 pixels, compared with PSF

- **Dedicated analysis software** in the 0.2 - 10 keV range

xspec (HEASoft v.6.32.1) with ancillary files for detector response

spectra extraction with ≥ 30 counts per channel bin

Swift Master Catalog (swiftmastr) Bulletin
Search radius used: 25.00'

https://heasarc.gsfc.nasa.gov/db-perl/W3Browse/w3table.pl

Select All	Related Links	Services	name	obsid	ra	dec	start time	processing date	xrt exposure [s]	uvot exposure [s]	bat exposure [s]	archive date	Search Offset [']
	BAT UVOT XRT	O R N S D B	TXCVN	00090484001	12 44 36.19	+36 45 17.2	2010-04-08 16:46:00	2016-07-11	4488.16200	4480.38100	4551.00000	2010-04-19	24.261 (TON 116)
	BAT UVOT XRT	O R N S D B	TXCVN	00090484002	12 44 33.79	+36 45 13.7	2010-04-21 06:28:00	2016-07-12	3420.78900	3416.20100	3488.00000	2010-05-02	23.888 (TON 116)
	BAT UVOT XRT	O R N S D B	TXCVN	00090484004	12 44 39.89	+36 43 47.2	2010-05-18 04:21:00	2016-07-13	2861.86000	2859.82200	2912.00000	2010-05-29	23.742 (TON 116)
	BAT UVOT XRT	O R N S D B	1RXSJ124312.5	00038445002	12 43 12.44	+36 30 08.7	2010-10-19 02:25:59	2016-08-15	2403.15100	2397.25500	2538.00000	2010-10-30	2.413 (TON 116)
	BAT UVOT XRT	O R N S D B	1RXSJ124312.5	00038445001	12 43 16.40	+36 28 29.6	2009-02-13 20:37:00	2015-12-27	2143.72100	2071.67300	2196.00000	2009-02-24	1.058 (TON 116)
	BAT UVOT XRT	O R N S D B	1RXSJ124312.5	00038445028	12 43 13.17	+36 27 59.7	2024-01-06 04:15:55	2024-01-16	2141.23400	2110.16600	2172.00000	2024-01-17	0.275 (TON 116)
	BAT UVOT XRT	O R N S D B	1RXSJ124312.5	00038445004	12 43 15.82	+36 29 08.3	2017-12-27 00:24:57	2018-01-06	2075.93700	2060.72800	2090.00000	2018-01-07	1.536 (TON 116)
	BAT UVOT XRT	O R N S D B	1RXSJ124312.5	00038445027	12 43 14.92	+36 26 22.4	2022-03-09 01:17:36	2022-03-19	1978.96300	1904.96400	2000.00000	2022-03-20	1.429 (TON 116)
	BAT UVOT XRT	O R N S D B	1RXSJ124312.5	00038445016	12 43 14.36	+36 28 14.7	2021-02-18 10:35:36	2021-02-28	1955.68500	1954.23900	1873.00000	2021-03-01	0.607 (TON 116)
	BAT UVOT XRT	O R N S D B	1RXSJ124312.5	00038445017	12 43 06.79	+36 28 56.0	2021-02-18 08:54:34	2021-02-28	1880.40800	1879.62300	2038.00000	2021-03-01	1.693 (TON 116)
	BAT UVOT XRT	O R N S D B	1RXSJ124312.5	00038445021	12 43 12.39	+36 27 00.6	2021-02-22 11:20:35	2021-03-04	1699.41800	1698.69400	1706.00000	2021-03-05	0.727 (TON 116)
	BAT UVOT XRT	O R N S D B	1RXSJ124312.5	00038445019	12 43 19.30	+36 27 49.2	2021-02-20 09:58:35	2021-03-02	1689.38800	1689.60300	1697.00000	2021-03-03	1.323 (TON 116)
	BAT UVOT XRT	O R N S D B	1RXSJ124312.5	00038445018	12 43 14.04	+36 29 33.4	2021-02-19 11:40:35	2021-03-01	1671.83600	1670.57200	1678.00000	2021-03-02	1.842 (TON 116)
	BAT UVOT XRT	O R N S D B	1RXSJ124312.5	00038445020	12 43 21.42	+36 24 24.6	2021-02-21 11:27:34	2021-03-03	1633.85600	1634.53800	1642.00000	2021-03-04	3.754 (TON 116)
	BAT UVOT XRT	O R N S D B	1RXSJ124312.5	00038445023	12 43 10.93	+36 26 30.9	2021-03-12 08:05:35	2021-03-22	1429.59900	1428.28900	1444.00000	2021-03-23	1.271 (TON 116)
	BAT UVOT XRT	O R N S D	TXCVN	00091453007	12 44 37.83	+36 44 38.9	2013-03-10 05:58:59	2017-11-04	1387.57100	1381.92800	1413.00000	2013-03-21	24.036 (TON 116)
	BAT UVOT XRT	O R N S D B	1RXSJ124312.5	00038445025	12 43 10.13	+36 26 31.9	2021-03-19 08:52:35	2021-03-29	1368.18100	1367.67400	1376.00000	2021-03-30	1.311 (TON 116)
	BAT UVOT XRT	O R N S D B	1RXSJ124312.5	00038445006	12 43 15.52	+36 27 56.1	2018-01-24 13:44:57	2018-02-03	1318.83500	1311.03100	1326.00000	2018-02-04	0.595 (TON 116)
	BAT UVOT XRT	O R N S D B	1RXSJ124312.5	00038445024	12 43 10.01	+36 25 40.9	2021-03-16 09:13:35	2021-03-26	1303.16400	1300.77000	1309.00000	2021-03-27	2.124 (TON 116)
	BAT UVOT XRT	O R N S D	TXCVN	00091453008	12 44 40.75	+36 43 44.4	2013-03-25 16:10:59	2017-11-06	1278.22800	1278.10900	1285.00000	2013-04-05	23.839 (TON 116)
	BAT UVOT XRT	O R N S D B	1RXSJ124312.5	00038445010	12 43 14.83	+36 26 45.9	2018-03-21 15:03:57	2018-04-23	1119.68200	1104.87000	1133.00000	2018-04-01	1.057 (TON 116)
	BAT UVOT XRT	O R N S D B	1RXSJ124312.5	00038445014	12 42 57.16	+36 27 47.3	2018-05-02 15:54:56	2018-05-12	1118.20300	1109.55800	1124.00000	2018-05-13	3.132 (TON 116)
	BAT UVOT XRT	O R N S D B	1RXSJ124312.5	00038445008	12 43 23.25	+36 26 15.1	2018-02-21 14:17:57	2018-03-03	1020.46900	1012.14900	1027.00000	2018-03-04	2.583 (TON 116)
	BAT UVOT XRT	O R N S D B	1RXSJ124312.5	00038445007	12 43 16.68	+36 27 26.3	2018-02-07 18:56:57	2018-02-17	1007.93000	998.56700	1013.00000	2018-02-18	0.846 (TON 116)
	BAT UVOT XRT	O R N S D B	1RXSJ124312.5	00038445003	12 43 18.62	+36 28 51.7	2017-12-13 17:12:57	2017-12-23	1002.91600	993.73500	1008.00000	2017-12-24	1.634 (TON 116)

TON 116 SED by Swift-XRT

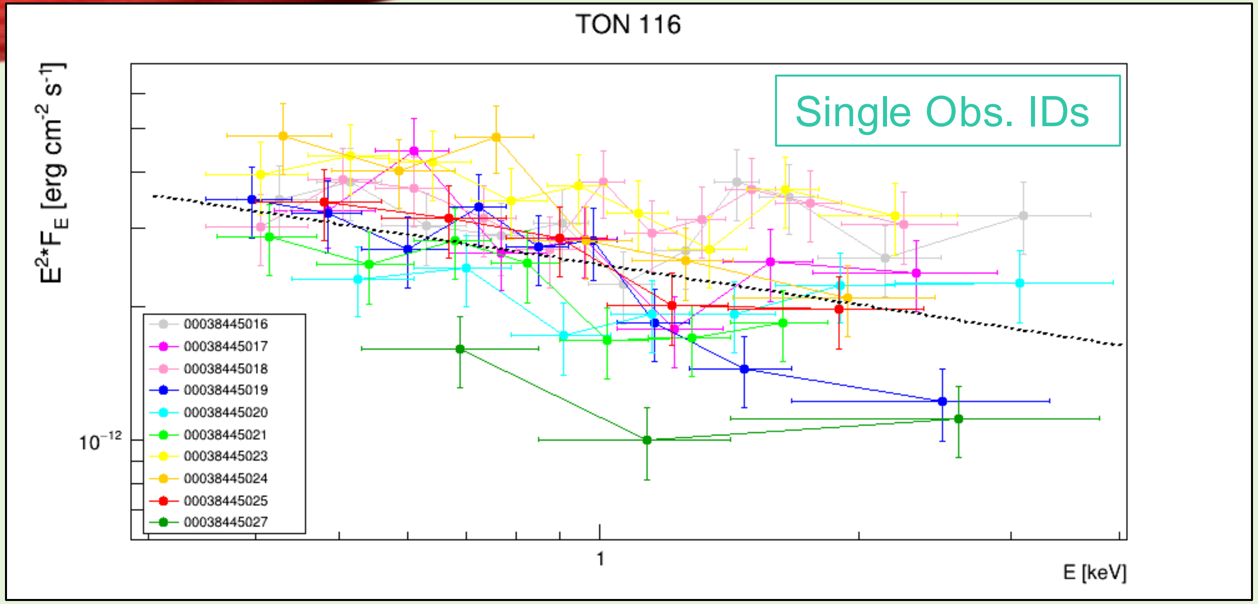

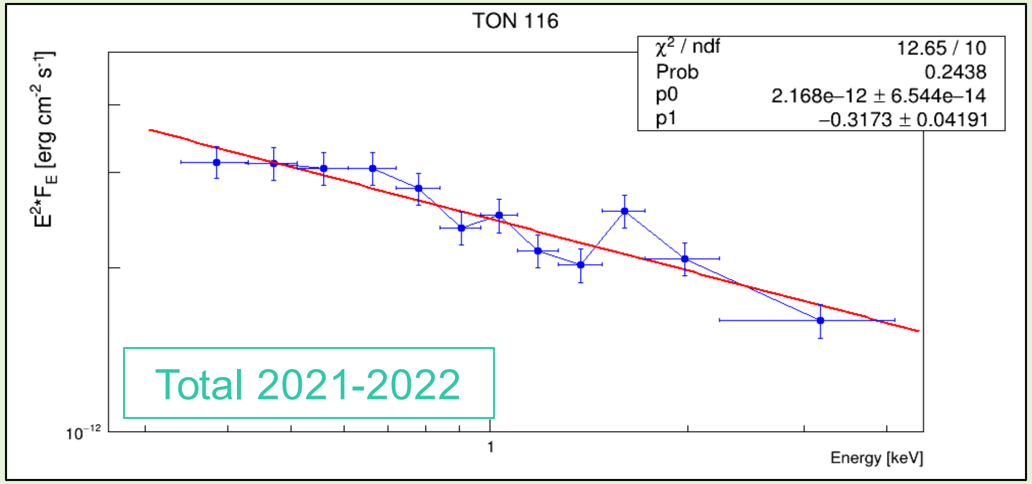

Obs. ID	Archive Date	Exposure [ks]	k_x [10^{-12} erg cm^{-2} s^{-1}]	p_x
38445016	2021-03-01	2.0	2.9 ± 0.2	2.1 ± 0.2
38445017	2021-03-01	1.9	2.2 ± 0.3	2.4 ± 0.2
38445018	2021-03-02	1.7	3.2 ± 0.3	2.0 ± 0.2
38445019	2021-03-03	1.7	1.7 ± 0.2	2.6 ± 0.2
38445020	2021-03-04	1.6	2.1 ± 0.2	2.0 ± 0.2
38445021	2021-03-05	1.7	1.7 ± 0.2	2.4 ± 0.2
38445023	2021-03-23	1.4	3.2 ± 0.3	2.2 ± 0.2
38445024	2021-03-27	1.3	2.4 ± 0.4	2.6 ± 0.2
38445025	2021-03-30	1.4	2.1 ± 0.3	2.5 ± 0.3
38445027	2022-03-20	2.0	1.1 ± 0.2	2.3 ± 0.4

$$F(E) = k_x \left(\frac{E}{E_x}\right)^{t_x}$$

TON 116 SED by Swift-XRT

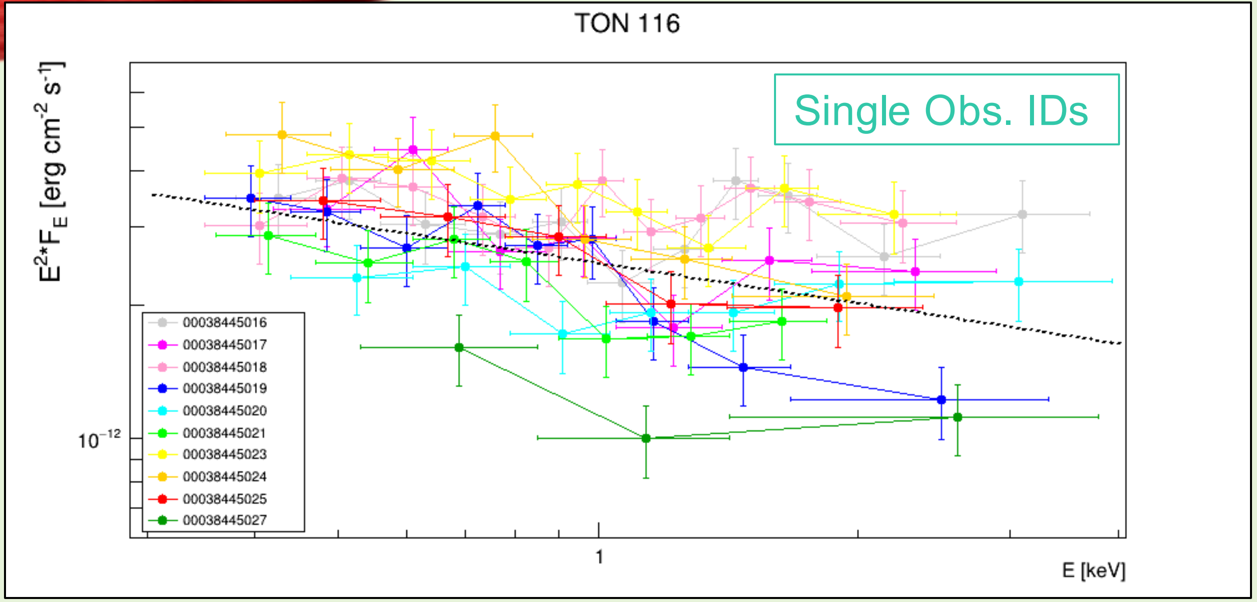

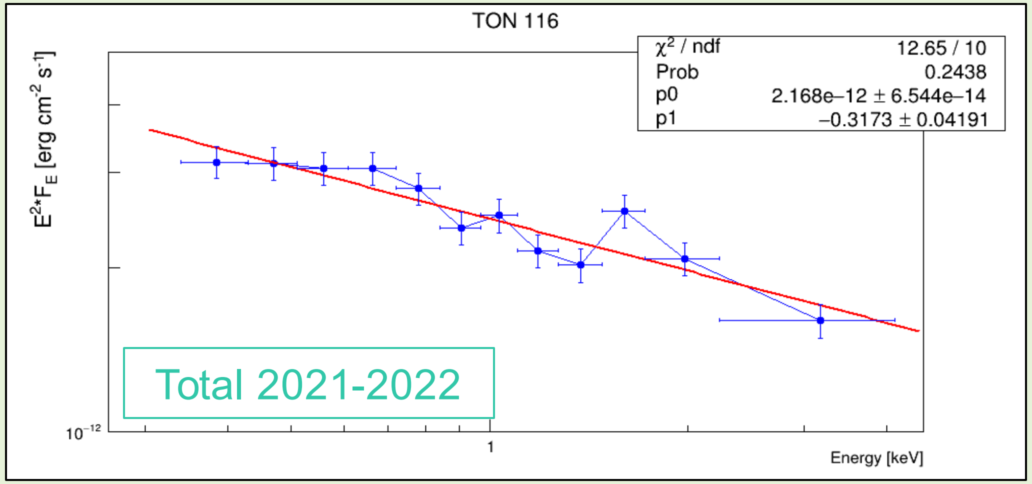

Obs. ID	Archive Date	Exposure [ks]	k_x [10^{-12} erg cm^{-2} s^{-1}]	p_x
38445016	2021-03-01	2.0	2.9±0.2	2.1±0.2
38445017	2021-03-01	1.9	2.2±0.3	2.4±0.2
38445018	2021-03-02	1.7	3.2±0.3	2.0±0.2
38445019	2021-03-03	1.7	1.7±0.2	2.6±0.2
38445020	2021-03-04	1.6	2.1±0.2	2.0±0.2
38445021	2021-03-05	1.7	1.7±0.2	2.4±0.2
38445023	2021-03-23	1.4	3.2±0.3	2.2±0.2
38445024	2021-03-27	1.3	2.4±0.4	2.6±0.2
38445025	2021-03-30	1.4	2.1±0.3	2.5±0.3
38445027	2022-03-20	2.0	1.1±0.2	2.3±0.4

Normalization constant

PL Model

Deabsorbed · data/absorbed

$$F(E) = k_x \left(\frac{E}{E_x}\right)^{t_x}$$

Weighted slope
(**intrinsic: $p_x = 2 - t_x$**)

1.5 keV

Galactic absorption (*Ben Bekhti et al. 2016*):

$n_H \approx 1.29 \cdot 10^{22}$ cm^{-2}

TON 116 SED by Swift-XRT

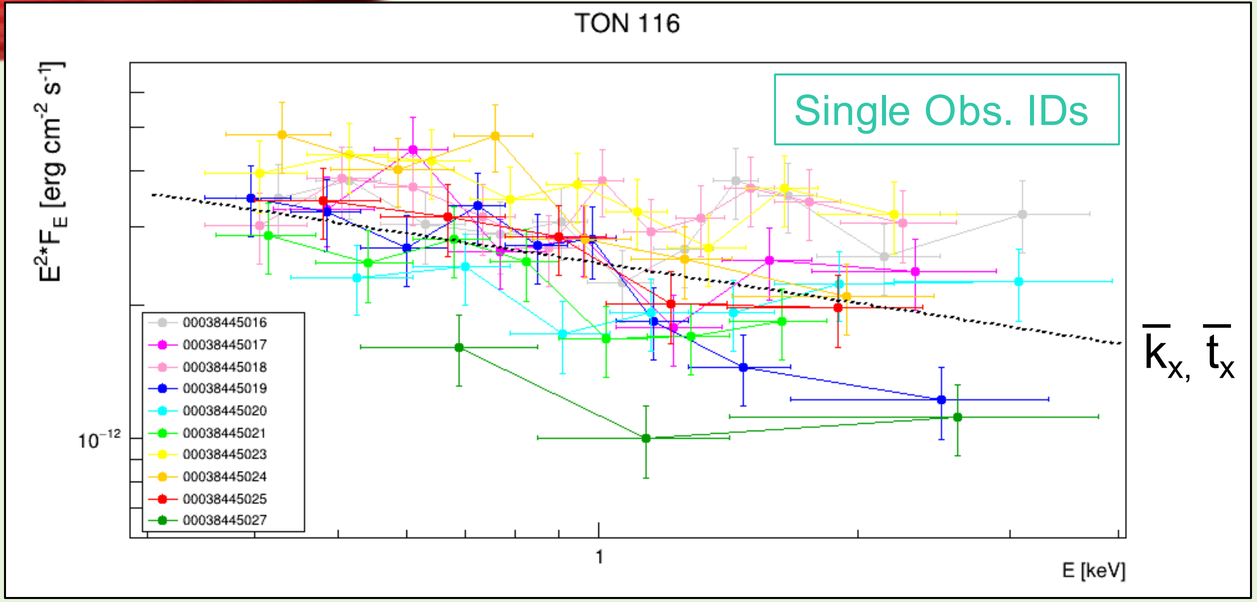

$\overline{k}_x$, $\overline{t}_x$

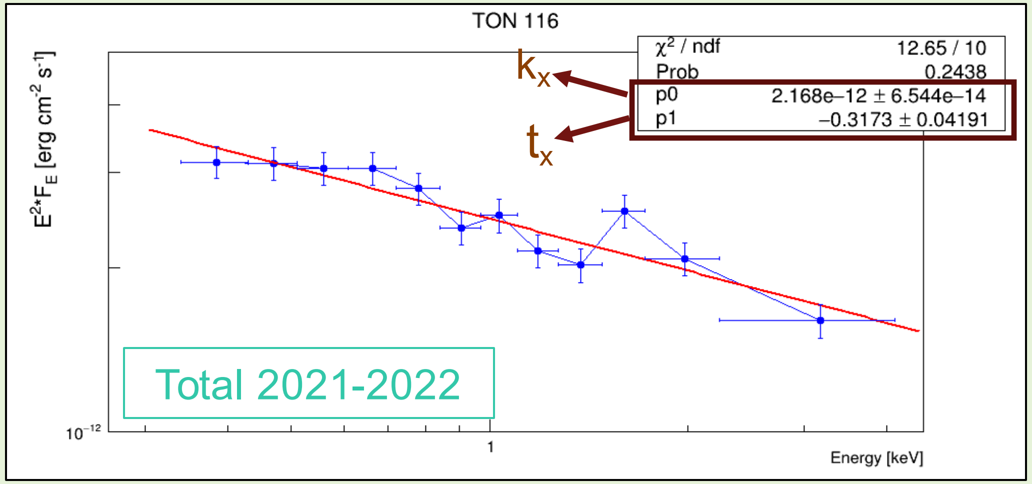

Obs. ID	Archive Date	Exposure [ks]	k_x [10^{-12} erg cm^{-2} s^{-1}]	p_x
38445016	2021-03-01	2.0	2.9 ± 0.2	2.1 ± 0.2
38445017	2021-03-01	1.9	2.2 ± 0.3	2.4 ± 0.2
38445018	2021-03-02	1.7	3.2 ± 0.3	2.0 ± 0.2
38445019	2021-03-03	1.7	1.7 ± 0.2	2.6 ± 0.2
38445020	2021-03-04	1.6	2.1 ± 0.2	2.0 ± 0.2
38445021	2021-03-05	1.7	1.7 ± 0.2	2.4 ± 0.2
38445023	2021-03-23	1.4	3.2 ± 0.3	2.2 ± 0.2
38445024	2021-03-27	1.3	2.4 ± 0.4	2.6 ± 0.2
38445025	2021-03-30	1.4	2.1 ± 0.3	2.5 ± 0.3
38445027	2022-03-20	2.0	1.1 ± 0.2	2.3 ± 0.4

Normalization constant

$$F(E) = k_x \left(\frac{E}{E_x}\right)^{t_x}$$

Weighted slope (**intrinsic: $p_x = 2 - t_x$**)

1.5 keV

PL Model

Deabsorbed · data/absorbed

Galactic absorption *(Ben Bekhti et al. 2016)*:

$n_H \approx 1.29 \cdot 10^{22}$ cm^{-2}

$\overline{k}_x \approx 2.2 \cdot 10^{-12}$ erg cm^{-2} s^{-1}, $\overline{t}_x \approx -0.3$ ↔ $\overline{p}_x \approx 2.3$

TON 116 daily index by Swift-XRT

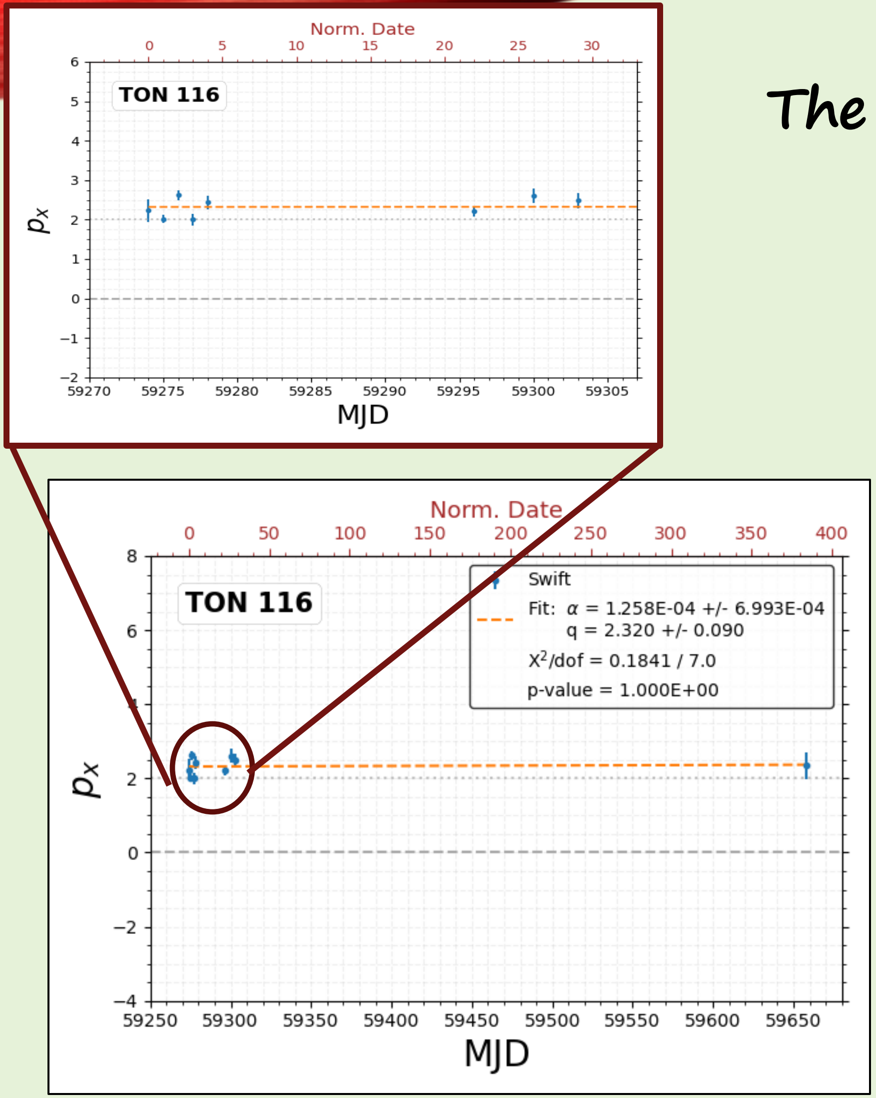

The soft-X slope is also found to be ~ constant over time

$$p_x = \begin{cases} \alpha_x D + p_{x,q} \\ p_{x,q} \end{cases}$$

Method	α_x [10^{-4} dy^{-1}]	$p_{x,q}$	χ^2_{np}/dof	*p-val$_{sf}$*	χ^2_{sp}/dof	*p-val$_{chi}$*	χ^2_{crit}
1-polyfit	1.26 ± 6.99	2.32 ± 0.09	0.184/7	1.000	0.184/7	1.000	14.07
1-curve_fit	1.26 ± 6.99	2.32 ± 0.09	0.184/7	1.000	0.184/7	1.000	14.07
0-polyfit	0	2.33 ± 0.08	0.185/8	1.000	0.185/8	1.000	15.51
0-curve_fit	0	2.33 ± 0.08	0.185/8	1.000	0.185/8	1.000	15.51

TON 116 daily index by Swift-XRT

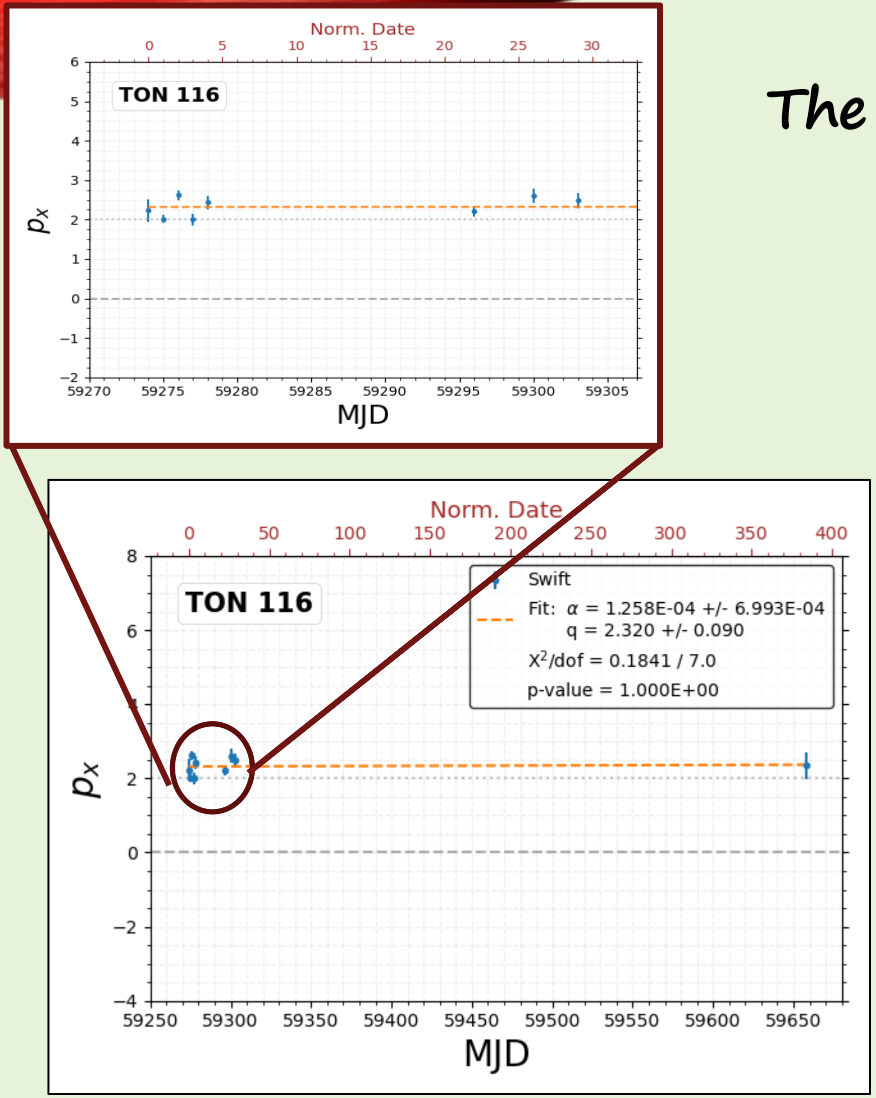

The soft-X slope is also found to be ~ constant over time

$$p_x = \begin{cases} \alpha_x D + p_{x,q} \\ p_{x,q} \end{cases}$$

Method	α_x $[10^{-4}\,\mathrm{dy}^{-1}]$	$p_{x,q}$	χ^2_{np}/dof	$p\text{-}val_{sf}$	χ^2_{sp}/dof	$p\text{-}val_{chi}$	χ^2_{crit}
1-polyfit	1.26 ± 6.99	2.32 ± 0.09	0.184/7	1.000	0.184/7	1.000	14.07
1-curve_fit	1.26 ± 6.99	2.32 ± 0.09	0.184/7	1.000	0.184/7	1.000	14.07
0-polyfit	0	2.33 ± 0.08	0.185/8	1.000	0.185/8	1.000	15.51
0-curve_fit	0	2.33 ± 0.08	0.185/8	1.000	0.185/8	1.000	15.51

Linear fit (generic slightly better than constant):

$\alpha_x \approx 1.3 \cdot 10^{-4}$ /day ➡ **still negligible in our case (384 days)**

$p_{x,q} \approx 2.3$ ➡ **mean slope (basically invariant)**

$$\chi^2 = \sum_{i=1}^{N} \frac{(p_{xi,obs} - p_{xi,exp})^2}{p_{xi,exp}}$$

➡ **TS for goodness-of-fit**
(numpy and scipy routines)

TON 116 by OSN

Data-taking period: 23rd Feb 2022 – 12th Feb 2023

Telescope(s): T090, T150

Scientific outcomes: *R mag* values

TON 116 by OSN

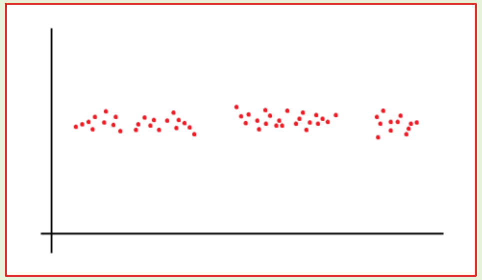

Data-taking period: 23rd Feb 2022 – 12th Feb 2023

Telescope(s): T090, T150

Scientific outcomes: *R mag* values

Few entries per night (mag range: 15-17)
Empty periods of 5-15 days (source not observed)

TON 116 by OSN

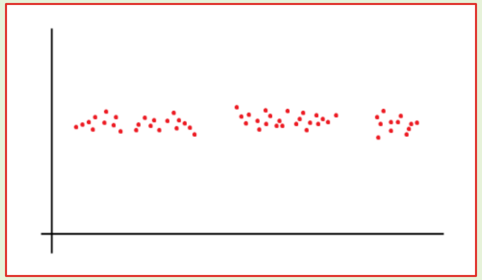

Data-taking period: 23rd Feb 2022 – 12th Feb 2023

Telescope(s): T090, T150

Scientific outcomes: R mag values ⇒ Few entries per night (mag range: 15-17)
Empty periods of 5-15 days (source not observed)

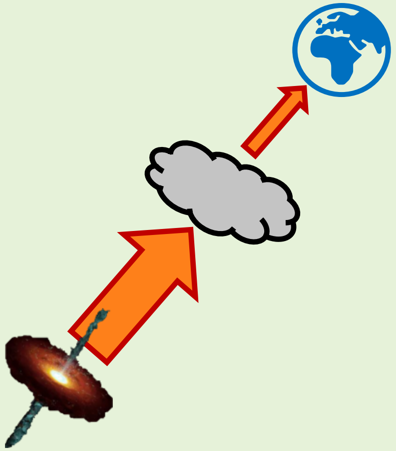

i) *Galactic extinction correction* (true magnitude from observed magnitude)

$$m_{R,t} = m_{R,o} - A_R$$

A_R → 0.026 mag (Landolt R bandpass, *Schlafly & Finkbeiner 2011*)

ii) True magnitudes ($m_{R,t}$) → flux densities ($f_{R,t}$) conversion (*Bessell et al. 1998*)

MagToFluxDensity_bessell98 method (**PyAstronomy.pyasl** python package)

TON 116 Light Curve by OSN

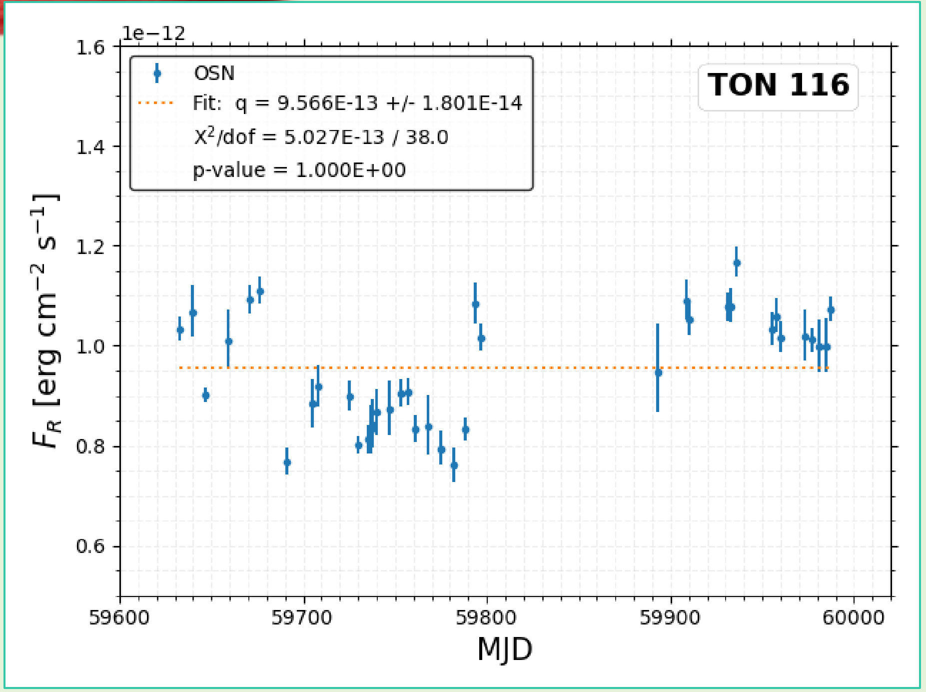

39 data points from a 1-per-day average:

$$f_R = \frac{\sum_{i=1}^{n} f_{R,i}}{n}$$

Flux value

$$\Delta f_R = \frac{1}{n}\sqrt{\sum_{i=1}^{n}(\Delta f_{R,i})^2}$$

Flux error

TON 116 Light Curve by OSN

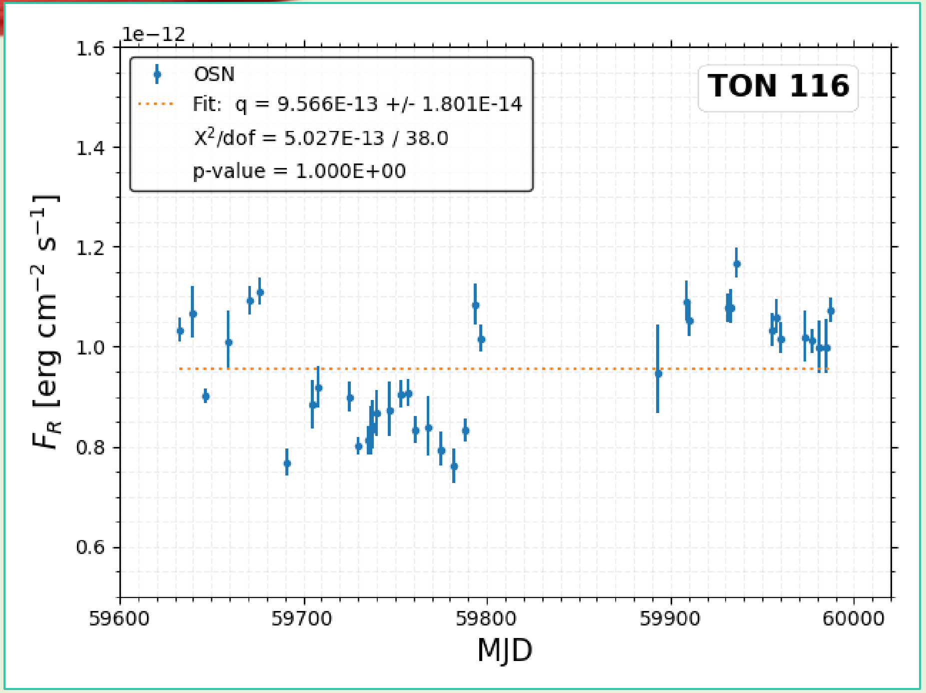

39 data points from a 1-per-day average:

$$f_R = \frac{\sum_{i=1}^{n} f_{R,i}}{n}$$

Flux value

$$\Delta f_R = \frac{1}{n}\sqrt{\sum_{i=1}^{n} (\Delta f_{R,i})^2}$$

Flux error

- $f_{R,i}$ → single measurement at given MJD
- $\Delta f_{R,i}$ → single measurement error
- n → n. of measurements at same MJD

TON 116 Light Curve by OSN

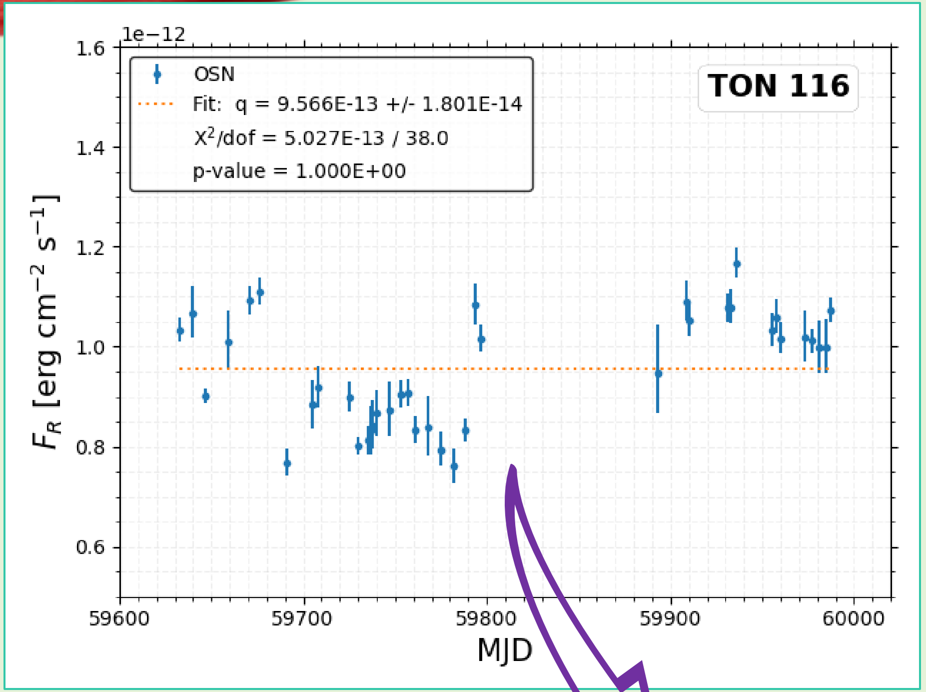

39 data points from a 1-per-day average:

$$f_R = \frac{\sum_{i=1}^{n} f_{R,i}}{n}$$

Flux value

Simple mean

$$\Delta f_R = \frac{1}{n}\sqrt{\sum_{i=1}^{n}(\Delta f_{R,i})^2}$$

Flux error

Upper ≈ lower

- $f_{R,i}$ → single measurement at given MJD
- $\Delta f_{R,i}$ → single measurement error
- n → n. of measurements at same MJD

No flaring state supported

Daily flux showing a constant trend with ≲ 22% fluctuations

$\bar{F}_R \approx (9.6 \pm 0.1) \cdot 10^{-13}$ erg cm^{-2} s^{-1} (confirmed by constant fit)

TON 116 average broadband SED

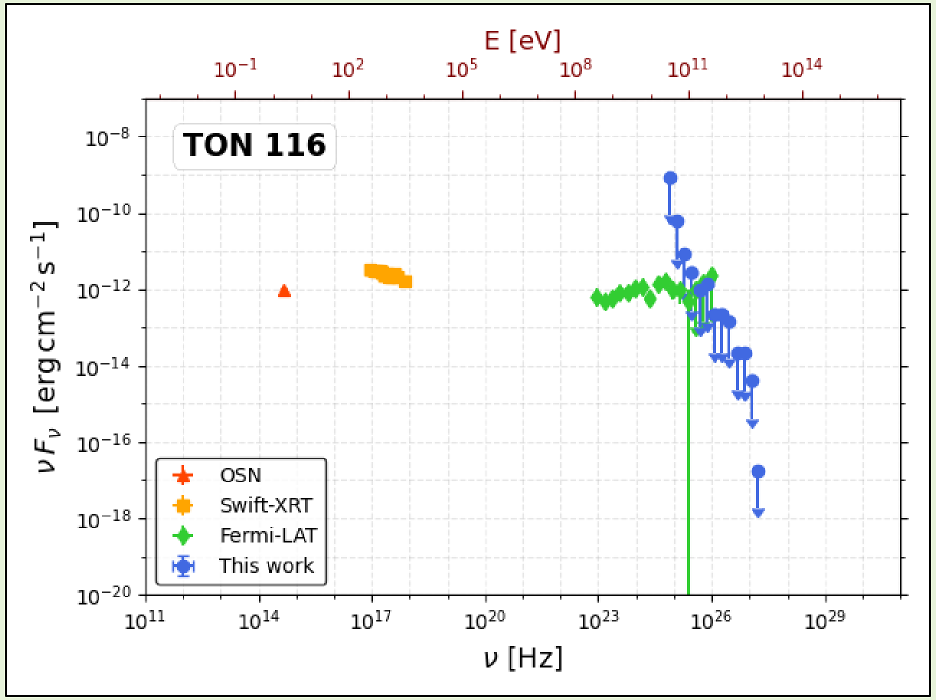

TON 116 average broadband SED

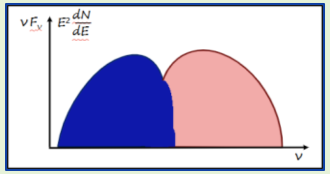

OSN + Swift-XRT

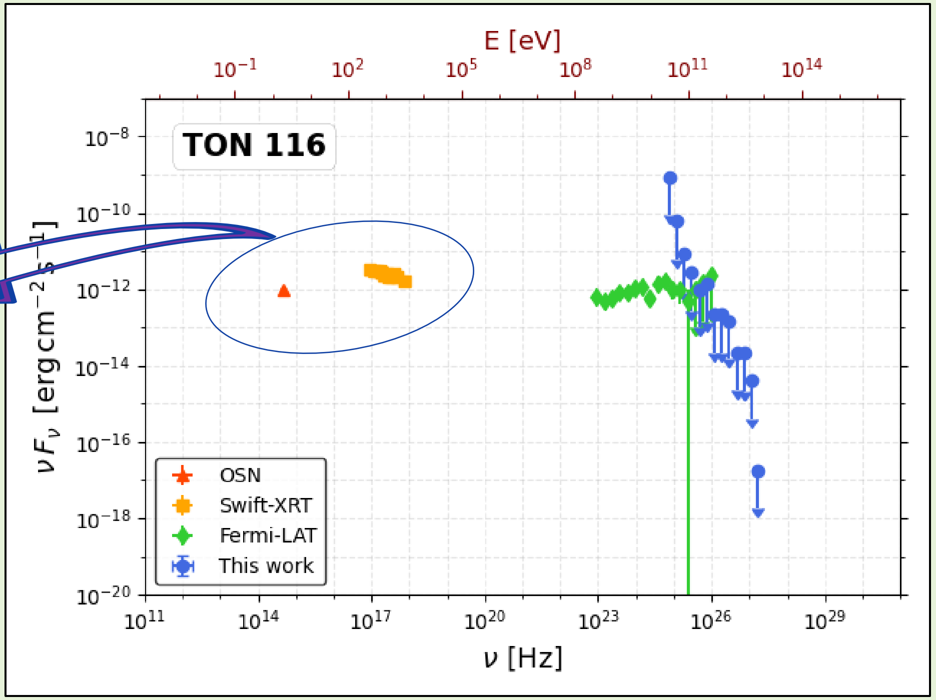

Probing the synchrotron bump (Optical + X band)

TON 116 average broadband SED

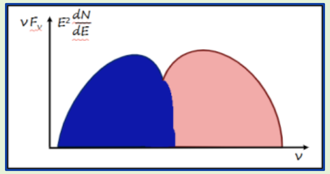

OSN + Swift-XRT

Probing the synchrotron bump (Optical + X band)

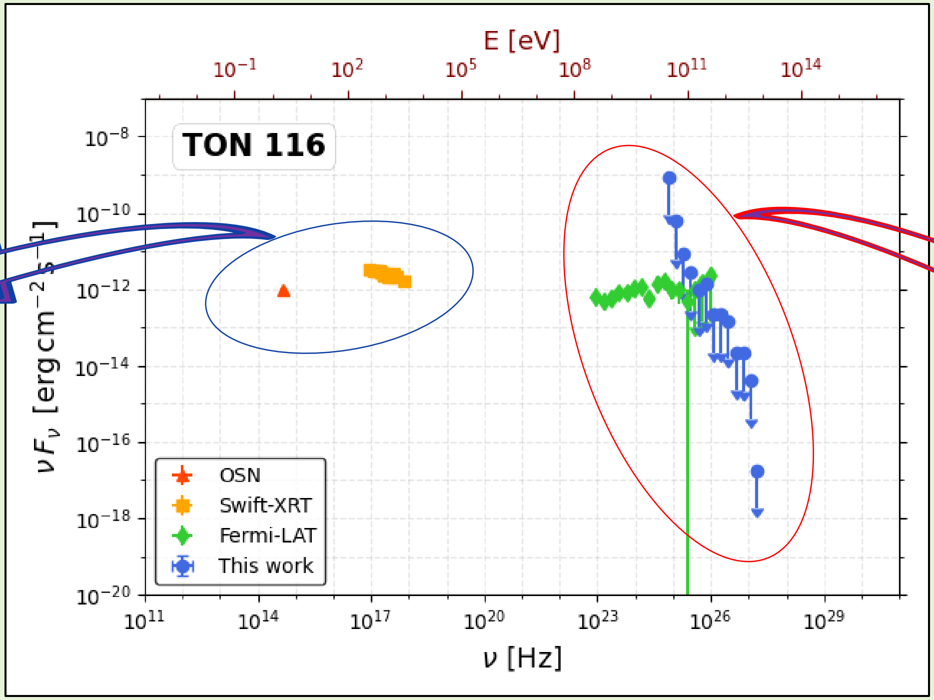

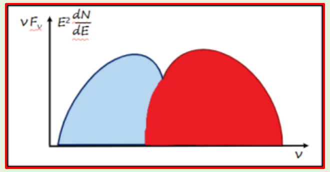

Fermi-LAT + MAGIC

Probing the inverse-Compton bump (HE + VHE γ band)

TON 116 average broadband SED

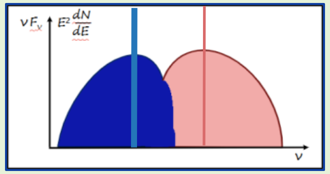

OSN + Swift-XRT

Probing the synchrotron bump (Optical + X band)

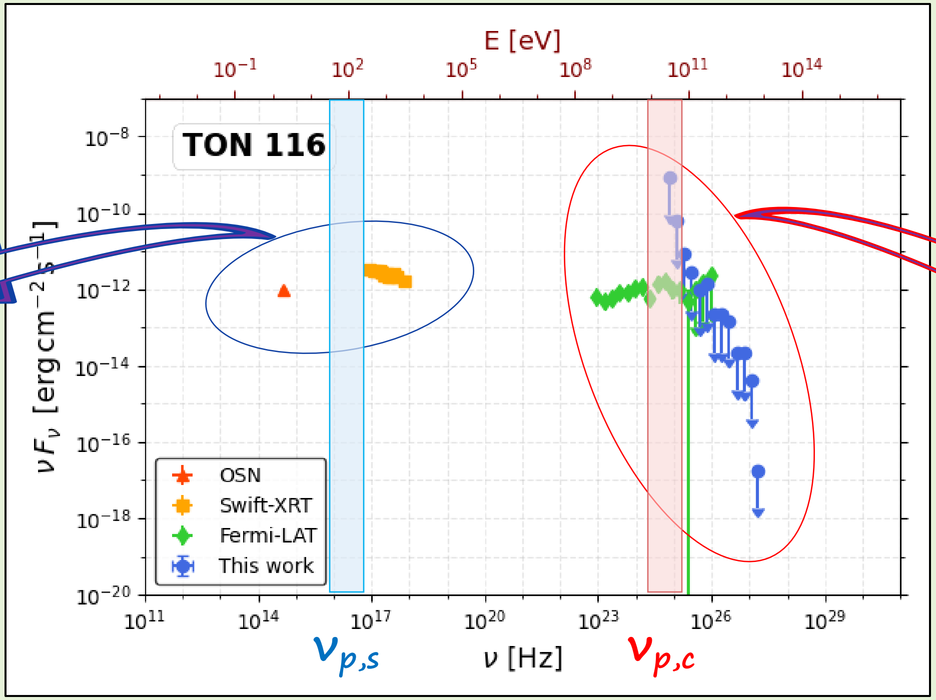

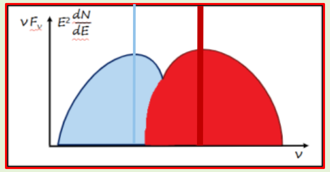

Fermi-LAT + MAGIC

Probing the inverse-Compton bump (HE + VHE γ band)

- *No Compton dominance (as expected for BL Lacs, Ghisellini et al. 2017)*
- $\nu_{p,s} \gtrsim 10^{16}$ Hz → *HBL nature (in agreement with 4LAC Fermi catalogue)*
  $\nu_{p,c} \lesssim 10^{25}$ Hz → *Compton peak before 100 GeV (as seen by Fermi)*
- *Emission highly suppressed at the most extreme energies (< 1 TeV)*

Broadband SED interpretation

Can we reach the model providing the best explanation?

Broadband SED interpretation

Can we reach the model providing the best explanation?

Nigro et al. (2022)

- 👍 Open-source, publicly-available python package for modeling radiative processes in the jets of AGNs
- 👍 Multiple AGN components considered (→ thermal/line emission sources), EBL and γ-γ absorption included
- 👎 No ν < 10^{11} Hz, no time evolution (but self-consistency)
- 👎 No data handling/fitting (but external *wrappers* available)

agnpy

Bégué et al. (2023)

- 👍 Publicly-available innovative platform for archival data searching and fitting (huge list of known blazars)
- 👍 Fast fitting procedure on archival/uploaded data relying on Convolutional Neural Networks (SOPRANO spectra training)
- 👎 No ν < 10^{11} Hz, no ULs handling
- 👎 Initial phase: SSC model only included (but self-consistency for secondary processes e.g. cooling, pairs, EBL)

MMDC

agnpy-sherpa fit results

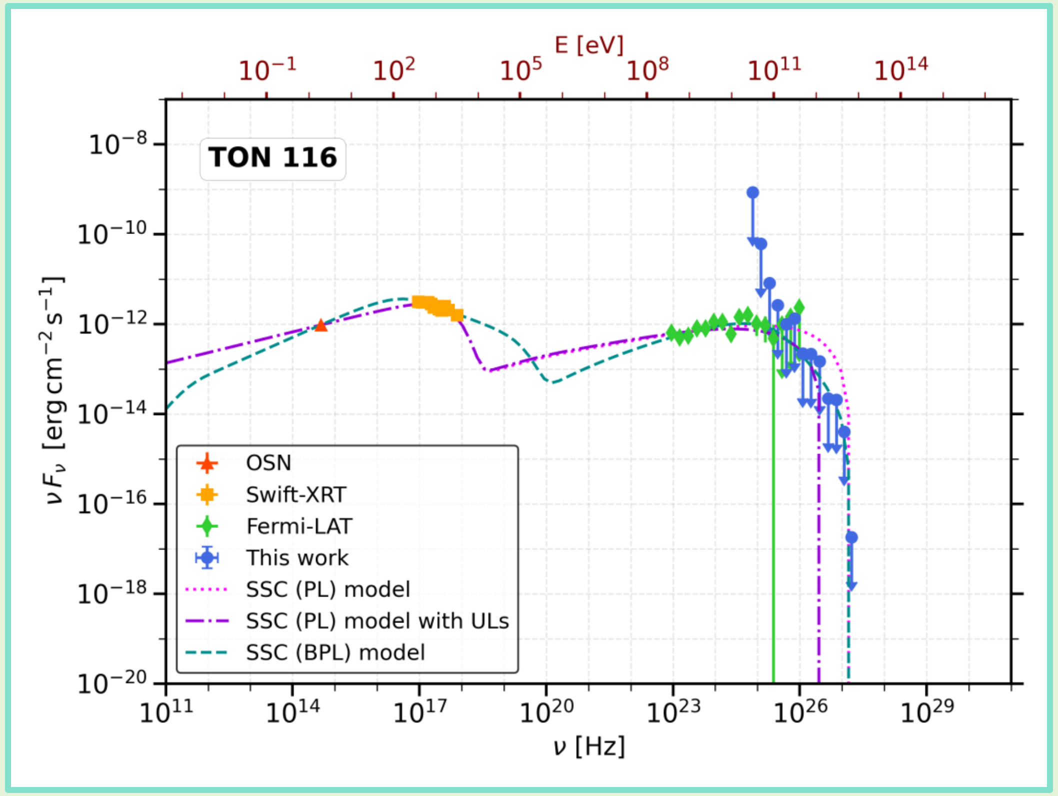

SynchrotronSelfComptonModel **method initializations:**

- PL/BPL (± ULs) as e- energy distribution
- z = 0.5
- *sherpa* wrapper for data handling

agnpy-sherpa fit results

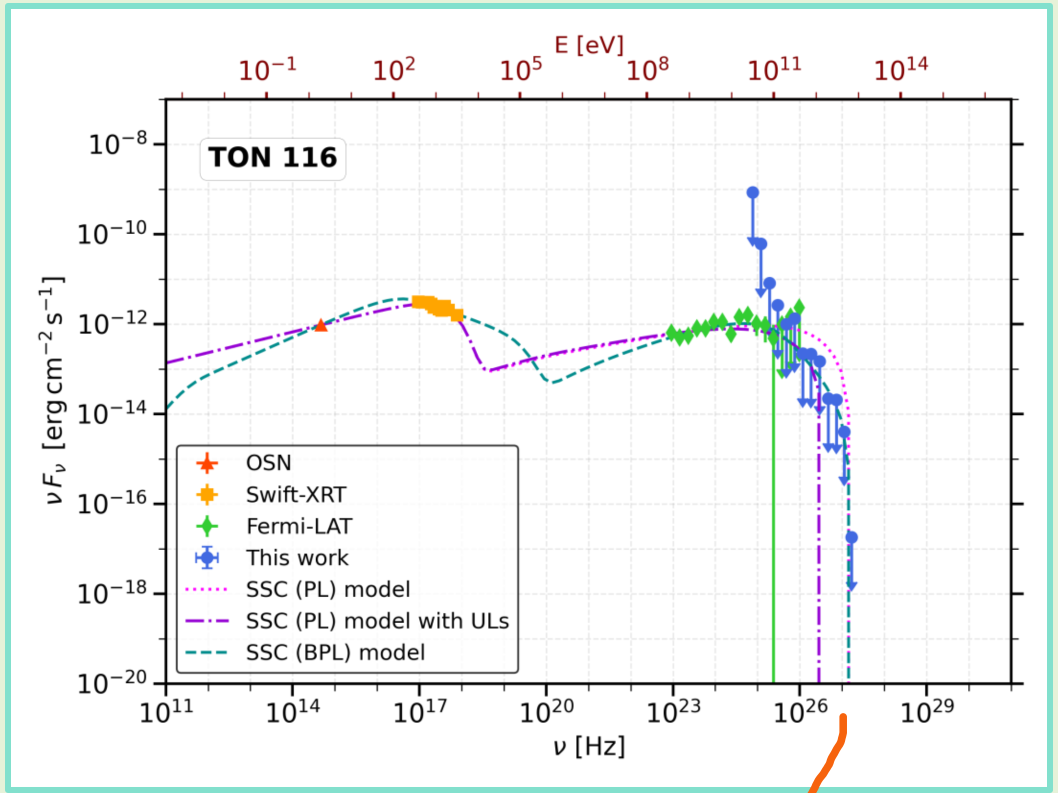

Strong VHE suppression

SynchrotronSelfComptonModel **method initializations:**

- PL/BPL (± ULs) as e^- energy distribution
- z = 0.5
- *sherpa* wrapper for data handling

Power-law case

For $\nu < 10^{25}$ Hz ⟶ PL (- ULs) ≈ PL (+ ULs)
For $\nu > 10^{25}$ Hz ⟶ PL (+ ULs) improving the VHE fit
But EHBL behaviour suggested ($\nu_{p,s} > 10^{17}$ Hz)...

Broken Power-law case

Harder rise & decrease of synchrotron bump
Bumps' connection at higher E, harder rise of IC bump
Good fit also at VHE even if ULs not included!

MMDC fit results

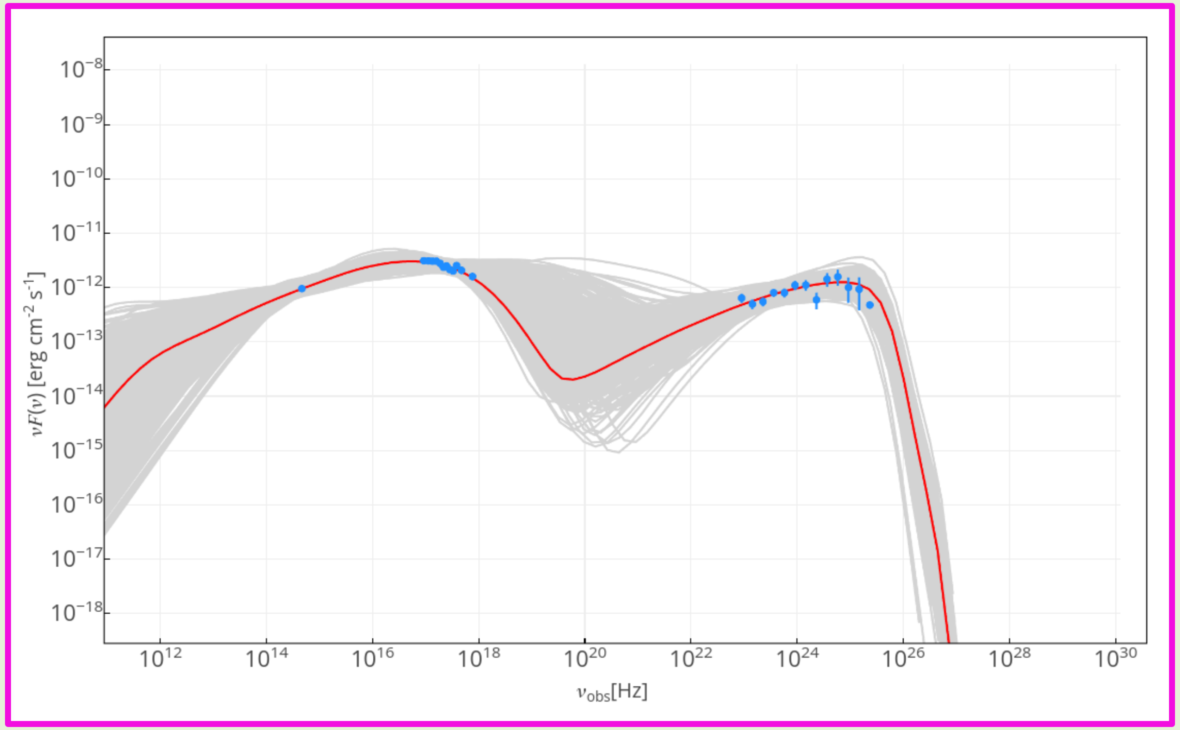

Main ingredients:

- **Leptonic SSC one-zone model**
- **Simple PL as electron energy distribution**
- **All TON 116 broadband datasets w/o ULs (HE, VHE), no TON 116 archival data (mostly out of 2021-2023)**
- **EBL absorption considered (*Domìnguez et al. 2011*)**

MMDC fit results

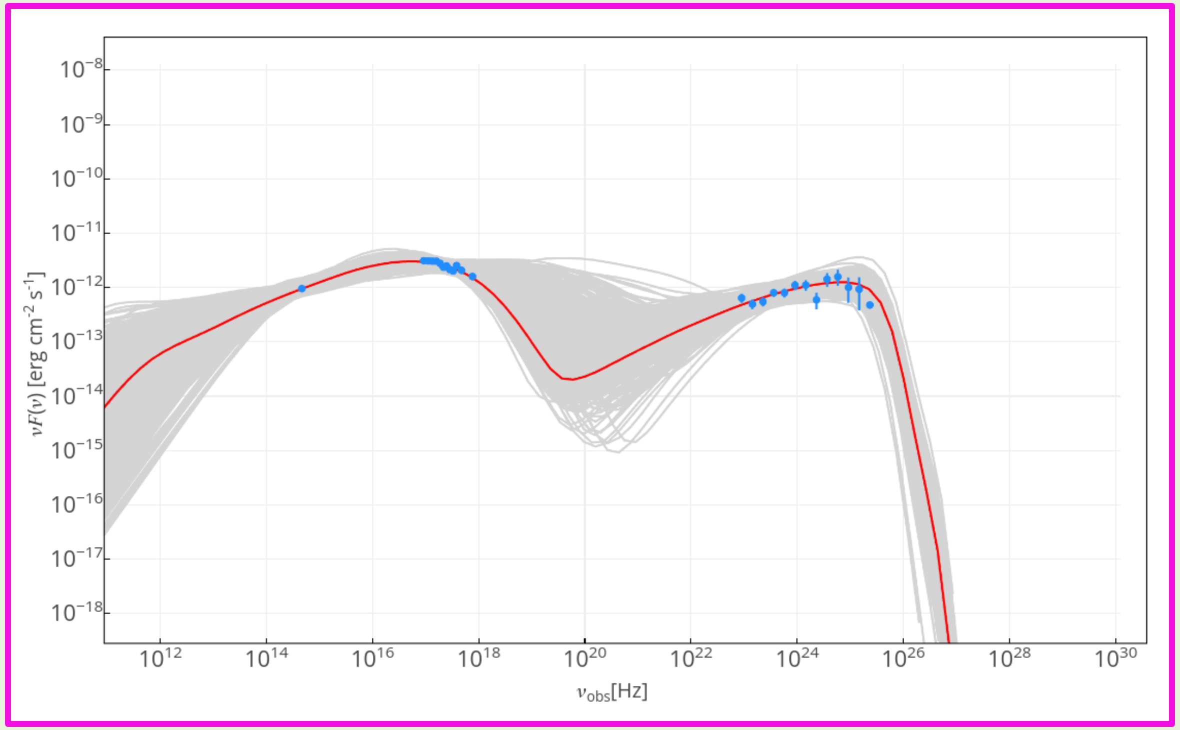

Main ingredients:

- **Leptonic SSC one-zone model**
- **Simple PL as electron energy distribution**
- **All TON 116 broadband datasets w/o ULs (HE, VHE), no TON 116 archival data (mostly out of 2021-2023)**
- **EBL absorption considered (*Domìnguez et al. 2011*)**

Overall trend very similar to agnpy BPL model (smallest slope *p*, close to the first of BPL)

VHE strong suppression confirmed

Parameter comparison

agnpy

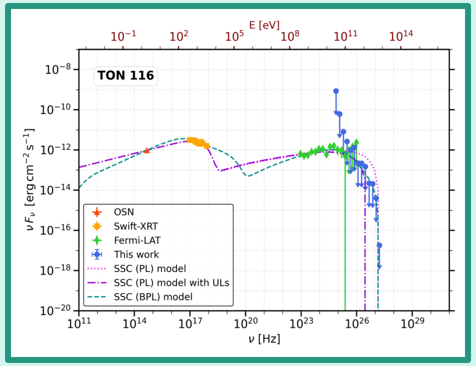

	PL (no ULs)	PL (ULs included)	BPL (no ULs)
χ^2/dof	26.35/19	40.74/36	17.28/17
Q-val	0.121	0.270	0.435
Log (k [cm^{-3}])	5.74 ± 0.84	5.14 ± 0.15	-6.1 ± 1.1
p_1	2.54 ± 0.04	2.54 ± 0.03	2.16 ± 0.23
p_2	–	–	3.68 ± 0.16
γ_{min}	1.00	1.00	100
Log (γ_{br})	–	–	4.59 ± 0.31
γ_{max} [10^5]	2.10	2.10	10.0
δ_D	100 ± 189	23.1 ± 1.5	19.4 ± 7.5
Log (B [G])	-1.32 ± 0.81	-0.683 ± 0.077	-0.329 ± 0.556
t_{var} [ks]	1.93 ± 7.26	35.0	29.3

Normalization to the **total numerical density**

No R_b reported, but **t_{var} predicted -> 0.5-10 h**

MMDC

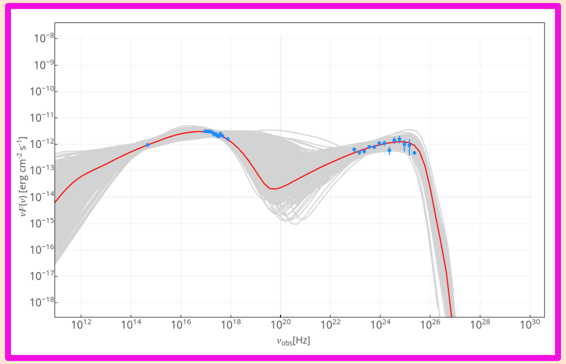

p	δ_D	γ_{min}	γ_{max}	B [G]	R_b [cm]	L_e [erg s^{-1}]
2.11	22.0	256	$2.57 \cdot 10^5$	0.0929	$1.25 \cdot 10^{16}$	$2.61 \cdot 10^{43}$

Normalization to the **total electron luminosity**

R_b reported, but no goodness-of-fit information

Parameter comparison

agnpy

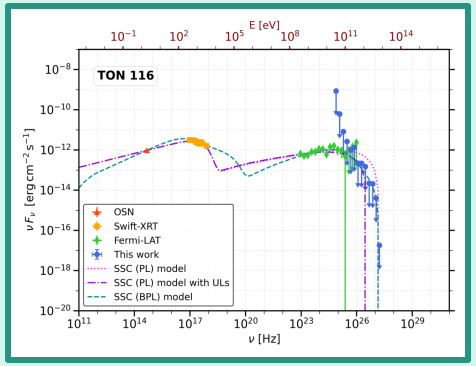

	PL (no ULs)	PL (ULs included)	BPL (no ULs)
χ^2/dof	26.35/19	40.74/36	17.28/17
Q-val	0.121	0.270	0.435
Log (k [cm^{-3}])	5.74 ± 0.84	5.14 ± 0.15	−6.1 ± 1.1
p_1	2.54 ± 0.04	2.54 ± 0.03	2.16 ± 0.23
p_2	–	–	3.68 ± 0.16
γ_{min}	1.00	1.00	100
Log (γ_{br})	–	–	4.59 ± 0.31
γ_{max} [10^5]	2.10	2.10	10.0
δ_D	100 ± 189	23.1 ± 1.5	19.4 ± 7.5
Log (B [G])	−1.32 ± 0.81	−0.683 ± 0.077	−0.329 ± 0.556
t_{var} [ks]	1.93 ± 7.26	35.0	29.3

Normalization to the **total numerical density**
No R_b reported, but **t_{var} predicted -> 0.5-10 h**

MMDC

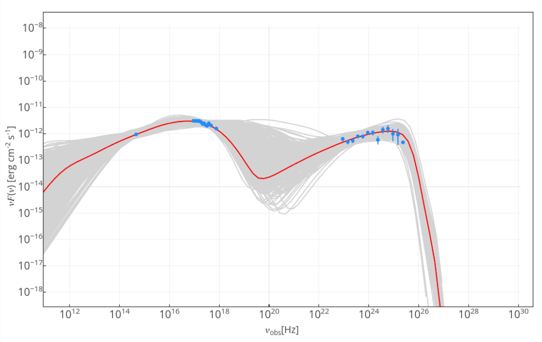

p	δ_D	γ_{min}	γ_{max}	B [G]	R_b [cm]	L_e [erg s^{-1}]
2.11	22.0	256	$2.57 \cdot 10^5$	0.0929	$1.25 \cdot 10^{16}$	$2.61 \cdot 10^{43}$

Normalization to the **total electron luminosity**
R_b reported, but no goodness-of-fit information

Overall agreement (fluctuations within ~ 1 order of magnitude mostly)
What about the literature…?

Literature check

PKS 1424+240 (*Aleksić et al. 2014*)

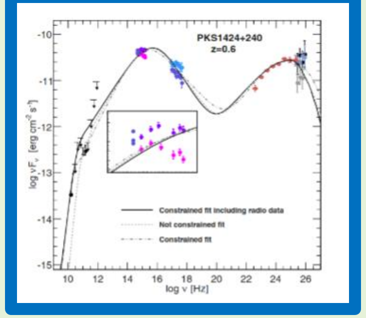

	p_1	p_2	δ_D	γ_{min}	γ_{br} [$\cdot 10^4$]	γ_{max} [$\cdot 10^7$]	B [G]	k [cm^{-3}]	R_b [cm]	$L_{e,kin}$ [erg s^{-1}]
1-zone	1.7	3.7	131	16	2.6	3.9	0.006	50	$5 \cdot 10^{16}$	$2.1 \cdot 10^{46}$
(no radio)	1.9	3.9	70	260	3.2	89	0.018	200	$6.5 \cdot 10^{16}$	$7.0 \cdot 10^{45}$

HBL detected by MAGIC (after *Fermi* and VERITAS)

z $\gtrsim$ 0.604 (*Furniss et al. 2013*)

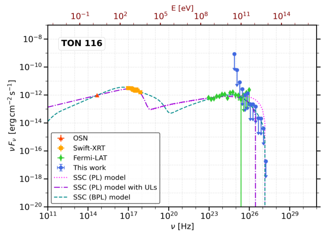

	p_1	p_2	δ_D	γ_{min}	γ_{br} [$\cdot 10^4$]	γ_{max} [$\cdot 10^5$]	B [G]	k [cm^{-3}]	R_b [$\cdot 10^{15}$ cm]
PL (no ULs)	2.54	–	100	1.0	–	2.1	0.0479	$5.50 \cdot 10^5$	3.86
PL (+ ULs)	2.54	–	23.1	1.0	–	2.1	0.207	$1.38 \cdot 10^5$	16.2
BPL (no ULs)	2.16	3.68	19.4	100	3.89	10	0.469	$7.94 \cdot 10^{-7}$	11.4

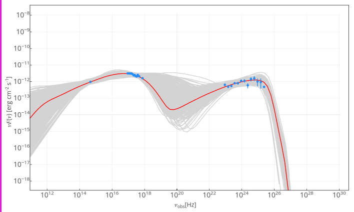

p_1	p_2	δ_D	γ_{min}	γ_{br}	γ_{max}	B [G]	R_b [cm]	L_e [erg s^{-1}]
2.11	–	22.0	256	–	$2.57 \cdot 10^5$	0.0929	$1.25 \cdot 10^{16}$	$2.61 \cdot 10^{43}$

Literature check

PKS 1424+240 (*Aleksić et al. 2014*)

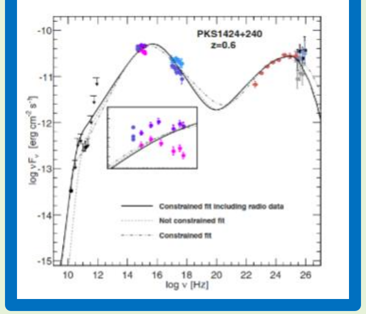

	p_1	p_2	δ_D	γ_{min}	γ_{br} $[\cdot 10^4]$	γ_{max} $[\cdot 10^7]$	B [G]	k $[\mathrm{cm}^{-3}]$	R_b [cm]	$L_{e,kin}$ $[\mathrm{erg\ s}^{-1}]$
1-zone	1.7	3.7	131	16	2.6	3.9	0.006	50	$5 \cdot 10^{16}$	$2.1 \cdot 10^{46}$
(no radio)	1.9	3.9	70	260	3.2	89	0.018	200	$6.5 \cdot 10^{16}$	$7.0 \cdot 10^{45}$

HBL detected by MAGIC (after *Fermi* and VERITAS)

z ≳ 0.604 (*Furniss et al. 2013*)

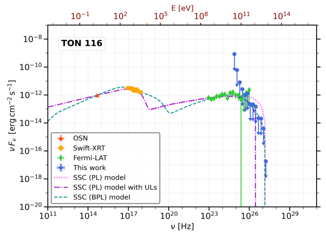

	p_1	p_2	δ_D	γ_{min}	γ_{br} $[\cdot 10^4]$	γ_{max} $[\cdot 10^5]$	B [G]	k $[\mathrm{cm}^{-3}]$	R_b $[\cdot 10^{15}\ \mathrm{cm}]$
PL (no ULs)	2.54	–	100	1.0	–	2.1	0.0479	$5.50 \cdot 10^5$	3.86
PL (+ ULs)	2.54	–	23.1	1.0	–	2.1	0.207	$1.38 \cdot 10^5$	16.2
BPL (no ULs)	2.16	3.68	19.4	100	3.89	10	0.469	$7.94 \cdot 10^{-7}$	11.4

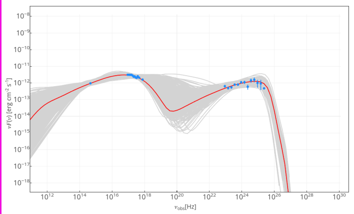

p_1	p_2	δ_D	γ_{min}	γ_{br}	γ_{max}	B [G]	R_b [cm]	L_e $[\mathrm{erg\ s}^{-1}]$
2.11	–	22.0	256	–	$2.57 \cdot 10^5$	0.0929	$1.25 \cdot 10^{16}$	$2.61 \cdot 10^{43}$

Plausible parameters and expected trends

Conclusions

- Thesis work on investigation of possible outliers of the blazar sequence → TON 116 good candidate if $z \approx 1$ (*Ajello et al. 2020*), but $z \geq 0.483$ (*Paiano et al. 2017*)

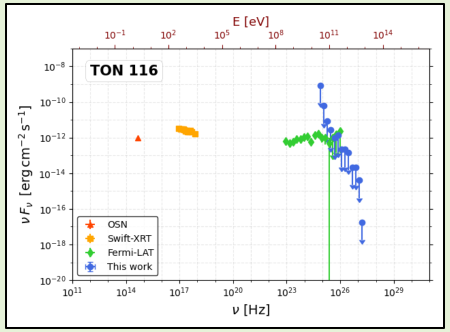

- 1st VHE observations ever with MAGIC (2021-2023), excess hint for 2021 + 2022, but no detection → no new z constraint (*Prandini et al. 2010*) possible

Conclusions

- ✓ Thesis work on investigation of possible outliers of the blazar sequence ➡ TON 116 good candidate if $z \approx 1$ (*Ajello et al. 2020*), but $z \geq 0.483$ (*Paiano et al. 2017*)

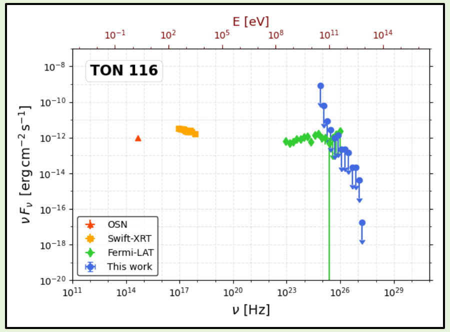

- ✓ 1st VHE observations ever with MAGIC (2021-2023), excess hint for 2021 + 2022, but no detection → no new z constraint (*Prandini et al. 2010*) possible

- ✓ Fermi-LAT, Swift-XRT, OSN observations also combined → broadband SED (~ constant low state)

- ✓ 1st emission model ever for TON 116 SED via innovative agnpy-sherpa and MMDC tools

Leptonic 1-zone SSC model
Broken/**Simple** power-law as e^- distribution

BPL best-fit model (at VHE also, despite no ULs)

PL model, trend similar to BPL
Strong VHE suppression confirmed

Conclusions

✓ *Thesis work on investigation of possible outliers of the blazar sequence ➡ TON 116 good candidate if z ≈ 1 (Ajello et al. 2020), but z ≥ 0.483 (Paiano et al. 2017)*

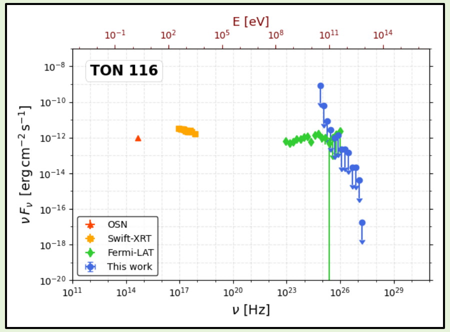

✓ *1st VHE observations ever with MAGIC (2021-2023), excess hint for 2021 + 2022, but no detection → no new z constraint (Prandini et al. 2010) possible*

✓ *Fermi-LAT, Swift-XRT, OSN observations also combined → broadband SED (~ constant low state)*

✓ *1st emission model ever for TON 116 SED via innovative agnpy-sherpa and MMDC tools*

Leptonic 1-zone SSC model
Broken/**Simple** power-law as e^- distribution

BPL best-fit model
(at VHE also, despite no ULs)

PL model, trend similar to BPL
Strong VHE suppression confirmed

✓ ***Perspectives:*** *VHE monitoring for new distance/nature clarification (especially with CTAO)*

11/07/2024

MAGIC Observations of the Blazar TON 116 in a Multi-wavelength Context

PhD candidate: Andrea Lorini

Supervisor: Dr. Sofia Ventura

Co-supervisor: Dr. Giacomo Bonnoli

MAGIC
Major Atmospheric Gamma Imaging Cerenkov Telescopes

DSFTA
DIPARTIMENTO DI SCIENZE FISICHE, DELLA TERRA E DELL'AMBIENTE

Thank you for your attention!

INFN
Istituto Nazionale di Fisica Nucleare
SEZIONE DI PISA

Backup slides

What is an Active Galactic Nuclei?

6 Eventual radio jets made up by collimated ultra-high-speed particles reaching up to ~ 1 Mpc distance (relativistic effects e.g. boosting)

1 Central U.A.-scale Super Massive Black Hole (SMBH) of ~ 10^6 - 10^{10} $M_\odot$

4 Optically-thick dusty torus (at ~ 1-100 pc) absorbing optical and UV radiation, mostly re-emitting in the far-IR

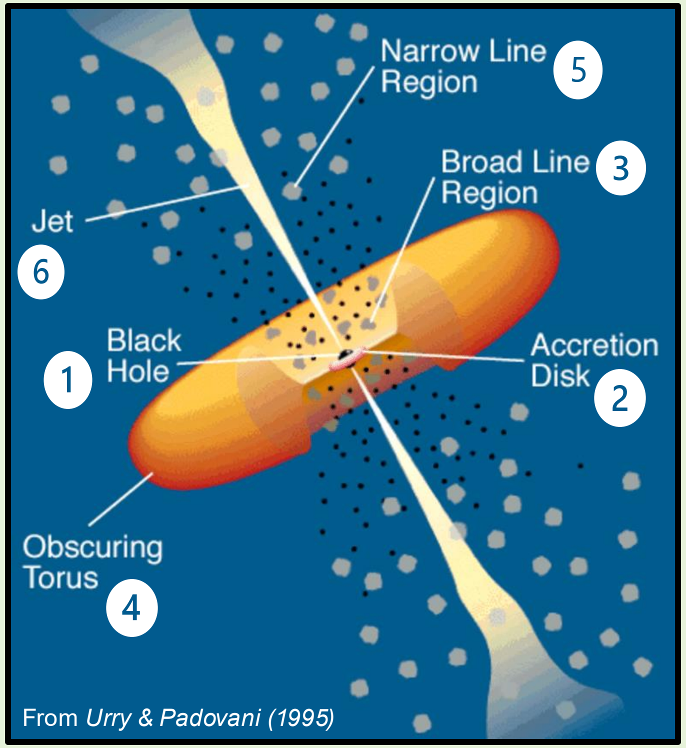

Narrow Line Region (NLR, ≲ 100 pc) with slower (~ 300 - 500 km/s), more sparse, and much less dense clumps 5

Broad Line Region (BLR, ~ 0.1-1 pc) with fastly-moving (~ 10^3 - 10^4 km/s) clumps excited/ionized by disk 3

Sub-pc-scale accretion disk of infalling material emitting as a black-body (hotter inward) 2

In 1% of all known galaxies, non-thermal (accretion) radiation greatly overcomes the thermal (stars + gas + dust) one!

Fermi-LAT

Atwood et al. (2009)

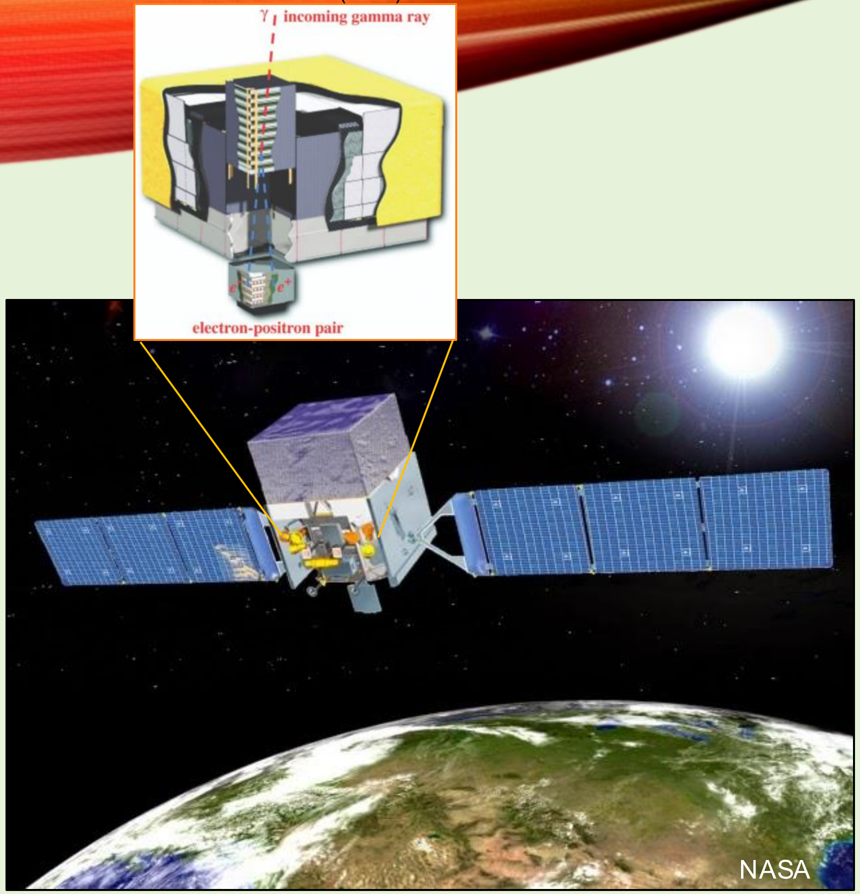

- Launched in Jun 2008 and operational since Nov 2008
- Sky monitorer in the HE γ-ray domain ($\gtrsim$ 20 MeV – 300 GeV)
- Long duty cycle ($\gtrsim$ 90%), large FoV ($\approx$ 3 sr)

- ***anti-coincidence scintillator*** *rejecting background signals*
- ***converter tracker*** *of tungsten plates (Z = 74) and silicon detectors hosting a produced e^-–e^+ pair from an incoming γ-ray*
- ***calorimeter*** *measuring the e^-–e^+ energy losses*

Breakthrough for HE sources and TeV candidates

Caveat:

small collection area (~ 1 m^2)
inefficient at VHE range...

Swift

- **Modular satellite launched in Nov 2004 to study GRBs**
- **Continuous MWL sky survey, ≈ 88% covered daily**
- ***Swiftly* reacting with three coaligned instruments**

BAT
Burst Alert Telescope

E ~ 15-150 keV
FoV ~ 2 sr

Transient position estimation (Δx ~ 1') and trigger

XRT
X-ray Telescope

E ~ 0.3-10 keV

UVOT
Ultraviolet-Optical Telescope

λ ~ 170-600 nm

Triggered within ~ 90 s
Images + spectra + LCs
Transient localization improved

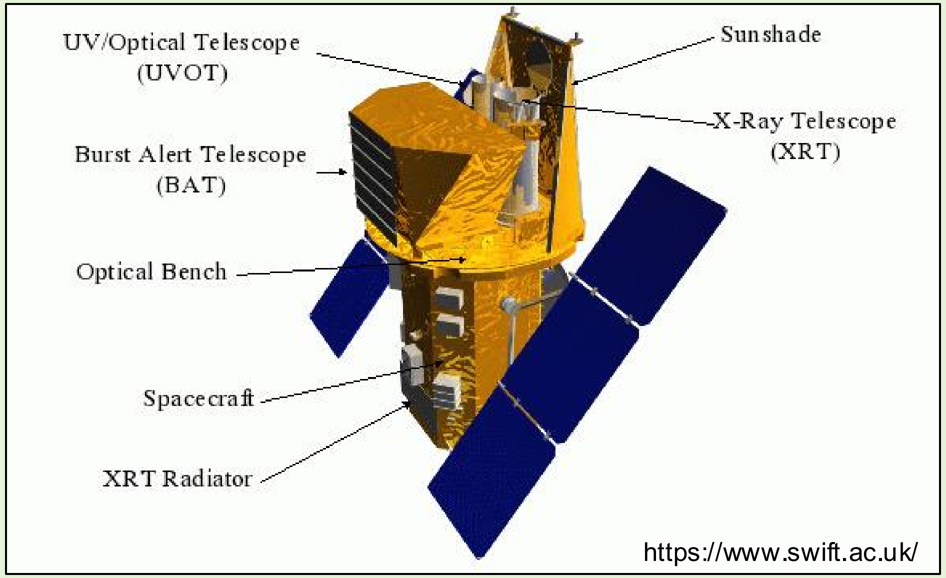

Key role for further follow-up (ground-based instruments also)

Transient's redshift possible (few cases)

Observatorio de Sierra Nevada (OSN)

IAA-CSIC

- Inaugurated in 1981 at Loma de Dìlar (03°23'05" W, 37°03'51" N), Sierra Nevada (Granada, Spain), 2896 m a.s.l.

- Two optical telescopes with Ritchey-Chrétien mirror displacement and Nasmyth focus configuration managed by IAA-CSIC

T150
1.50 m diameter

T090
0.90 m diameter

Bessell 2005

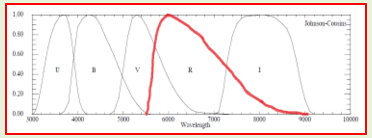

R-band (Johnson-Cousins filter, $\lambda_{ref} \approx 640.7$ nm, $\Delta\lambda_{fwhm} \approx 1580$ Å**)**

- *Photometric data*
- *Polarimetric data*

iop4 pipeline (*Escudero et al. 2024*)

Detection insights

Primary VHE γ-ray interacting with atmospheric nuclei (h ~ 10 km)

Cascade of generated e^--e^+ (pair production) and γ (bremsstrahlung)

Cherenkov pool (~ ns pulse) focused by M1 and M2 reflectors

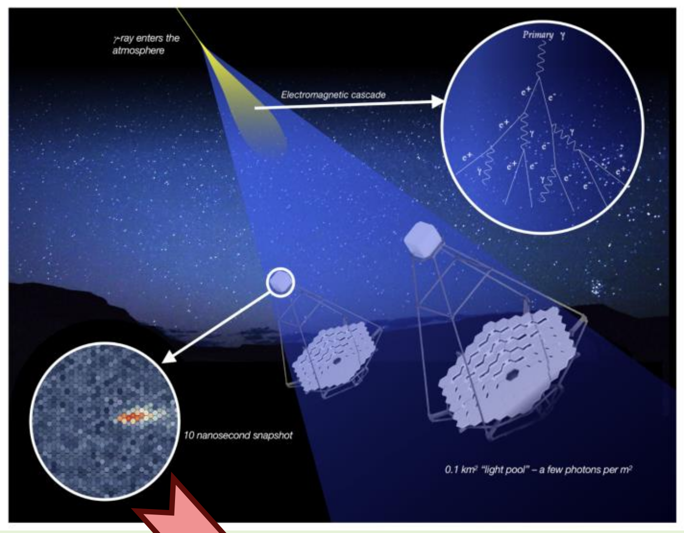

MAGIC Analysis and Reconstruction Software (MARS)

- C++ - based scripts (ROOT environment): from **DAQ raw files** (space/ time distribution of camera p.e.) to **high-level results** (e.g. SED, LC)
- **Signal significance (s)**: statistical comparison of ON/OFF regions (*Li & Ma 1983*), **Wobble** being the standard observation mode
- Reconstructed quantities (by RF per MC): **direction**, **energy**, **hadronness**

Background to be rejected!

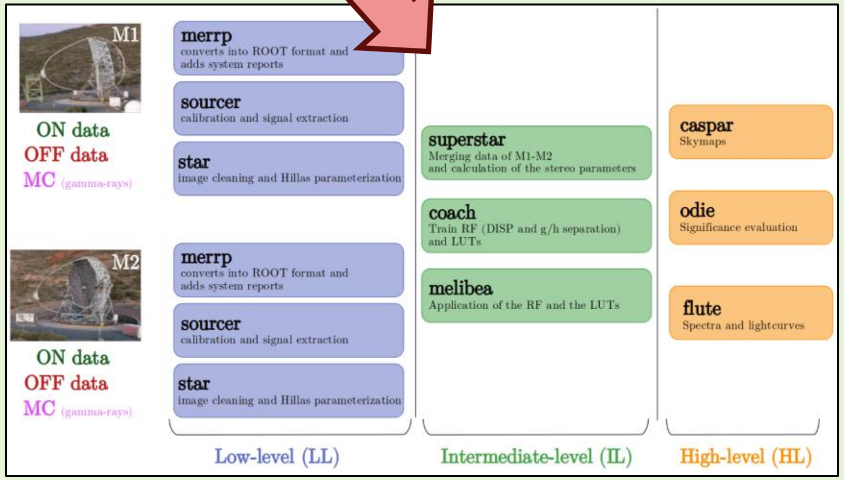

TON 116 by MAGIC (2021, 2022)

Zenith: 7°-36°; DTs: Dark Extragalactic; DCMax = 3000 nA; LIDAR@9km: > 0.7; Cloudiness: < 30; En. range: LE

2021 (~ 17.8/18.7 h) | **2022 (~ 7.0/8.0 h)** | **2021+2022**

Andrea Lorini

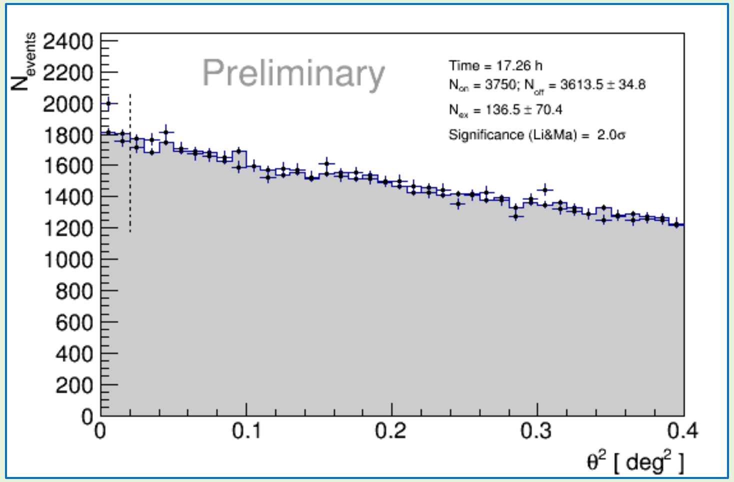

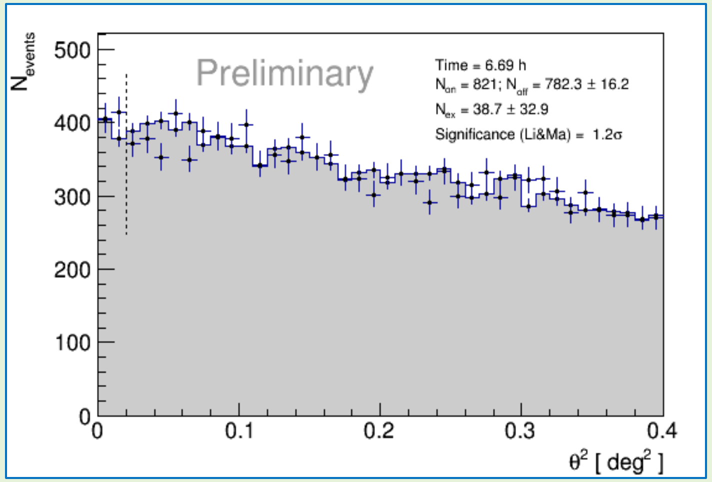

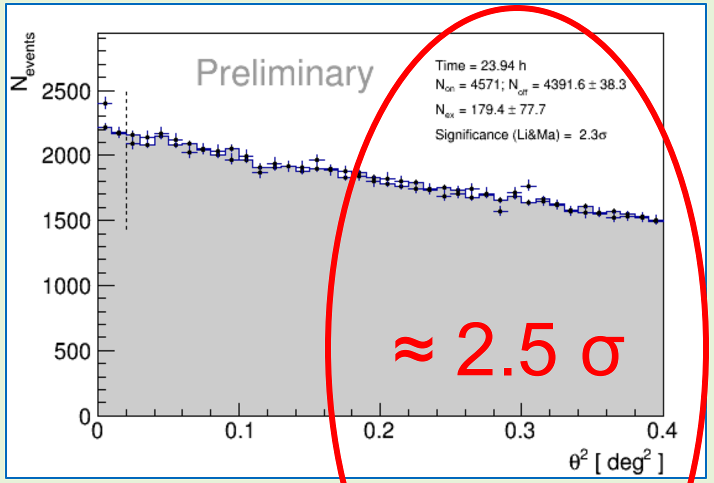

Dr. Paolo Da Vela

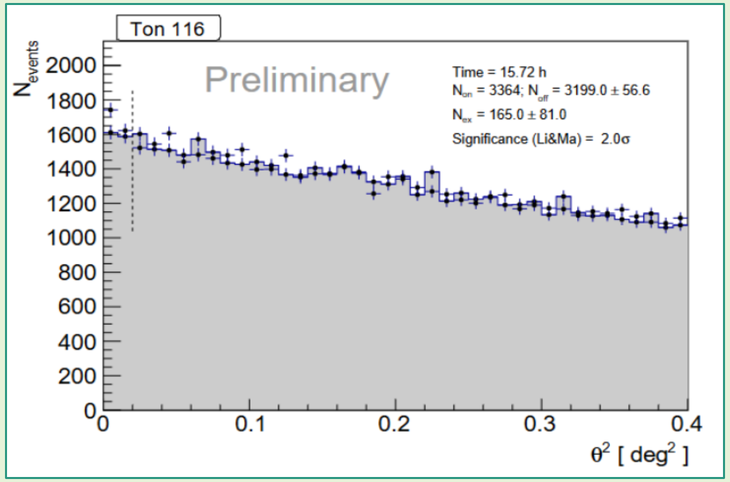

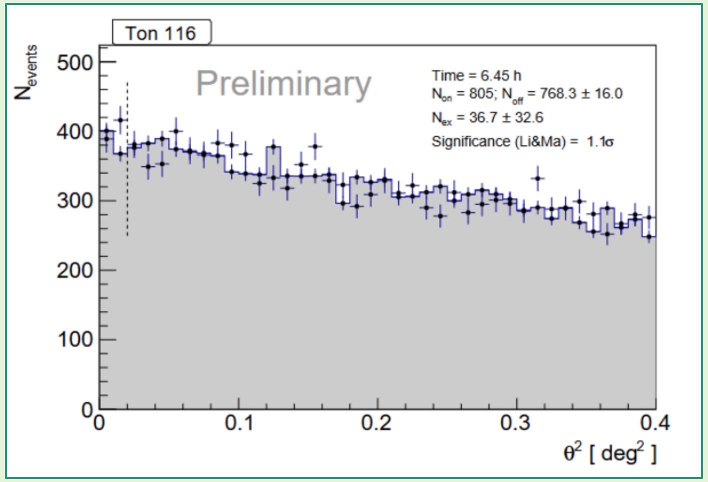

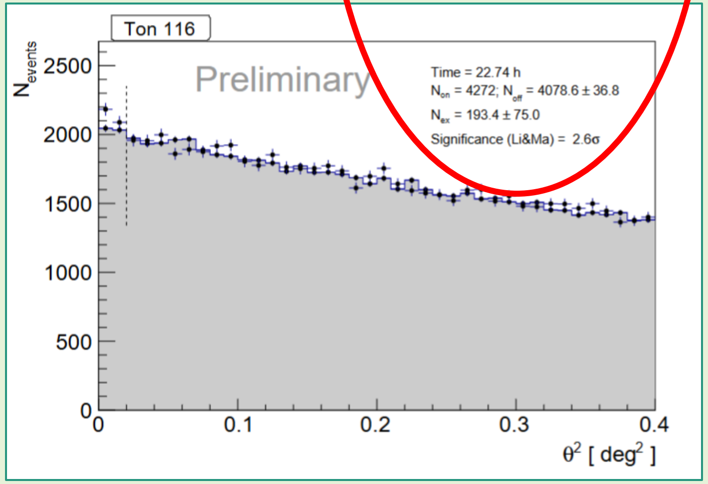

VHE excess hint

2021 (flute) | **2021+2022 (foam)**

A

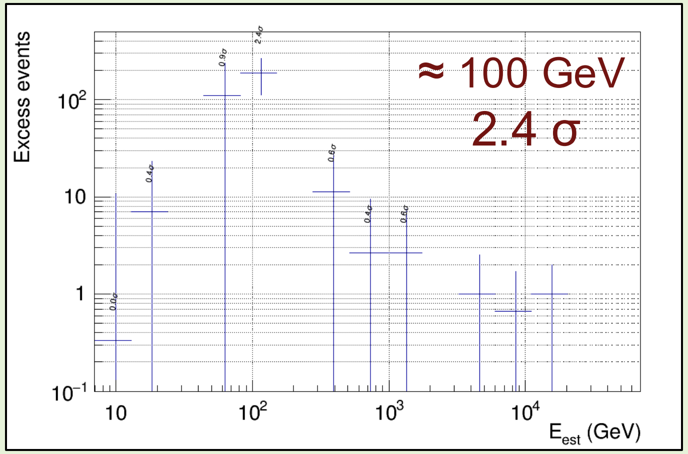

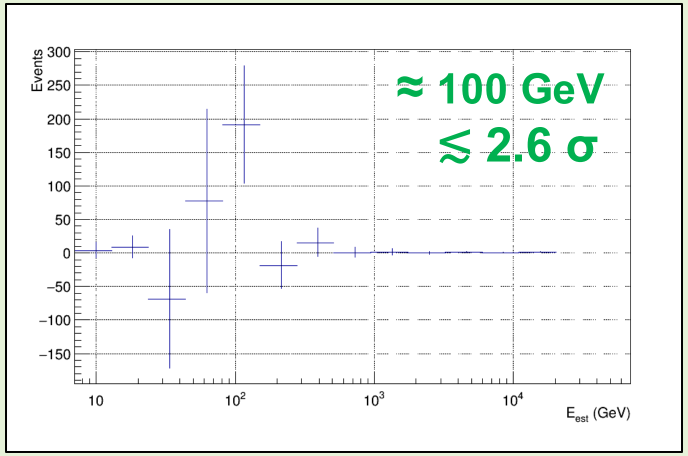

P

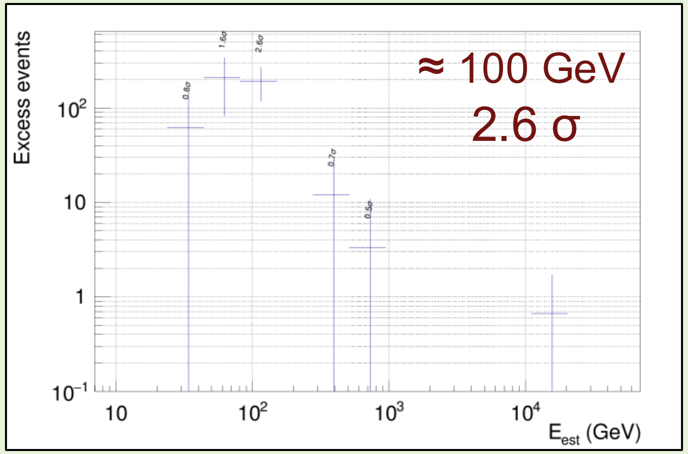

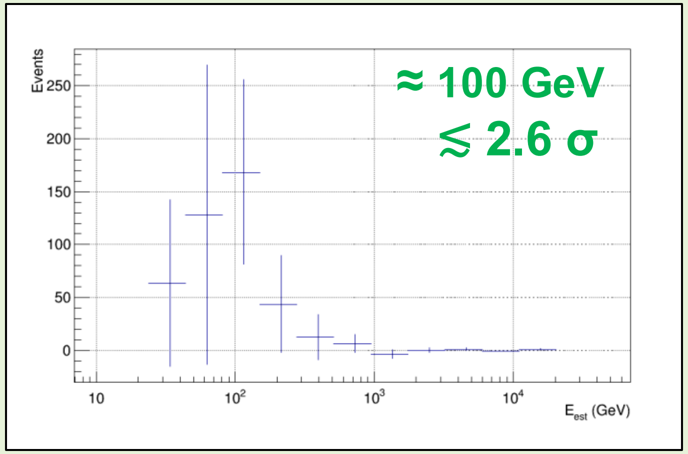

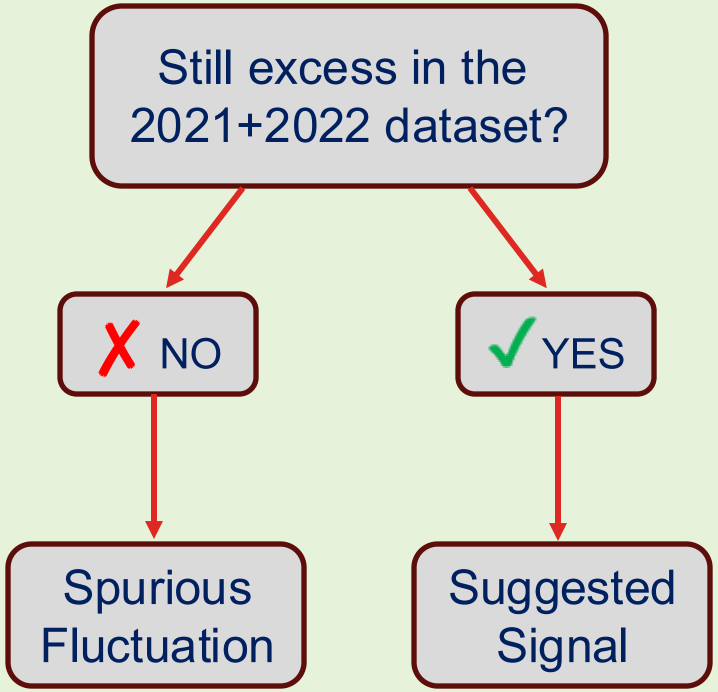

Dedicated odie execution (standard/fitted ON & OFF distrib.):

$2.0\,\sigma \lesssim s \lesssim 2.6\,\sigma$

TON 116 by Fermi-LAT (recap)

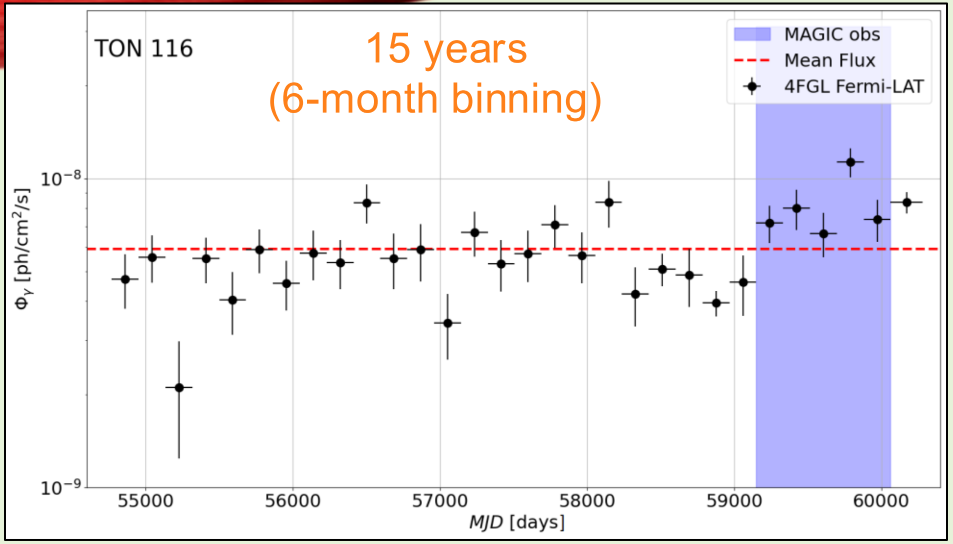

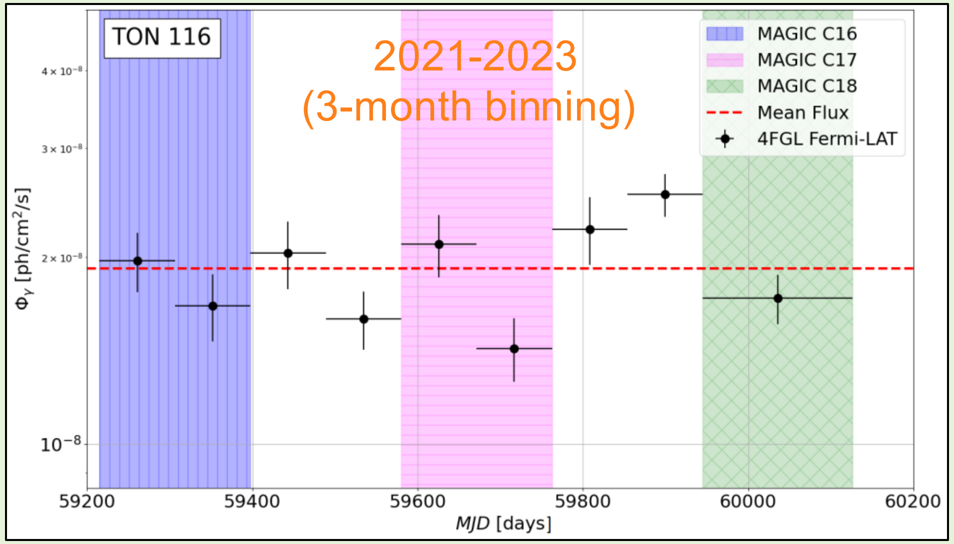

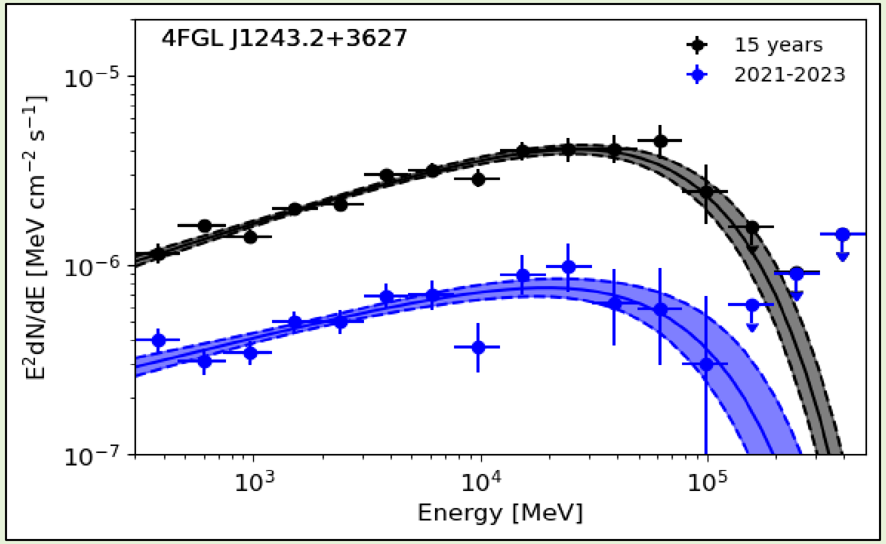

300 MeV – 500 GeV range, 2021-2023 period:

- *Overall non-variability (LC)*
- *Particularly low activity (SED) also preventing VHE detection (but still possible in case of flare...)*

agnpy-sherpa fit results

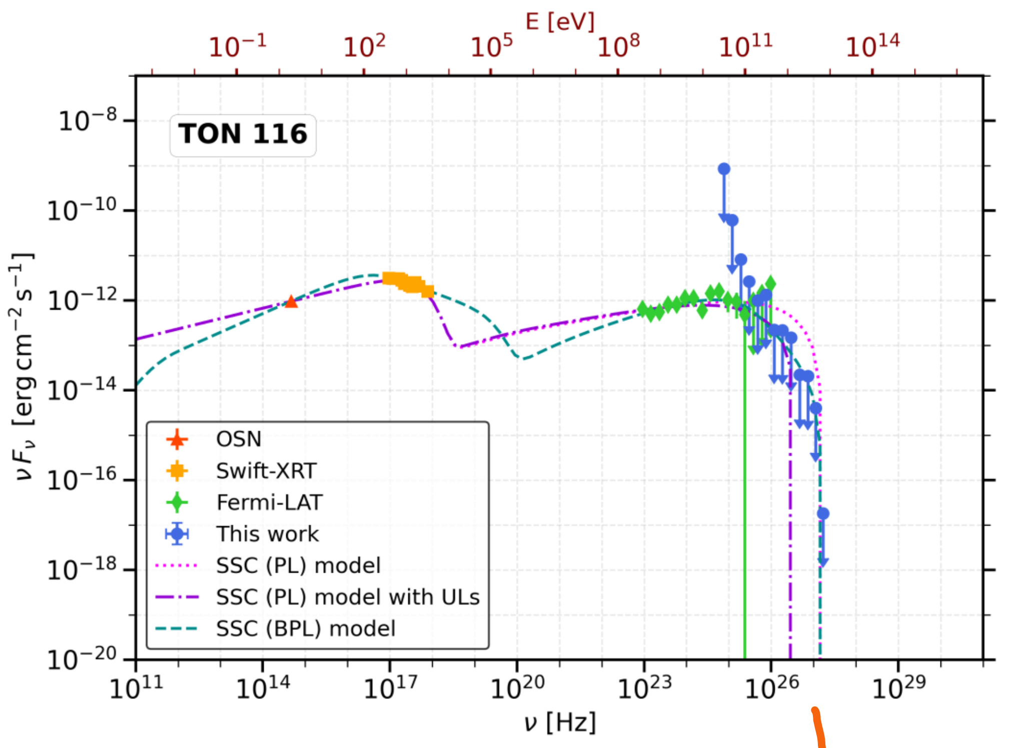

	PL (no ULs)	PL (ULs included)	BPL (no ULs)
χ^2/dof	26.35/19	40.74/36	17.28/17
Q-val	0.121	0.270	0.435
Log (k [cm^{-3}])	5.74 ± 0.84	5.14 ± 0.15	-6.1 ± 1.1
p_1	2.54 ± 0.04	2.54 ± 0.03	2.16 ± 0.23
p_2	–	–	3.68 ± 0.16
γ_{min}	1.00	1.00	100
Log (γ_{br})	–	–	4.59 ± 0.31
γ_{max} [10^5]	2.10	2.10	10.0
δ_D	100 ± 189	23.1 ± 1.5	19.4 ± 7.5
Log (B [G])	-1.32 ± 0.81	-0.683 ± 0.077	-0.329 ± 0.556
t_{var} [ks]	1.93 ± 7.26	35.0	29.3

Strong VHE suppression

SynchrotronSelfComptonModel **method initializations:**

- PL (ULs excluded/included), BPL (no ULs) as e$^-$ distribution
- z = 0.5
- *sherpa* wrapper for data handling (ecsv format)
- Systematics added (OSN 5%, XRT & LAT 10%, MAGIC 30%)

Power-law case

For $\nu < 10^{25}$ Hz → PL (- ULs) ≈ PL (+ ULs)

For $\nu > 10^{25}$ Hz → PL (+ ULs) improving the VHE fit

But EHBL behaviour suggested ($\nu_{p,s} > 10^{17}$ Hz)...

Broken Power-law case

Harder rise & decrease of synchrotron bump

Bumps' connection at higher E, harder rise of IC bump

Good fit also at VHE even if ULs not included!

MMDC fit results

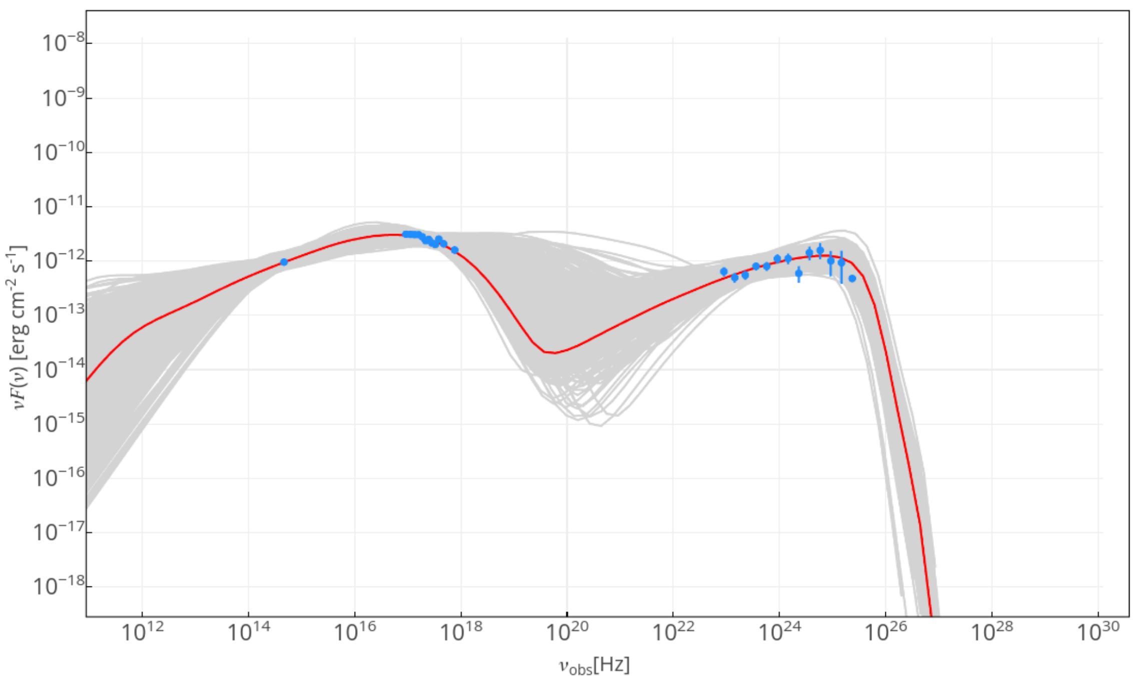

p	δ_D	γ_{min}	γ_{max}	B [G]	R_b [cm]	L_e [erg s^{-1}]
2.11	22.0	256	$2.57 \cdot 10^5$	0.0929	$1.25 \cdot 10^{16}$	$2.61 \cdot 10^{43}$

Main ingredients:

- **Leptonic SSC one-zone model**
- **Simple PL as electron energy distribution**
- **All TON 116 broadband datasets w/o ULs (HE, VHE), no TON 116 archival data (mostly out of 2021-2023)**
- **EBL absorption considered (*Domìnguez et al. 2011*)**

Overall trend very similar to agnpy BPL model (smallest slope *p*, close to the first of BPL)

VHE strong suppression confirmed

Literature check

Parameter	Mrk 421 Gammapy	Mrk 421 sherpa	PKS 1510-089 Gammapy	PKS 1510-089 sherpa
(a) Best-fit parameters				
$\log_{10}(\frac{k_e}{cm^{-3}})$	−7.89	−7.89	−2.06	−2.05
p_1	2.06	2.06	2.00	2.00
p_2	3.54	3.54	3.16	3.16
$\log_{10}(\gamma'_b)$	4.99	4.99	3.01	3.01
$\log_{10}(B/G)$	−1.33	−1.33	−0.42	−0.42
δ_D	19.74	19.76	–	–
χ^2/d.o.f.	271.2/80	271.2/80	230.5/36	230.5/36

(b) Fixed parameters

Parameter	Mrk421	PKS 1510-089
δ_D	–	25
γ'_{min}	500	1
γ'_{max}	10^6	3×10^4
R_b / cm	5.3×10^{16}	2.4×10^{16}
θ_s	2.90°	2.22°
r/cm	–	6×10^{17}
L_{disc}/(erg s^{-1})	–	6.7×10^{45}
η	–	1/12
$M_{BH}/M_\odot$	–	5.71×10^7
R_{in}/R_g	–	6
R_{out}/R_g	–	10^4
ξ_{DT}	–	0.6
R_{DT} / cm	–	6.5×10^{18}
T_{DT} / K	–	10^3
z	0.0308	0.361

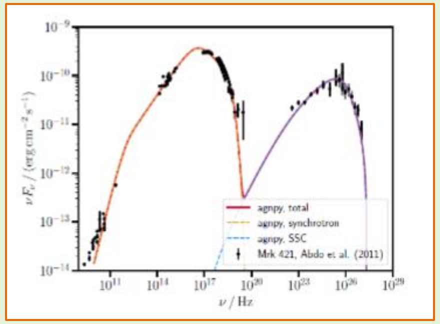

Mrk 421, Nigro et al. (2022)

Well known, TeV-emitter HBL
Close, z ≈ 0.031 (*Ulrich et al. 1975*)
Lower ρ and B, larger R_b and γ_{min}

PKS 1424+240, Aleksić et al. (2014)

HBL seen by *Fermi*, VERITAS, MAGIC
Far, z ≳ 0.604 (*Furniss et al. 2013*)
Lower ρ (BPL) and B, larger R_b, γ_{max}, δ_D

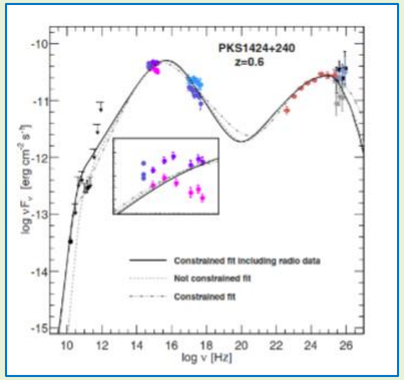

Model	γ_{min} [10^3]	γ_b [10^4]	γ_{max} [10^5]	n_1	n_2	B [G]	K [cm^{-3}]	R [10^{16} cm]	δ	$L_{kin(p)}$ [10^{45} erg s^{-1}]	$L_{kin(e)}$ [10^{45} erg s^{-1}]	L_B [10^{43} erg s^{-1}]
One-zone (No radio)	0.260	3.2	8.9×10^3	1.9	3.9	0.018	2×10^2	6.5	70	5	7.0	3
One-zone	0.016	2.6	3.9×10^2	1.7	3.7	0.006	50	5	131	64	21	0.8
One-zone (Constrained)	0.004	5.3	3.2×10^4	2.0	4.0	0.017	1.7×10^2	19	40	371	11	8.8
2 zones (in)	8.0	3.9	7.0	2.0	3.1	0.033	3.1×10^3	4.8	30	0.07	1.2	1.1
2 zones (out)	0.6	3.0	0.5	2.0	3.0	0.033	23	190	9	1.3	2.3	159

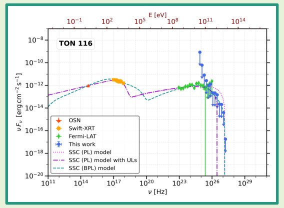

	PL (no ULs)	PL (ULs included)	BPL (no ULs)
χ^2/dof	26.35/19	40.74/36	17.28/17
Q-val	0.121	0.270	0.435
Log (k [cm^{-3}])	5.74 ± 0.84	5.14 ± 0.15	−6.1 ± 1.1
p_1	2.54 ± 0.04	2.54 ± 0.03	2.16 ± 0.23
p_2	–	–	3.68 ± 0.16
γ_{min}	1.00	1.00	100
Log (γ_{br})	–	–	4.59 ± 0.31
γ_{max} [10^5]	2.10	2.10	10.0
δ_D	100 ± 189	23.1 ± 1.5	19.4 ± 7.5
Log (B [G])	−1.32 ± 0.81	−0.683 ± 0.077	−0.329 ± 0.556
t_{var} [ks]	1.93 ± 7.26	35.0	29.3

Plausible parameters and expected trends

p	δ_D	γ_{min}	γ_{max}	B [G]	R_b [cm]	L_e [erg s^{-1}]
2.11	22.0	256	$2.57 \cdot 10^5$	0.0929	$1.25 \cdot 10^{16}$	$2.61 \cdot 10^{43}$

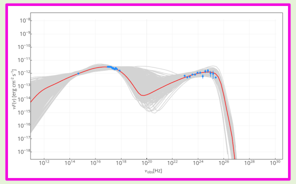

Literature check

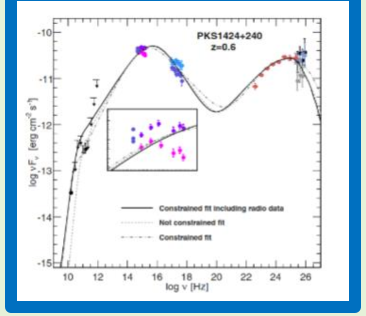

PKS 1424+240 (*Aleksić et al. 2014*)

	p_1	p_2	δ_D	γ_{min}	γ_{br} $[\cdot 10^4]$	γ_{max} $[\cdot 10^7]$	B [G]	k $[\mathrm{cm}^{-3}]$	R_b [cm]	$L_{e,kin}$ $[\mathrm{erg\ s^{-1}}]$
1-zone	1.7	3.7	131	16	2.6	3.9	0.006	50	$5 \cdot 10^{16}$	$2.1 \cdot 10^{46}$
(no radio)	1.9	3.9	70	260	3.2	89	0.018	200	$6.5 \cdot 10^{16}$	$7.0 \cdot 10^{45}$

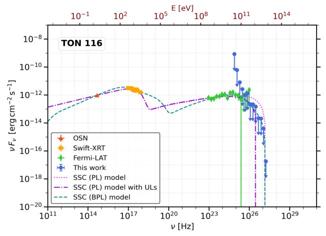

	p_1	p_2	δ_D	γ_{min}	γ_{br} $[\cdot 10^4]$	γ_{max} $[\cdot 10^5]$	B [G]	k $[\mathrm{cm}^{-3}]$	R_b $[\cdot 10^{15}\ \mathrm{cm}]$
PL (no ULs)	2.54	–	100	1.0	–	2.1	0.0479	$5.50 \cdot 10^5$	3.86
PL (+ ULs)	2.54	–	23.1	1.0	–	2.1	0.207	$1.38 \cdot 10^5$	16.2
BPL (no ULs)	2.16	3.68	19.4	100	3.89	10	0.469	$7.94 \cdot 10^{-7}$	11.4

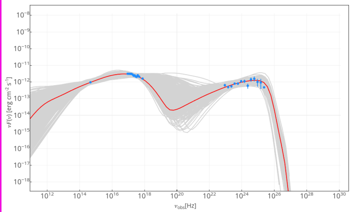

p_1	p_2	δ_D	γ_{min}	γ_{br}	γ_{max}	B [G]	R_b [cm]	L_e $[\mathrm{erg\ s^{-1}}]$
2.11	–	22.0	256	–	$2.57 \cdot 10^5$	0.0929	$1.25 \cdot 10^{16}$	$2.61 \cdot 10^{43}$

HBL detected by MAGIC (after *Fermi* and VERITAS) with $z \gtrsim 0.604$ (*Furniss et al. 2013*):

- p_1, p_2, γ_{min}, γ_{br}, δ_D compatible
- ρ ~ mean Log value
- Lower B, larger R_b, γ_{max}

Plausible parameters and expected trends